IN-VIVO DYNAMICS OF HIV-1 EVOLUTION

Tinevimbo Shiri

A thesis submitted to the Faculty of Science, University of the Witwatersrand, Johannesburg, in fulfillment of the requirements for the degree of Doctor of Philosophy

8 June 2011

DECLARATION

I declare that this thesis is my own, unaided work. It is being submitted for the degree of Doctor of Philosophy in the University of the Witwatersrand, Johannesburg. It has not been submitted before for any degree or examination in any other University.

_____

Signature

_____

Date

To my Family.

Table of Contents

List of Tables

List of Figures

Abstract

The evolution of drug resistance in human immunodeficiency virus (HIV) infection has been a focus of research in many fields, as it continues to pose a problem to disease prevention and HIV patient management. In addition to techniques of molecular biology, studies in mathematical modelling have contributed to the knowledge here, but many questions remain unanswered. This thesis explores the application of a number of hybrid stochastic/deterministic models of viral replication to scenarios where viral evolution may be clinically or epidemiologically important. The choice of appropriate measures of viral evolution/diversity is non-trivial, and this impacts on the choice of mathematical techniques deployed. The use of probability generating functions to describe mutations occurring during early infection scenarios suggest that very early interventions such as pre-exposure prophylaxis (PrEP) or vaccines may substantially reduce viral diversity in cases of breakthrough infection. A modified survival analysis coupled to a deterministic model of viral replication during transient and chronic treatment helps identify clinically measurable indicators of the time it takes for deleterious rare mutations to appear. Lastly, persistence of problematic mutations is studied through the use of deterministic models with stochastic averaging over initial conditions.

Acknowledgements

I would like to thank Dr Alex Welte, my supervisor, for his guidance, mentorship, many suggestions and constant support during this research. I am also thankful to Nina Fefferman for introducing me to the research field of social networks and her guidance throughout the year (March 2009 - March 2010) whilst visiting DIMACS at Rutgers University.

The SACEMA bursary, which was awarded to me for the period 2007–2010, was very crucial to the successful completion of this project. I would also like to thank Professor Fred Roberts for the DIMACS research fellowship at Rutgers University, and the useful contacts and friendly encouragement that he gave me.

I had the pleasure of meeting David Wick and his fellow SCHARP staff members in Seattle. They are wonderful people. Dave's invitation and advice made me enjoy my research and I would also like to thank him for the reading material (books and preprints). We also had stimulating discussions on modelling methods.

Of course, I am grateful to my wife and my parents for their patience and love. Without them my stay in South Africa would have been a nightmare (literally). Thank you for the calls every night, those made me keep going and proud to have such a loving family.

Finally, I wish to thank the following: Peter Olofsson and Marek Kimmel (for their technical assistance on branching processes); Alantha Newman (for stimulating discussions); Levin Lab Tea (for the stimulating talks in ecology and evolutionary biology) and Fefferman Lab members (for all the good times we had together). I might have forgotten the people who were involved in the early stages of my studies, my apologies to all those.

Chapter 1

Introduction

1.1 Background

In this chapter, we furnish the reader with current facts on the impact of HIV (Human Immunodeficiency Virus)/AIDS (Acquired Immune Deficiency Syndrome) disease and HIV pathogenesis. We also give a little essay about the general situation in modelling viral genetics, important modelling work in HIV evolution, what has been achieved so far in the field of HIV modelling and highlight questions that remain unanswered.

The Joint United Nations Programme on HIV/AIDS (UNAIDS) and the World Health Organization (WHO) 2009 [143] estimated that by December 2008, nearly 34.4 million individuals were living with the disease, the virus killed 2 million people and 2.7 million individuals were infected in 2008. Again, sub-Saharan Africa is still leading on the number of people living with the disease (22.4 million) and the epidemic is still the leading cause of death (1.44 million deaths in 2008) in sub-Saharan Africa [133]. The epidemic's effects are multi-faceted, affecting not only an individual's health but also impacting life style, the structure of families and society. This disproportionate burden of the global pandemic threatens sub-Saharan Africa's economic and social fabric.

Currently, science has produced no magic bullet, there is still no cure and vaccine although recently there were reports of a vaccine with some efficacy [124] and a modest efficacy afforded by 1% Tenofovir vaginal gel [70]. Given the ongoing burden of the HIV pandemic, new proposals for controlling the epidemic now include circumcising men [7], giving a daily prophylactic pill to high risk groups [121], and testing and treating as many infected individuals as countries can afford to reduce transmission [50]. These, together with the traditional prevention methods such as abstinence, faithfulness, use of condoms and treatment, form a comprehensive prevention package.

Although significant progress has been made in reducing new infections in some contexts and in prolonging individual lives, there are still challenges. Mechanisms of HIV disease progression are still unclear and there is still no convincing explanation why there is a long and variable asymptomatic phase. Some infected individuals have died within one or two years of infection, while others are still asymptomatic after 15 years [48, 94, 110]. The rapid accumulation of mutations in HIV, the theme of this thesis, presents a great challenge to treatment and therapeutic development efforts. Understanding key evolutionary and ecological processes underlying successful viral lineages, the timing of key events in viral emergence is relevant to vaccine design and other control efforts.

1.2 HIV Pathogenesis

HIV is a complex virus that belongs to the lentivirus (because it causes disease slowly) genus of the retroviridae family [76], which 'reversely' transcribe their ribonucleic acid (RNA) genome to deoxyribonucleic acid (DNA). Other examples of retroviruses are simian immunodeficiency viruses (SIV) that mainly infect sooty mangabeys and

rhesus macaques [82]. The virus encodes major precursor polypeptides and several accessory genes which are indispensable to its life cycle. As a retrovirus, HIV does not have the required mechanisms to prevent errors during the transcription process, and therefore it is prone to generating a large number of copying errors.

After infection, HIV leads to primary infection where there is high viral load and massive dissemination of the virus throughout the body. Subsequently, infected individuals enter an asymptomatic phase that can last for years. The hallmark of HIV-1 infection is the depletion and incapacitation of immune cells central to human antimicrobial defenses. The depletion of the CD4+ T cells with no medical intervention may result in a situation where the viral population flourishes, leading to a state where the immune system becomes heavily compromised in fighting off opportunistic infections, known as the AIDS stage [133]. Initiation of effective antiretroviral therapy results in a decay in plasma HIV-1 RNA levels and a concurrent increase in the CD4+ T cell count [62].

Currently, the use of antiviral therapies in HIV-1 infected individuals has significantly impacted on HIV/AIDS morbidity and mortality and this has greatly improved the prognosis of people living with the virus [118]. Clinical and immunologic stability are the favourable outcomes of antiretroviral treatment. Management of HIV-1 infected patients has become increasingly complex due to expanding choices of drug regimens, emergence of resistance and drug tolerability problems. With the increase in numbers of patients receiving antiviral therapy, concerns about the long term management of patients and resources are being explored on multiple fronts, from training and logistics, to mathematical modelling. It is clear that a novel portfolio of HIV-1 prevention ideas is required.

1.3 The Evolution of HIV

The techniques of modern molecular biology have elucidated many aspects of HIV-1 infection, and some fine details about the immune responses mounted by the host to fight infection [8, 19, 90, 93, 103]. To complement this knowledge, mathematical techniques may be used to facilitate the analysis and interpretation of dynamic processes such as viral transmission, multiple viral evolutions within the host and the interplay between viral population growth and drugs/immunological responses. Mathematical techniques allow the description of biological systems in terms of hazards or rates of the processes. Mathematical modelling of the dynamics of HIV-1 infection within an individual has become a substantial area of research. Genuine advances have been modest in number, but large in impact.

Historically, there have been three primary approaches to thinking about in-vivo viral evolution: population genetics, ecological genetics, and quasispecies (for a more complete review see Wick et al.[150]). Population genetics began with R. A. Fisher in his 1930s book [38]. In his thinking he included rivals (members of the same species) but not enemies (members of other species which act as predators or parasites). It was a conscious decision to leave ecology to others. This fixes the demographic population size, imagining that there are a particular number of niches; population dynamics became simply reproduction followed by random sampling, with the 'selection coefficient', or fitness of each sub-species determining the probability an offspring gets a niche, i.e. competition so strong that if one subspecies population goes up by x, another must decline by x. Under these assumptions, Fisher proved his Fundamental Theorem of Natural Selection: average fitness in every population always increases.

E. B. Ford invented the field of ecological genetics [40]. He investigated the role

of natural selection in nature by studying British birds and moths; the moths varied the spots on their wings to avoid predation by birds. Ford considered that ecological genetics dealt with adjustments and adaptations of wild populations to their natural environment. Characteristic of ecological genetics is that organism traits are related to fitness, which affect an organism's fitness.

Quasispecies were introduced by Eigen and Schuster in the 1970s [33, 34]. A quasispecies is a group of related genotypes that exist due to high mutation rates. The quasi-species model is a description of evolution of certain self-replicating entities within the framework of physical chemistry. They discovered the high mutation rate in RNA viruses and modelled populations using ordinary differential equations (ODEs).

Deterministic approaches, mainly using ODEs, have been the core of most ecological models, including virus population dynamics. Simple ODEs have been solved to fit to sets of observational HIV-1 RNA viral load data [62, 120] in order to estimate the parameters of viral and cellular kinetics. Significant insights into HIV-1 dynamics such as rates of viral turnover and virus clearance rates have been derived from the basic model of HIV-1 dynamics [115, 120, 145]. However, the basic model is simplistic in that it only describes a single strain, whereas in reality there are many coexisting strains.

It has been widely adopted and modified to model plasma viral load in HIV-1 infected patients, for example see [13, 105, 108, 113, 144]. Some of these models have been used to estimate viral growth rates, basic reproductive numbers and post peak decay rates [87, 114, 128]. Other extended versions of the basic model have been used to explore the evolution of drug resistant mutants [42, 98, 111, 115, 126, 127, 136, 144]. Nowak et al. explored the evolutionary mechanism for HIV disease

progression [111] and the effect of treatment in reducing viral diversity [116]. In another study, Wahl and Nowak [144] used modelling to assess the conditions under which resistance dominates as a result of imperfect adherence. Wodarz and Lloyd [152] also investigated the role of immune responses in emergency of drug resistant mutants.

ODEs are both elegant and powerful, but there are instances when they miss relevant aspects, as will be illustrated in chapter 2. Monte Carlo simulations of within host HIV dynamics have also been used as alternatives to ordinary differential equations [61, 106, 131, 139, 142]. Wick and Self have used compartmental Markov models to explore whether cytotoxic T lymphocytes (CTLs) really control HIV infection [147, 148] and assess the influence that the timing of immune responses and drugs have on the rate of disease progression [146]. Recently, a stochastic spatial model based on the Monte Carlo approach was developed to study the dynamics of HIV infection, and it successfully reproduced the three-phase pattern observed in HIV infection [83].

Recent advances through coupling data analysis and mathematical modelling have allowed the identification and characterization of the nature of the transmitted virus [71]. Monte Carlo methods have been used to capture the stochasticity of early infection focusing on sequence evolution of the virus [79]. These models of random mutations have been used successfully to assess viral diversity as an indicator of the number of transmission events or founder strains [71, 79] and also to simulate the effects of mutations and fitness on the correlation between HIV quasispecies evolution and disease progression [80].

1.4 Structure of the Thesis

The overall objective of this thesis is to test and develop appropriate methods for modelling the effects of immune system pressure and therapeutic intervention on virus diversification. We then use these models to investigate the impact of acute infection dynamics on the accumulation of mutations, the effect of suboptimal therapy on the appearance of rare higher order mutations (those that do not typically exist at most points in time) and the persistence of these new genomes.

In chapter 2[1], we give a critical review of some of the modelling techniques that have been used to explore virus evolution. We also compare various indicators of viral diversity and show how they impact on the choice of mathematical techniques.

Chapter 3[2] explores how the dynamics of early infection affects the accumulation of mutations which lay the seeds for long term evolution of drug resistance and immune system evasion, using a branching process model in a deterministically varying environment. We relate applications of these ideas to pre-exposure prophylaxis (PrEP) and vaccine strategies.

We present a strain-differentiated hybrid deterministic-stochastic population dynamic type model of healthy and infected cells in chapter 4[3] to explore how the transient increase in a population of cells transcribed with a common mutation, which occurs in response to a short course of monotherapy and chronic treatment, has an impact on the risk of appearance of rarer, higher-order, therapy-defeating mutations.

In chapter 5[4],we analyze the full hybrid model. The objective is to explore

[1]Part of the content was presented as a poster at: DIMACS Capstone Workshop on Mathematical Modelling of Infectious Diseases in Africa (25-27 June 2007)

[2]Published in J. Theor. Biol. 2011; 279(1): 44-54

[3]Most of the content was published in Theor. Biol. Med. Model. 2008; 5: 25

[4]Manuscript in Preparation

how long specific viral variants persist in the population, if suboptimal treatment is stopped. Finally, in chapter 6, we take stock of what was achieved in the thesis and suggest direction for future work.

Chapter 2

Review of Modelling Techniques

Introduction

The thesis is about how to construct and apply appropriate mechanistic models of in-vivo viral replication. We now give a review of some of the modelling techniques that have been used for viral dynamics. At a high level, we distinguish deterministic models from stochastic models, and note that they can be formulated in either continuous or discrete time. In each case, the defining elements are state variables and dynamical rules, but we also pay attention to 'metrics' of viral diversity that can be computed from the model ingredients.

2.1 Continuous Time Models

A large variety of in-vivo HIV models are based on continuous time processes, as these are often analytically tractable (closed form solution or efficient numerical schemes). Examples of these models are in the form of ODEs, stochastic differential equations (SDEs) and partial differential equations (PDEs). Of these models, ODEs have been

at the core in modelling the complex set of interacting concepts that are relevant to the dynamical understanding of HIV evolution. In the setting of HIV, which replicates very fast, some mutations, such as known single base mutations, cannot be avoided. They are repeatedly generated even though they might be kinetically compromised. By contrast, in a given patient/environmental context, there may be rare mutations which are unlikely to occur during an infected individual's lifetime. ODE models are appropriate to investigate the evolution of common mutants and are not appropriate to model rare events. In the following section, we demonstrate that ODEs fail to capture correctly the dynamics of rare mutations. For example, mutants which will almost certainly not happen in a stochastic model are instantaneously generated as infinitesimal populations in an ODE model. In reality, a new rare mutant shows up in a single productively infected cell, while continuous models such as ODEs produce infinitesimal population sizes which immediately become a dynamical entity without a waiting time.

Modelling Rare Mutation Events

The rate of evolution of HIV in-vivo is probably greater than for any other persistent infection, for example, the mutation rate per nucleotide per round of replication is about 3×10^{-5} [92]. This is very high considering that for eukaryotes is closer to 10^{-10} [77]. The number of productively infected cells is around 10^8 in chronic infection; therefore, every mutation in HIV's genome which is about 10^4 nucleotides is made everyday [24, 55]. We are interested in the dynamics of quasispecies, therefore we mainly consider different types of infected cells which will be denoted by P_i, i.e. which distinguishes cells infected by strain i. These different cell types reproduce at

different rates. Right now, we present a basic model of virus dynamics [115, 120] with a single strain labeled P_1. The single strain ODE model is given by

$$\begin{aligned} \frac{dT(t)}{dt} &= S_{\mathrm{T}} - k_1 T(t) P_1(t) - \mu_{\mathrm{T}} T(t); \\ \frac{dP_1(t)}{dt} &= f k_1 P_1(t) T(t) - \mu_{\mathrm{P}} P_1(t), \end{aligned} \tag{2.1.1}$$

where S_{T} is the rate at which healthy or target cells T are generated, k_1 is the wild-type strain infectivity parameter, μ_{T} is the natural target cell death rate, μ_{P} is the rate at which infected cells are cleared, and f is the probability of error free transcription.

The model (2.1.1) does not explicitly include the virus population. The free virion decay rate is much larger than the decay rate of virus-producing cell populations. By standard analysis of the separation of fast and slow dynamics, one shows that to a good approximation, the free virus population is in a quasi equilibrium with the lower mortality cell population, according to the relation $V_1(t) = \alpha P_1(t)$, where the constant α contains virion production rates and mortality. Thus, the dynamics of a model with virions can be reproduced by system (2.1.1) unless one is asking questions about very short time scales, i.e. short compared to the mean lifetime of a virion, which we do not do. Incorporating virions in our model can help distinguish how certain drugs work, for example, reverse transcriptase inhibitors (RTIs) that block reverse transcription early in infection cycle and protease inhibitors (PIs) that block viral maturation at the end of the virus life cycle. To distinguish the dynamics of these drugs clinically requires high quality HIV RNA data that may be separated by hours which means frequent blood drawing from patients.

The ODE model has a disease free equilibrium given by

$$\left(T^0, P_1^0\right) = \left(\frac{S_{\mathrm{T}}}{\mu_{\mathrm{T}}}, 0\right) \tag{2.1.2}$$

and an infected equilibrium state given by

$$\left(T^*, P_1^*\right) = \left(\frac{\mu_{\mathrm{P}}}{fk_1}, \frac{\mu_{\mathrm{T}}}{k_1}(R_0 - 1)\right), \tag{2.1.3}$$

where R_0 is the basic reproductive number (which can be thought as the number of new infections caused by one infection in an extremely susceptible population, i.e. at the beginning of infection [4]) given by

$$R_0 = \frac{fS_{\mathrm{T}}k_1}{\mu_{\mathrm{P}}\mu_{\mathrm{T}}}.$$

Theorem 2.1.1. *If $R_0 > 1$, then the infected equilibrium state (equation 2.1.3) is locally asymptotically stable.*

Proof. We investigate local stability by evaluating the linearized system at the infected equilibrium state. This equilibrium state is locally asymptotically stable if and only if all the eigenvalues of the Jacobian matrix J have a strictly negative real part. We determine the eigenvalues by solving the characteristic equation of the Jacobian matrix J given by

$$J\left(T^*, P_1^*\right) = \begin{pmatrix} -\mu_{\mathrm{T}}R_0 & -\dfrac{\mu_{\mathrm{P}}}{f} \\ f\mu_{\mathrm{T}}(R_0 - 1) & 0 \end{pmatrix}. \tag{2.1.4}$$

The characteristic equation is given by

$$\lambda^2 + \mu_{\mathrm{T}}R_0\lambda + \mu_{\mathrm{P}}\mu_{\mathrm{T}}(R_0 - 1) = 0, \tag{2.1.5}$$

such that the two eigenvalues are given by

$$\lambda_{1,2} = \frac{-\mu_{\mathrm{T}}R_0 \pm \sqrt{(\mu_{\mathrm{T}}R_0)^2 - 4\mu_{\mathrm{P}}\mu_{\mathrm{T}}(R_0 - 1)}}{2}. \tag{2.1.6}$$

Using the Routh-Hurwith stability criterion [49] we conclude the existence of roots with negative real parts if and only if $R_0 > 1$. □

In the setting of HIV infection, some common variants are created quickly early after infection with a single founder strain. This model can be extended to accommodate a new variant that can emerge, say mutant P_2. The new model that describes the dynamics of two strains is given as:

$$\begin{aligned}
\frac{dT(t)}{dt} &= S_{\text{T}} - k_1 T(t) P_1(t) - k_2 T(t) P_2(t) - \mu_{\text{T}} T(t); \\
\frac{dP_1(t)}{dt} &= f k_1 P_1(t) T(t) + \epsilon k_2 P_2(t) T(t) - \mu_{\text{P}} P_1(t); \\
\frac{dP_2(t)}{dt} &= f k_2 P_2(t) T(t) + \epsilon k_1 P_1(t) T(t) - \mu_{\text{P}} P_2(t),
\end{aligned} \tag{2.1.7}$$

where ϵ is the mutation rate and k_2 is the new mutant strain infectivity parameter. In this model, the wild-type strain P_1 is the initially infecting strain and the mutant strain P_2 is a result of mutations from the wild-type strain. Similarly, the two-strain deterministic model has two steady states: the uninfected steady state and a unique infected steady state which is either physical (a positive number of infected cells) or unphysical (a negative number of infected cells) depending on the fitness parameters. The uninfected steady state is given by

$$\left(T^0, P_1^0, P_2^0\right) = \left(\frac{S_{\text{T}}}{\mu_{\text{T}}}, 0, 0\right). \tag{2.1.8}$$

The exact infected steady state is given by

$$\begin{aligned}
\bar{T} &= \frac{\mu_{\text{P}}\Big(f(k_1+k_2) - \sqrt{f^2(k_1+k_2)^2 - 4(f^2-\epsilon^2)k_1k_2}\Big)}{2(f^2-\epsilon^2)k_1k_2}; \\
\bar{P_1} &= \frac{\big(S_{\text{T}} - \mu_{\text{T}}\bar{T}\big)\big(\mu_{\text{P}} - f k_2 \bar{T}\big)}{k_1 \bar{T}\big(\mu_{\text{P}} - (f-\epsilon)k_2\bar{T}\big)}; \\
\bar{P_2} &= \frac{\epsilon k_1 \bar{P_1} \bar{T}}{\mu_{\text{P}} - f k_2 \bar{T}}.
\end{aligned} \tag{2.1.9}$$

For a high value of the mutation production rate $\epsilon k_1 P_1 T$, i.e. for very small intervals between individual mutation events, mutant infected cells are quickly generated, thus we can call P_2 a common mutant. This model is sensible to capture the dynamics of common mutants, where the appearance of a new variant is captured by the parameter ϵ and its growth is captured by parameter k_2. For small values of $\epsilon k_1 P_1 T$, in reality the mutant might never occur, thus we call it a rare mutant. Here, we need to check whether it makes sense to model the appearance of rare mutations as a deterministic process, as was done by some of the authors including [115, 116, 136].

Now, we consider P_2 as a fitter rare mutant which may arise when healthy and wild-type infected cells are at equilibrium (infected steady state, equation 2.1.3). As an approximation, we assume that this mutant population grows exponentially during the initial stages such that its dynamics are given by a linear ODE

$$\frac{dP_2(t)}{dt} = \mu_P(\gamma - 1)P_2(t) + \epsilon s_T \left(\frac{R_0 - 1}{R_0}\right), \tag{2.1.10}$$

where $\gamma = k_2/k_1 > 1$. We have also assumed that healthy and wild-type infected cell populations are not significantly perturbed from their initial values (i.e. from the infected steady state) over the time it takes to produce one cell of the fitter rare mutant. Solving the equation $P_2(t) = 1$ for t, we have the evolutionary time required to have one cell infected by an advantageous mutant strain in the population, i.e.

$$t_1 = \frac{1}{\mu_{\mathrm{P}}(\gamma - 1)} \ln\left(1 + \frac{\mu_{\mathrm{P}}(\gamma - 1)R_0}{\epsilon S_{\mathrm{T}}(R_0 - 1)}\right). \tag{2.1.11}$$

On the other hand, the stochastic mean waiting time before the appearance of a mutant is given by

$$\begin{aligned} < t_w > &= \left(\frac{1}{\epsilon k_1 P_1^* T^*}\right); \\ &= \frac{R_0}{\epsilon S_{\mathrm{T}}(R_0 - 1)}. \end{aligned} \tag{2.1.12}$$

We numerically integrate the evolution of wild-type and mutant strain infected cells using the fourth order Runge-Kutta scheme when:

1. there is no waiting time for different values of γ in figure 2.1 and
2. there is a mean waiting time of 186 days calculated from equation 2.1.12 using the chosen parameters in figure 2.2 and figure 2.3.

Figure 2.1 and Table 2.1 show that the evolutionary time depends on the mutant infectivity parameter and the mutation rate in the deterministic framework.

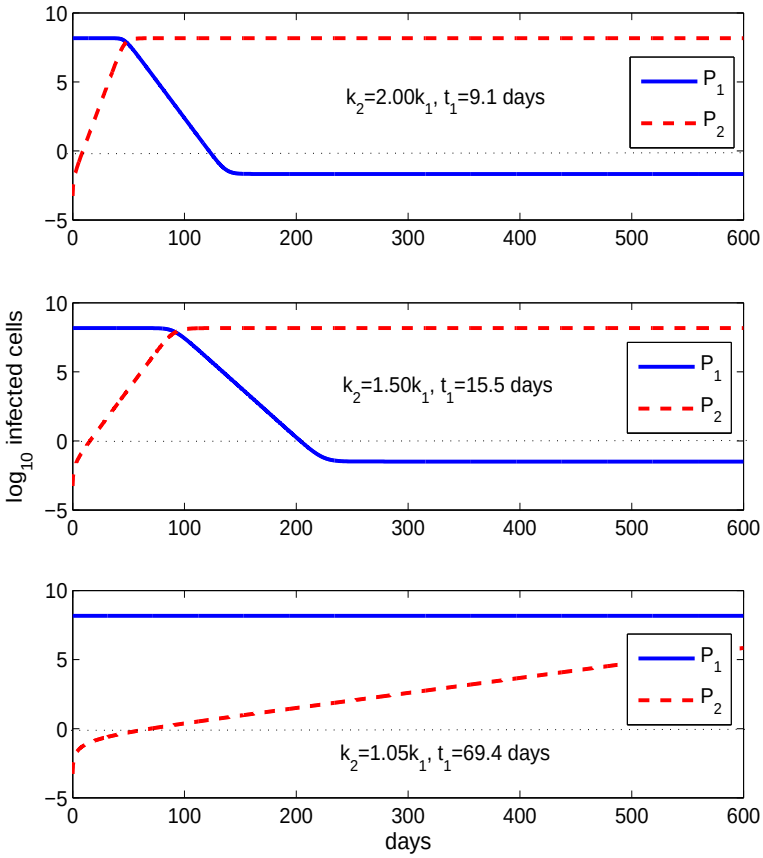

Figure 2.1: Growth of mutant strain with no waiting time. The other parameter values are $R_0 = 148$, $S_{\mathrm{T}} = 2 \times 10^8$, $\mu_{\mathrm{P}} = 0.5$, $k_1 = 2 \times 10^{-8}$ and $\epsilon = 2.7 \times 10^{-11}$. The initial values for the healthy T cells and the wild-type strain are given by equation 2.1.3 and that of the rare mutant is zero.

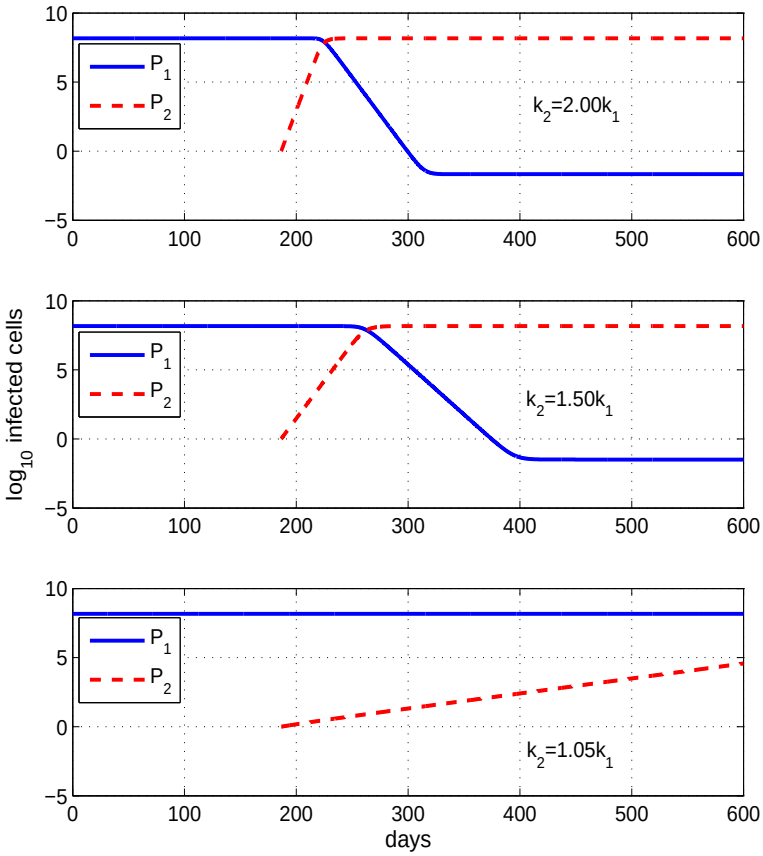

Figure 2.2: Growth of mutant strain including a mean waiting time of 186 days. The other parameter values are as in figure 2.1

We use equations 2.1.11 and 2.1.12 to generate values in Table 2.1.

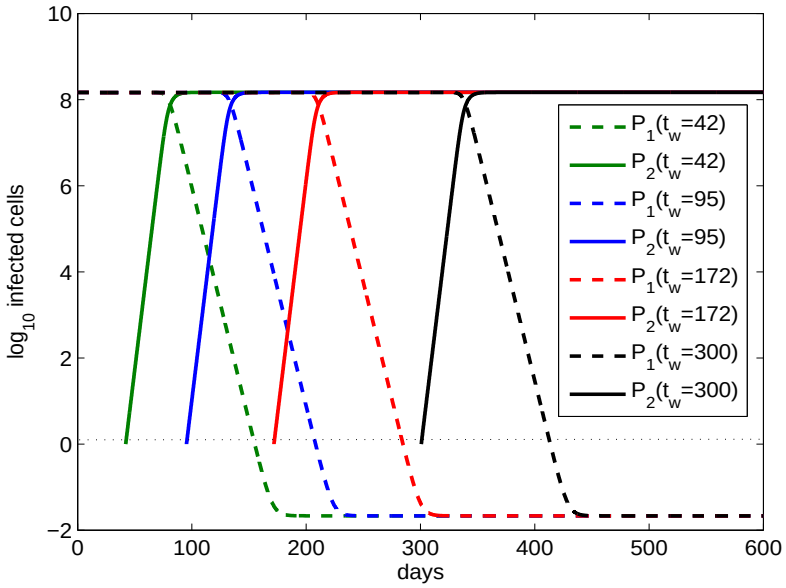

Figure 2.3: Growth of mutant strain including pseudo sampled waiting times. The times ($< t_w >$) chosen are 42, 95, 172 and 300 which are chosen so that there are spaced inversely proportional to the probability density. The other parameter values are as in figure 2.1 and $k_2 = 1.5k_1$.

The appearance of a rare mutation will almost certainly not happen in an individual's lifespan, for example numbers in brackets for $< t_w >$ in Table 2.1 as calculated from a stochastic model. In an ODE framework, there is an instantaneous creation of infinitesimal populations (from the mutation term) and the dynamic property (given by the infectivity parameter) of the strain will drive the growth such that there is a significant population size within days (see numbers in brackets for t_1 calculated from a deterministic model). In reality, the mean waiting time for the emergence of a mutant strain depends on the mutation rate and not on the selective advantage or disadvantage of the mutant.

In chapter 4, we use a combination of ODE and stochastic models to calculate the probability of appearance of rare mutations. We use concepts of survival analysis,

Table 2.1: Deterministic times (in days) to generate a single three-point mutant (t_1) and stochastic mean waiting times before the appearance of a mutant ($< t_w >$), for different values of R_0, $\gamma = k_2/k_1 > 1$ and $\epsilon = 2.7 \times 10^{-11}$. The figures in brackets are obtained when $\epsilon = 2.7 \times 10^{-14}$.

R_0	$< t_w >$	t_1		
		$\gamma = 2$	$\gamma = 1.5$	$\gamma = 1.05$
2	370 [370370]	10 [24]	18 [46]	93 [365]
10	206 [205760]	9 [23]	16 [43]	73 [342]
148	186 [186440]	9 [23]	16 [43]	69 [338]

i.e. we introduce mutations at random, as a state-dependent Poisson process. Within this framework, we use the conventional survival analysis to ask questions such as how long till a key event occurs or the probability that an event has not occurred. We then use a modified survival analysis to calculate the probability that the key event has not 'occurred recently'.

Furthermore, it is important not just for the rare mutant to appear in one productively infected cell, but for its lineage not to go extinct. However, the modified survival analysis framework does not allow us to investigate in a dynamically consistent way whether the new cell harboring the rare mutant will die before infecting other cells or before infecting enough other cells for the mutant to be fixed, i.e. the persistence of the new mutants. We run full simulations of the hybrid deterministic-stochastic model in chapter 5 to investigate persistence of new variants with a subcritical fitness. The new rare mutant has to compete with existing strains and its persistence depends on its characteristics such as viability and replication ability. Varying the new genome's replicative ability, we determine the period at which the new genome

lineage will be sustained in the face of competition from existing strains after the initial appearance of a single cell with a new genome.

2.2 Discrete Time Models

Mathematical biology is about modelling discrete populations, e.g. cells, usually changing over time. Continuous time models in the form of ODEs formally enforce that, in any time interval, actual population change equals the expected change of that population as it would be conceived in some stochastic model. While a deterministic model (formulated in either continuous or discrete time) predicts a single outcome for a given set of parameters, a stochastic model predicts a set of possible outcomes weighed by their likelihoods or probabilities. There are many types of deterministic and stochastic discrete models. Examples of stochastic discrete models include birth and death models, Markov models and branching processes. We compute important indicators of viral diversity using a branching process model of viral evolution.

The model folds in the notions of the mutation rate, reproductive ratio and generation time (implemented as discrete non-overlapping generations). The branching process model is as follows: one infected cell initiates the process. On replication, each cell produces a deterministic number of new cells (say R_0); the type of each new daughter cell may or may not be the same as that of the parent cell, i.e. infected cell populations evolve as a stochastic process with random choices for the type of offspring. This model assumes exponential viral growth with no selection pressure, no recombination and a constant mutation rate across sites and lineages. We consider two fundamentally similar approaches to calculate viral diversity properties. In the first

framework, we explicitly calculate diversity properties for each evolving individual species (simulation based computational approach - at every time point population sizes are updated). The second framework involves calculating statistical properties of ensembles (mean fields) using the theory of probability generating functions. Models of random mutations have been used successfully to assess viral diversity as an indicator of the number of transmission events or founder strains [71, 79].

Simulation Based Computational Approach

In this framework, proposed by Lee et al. [79], we consider infected cells carrying a genome of length N_B, i.e. a sequence of nucleotides A, T, C, and G. Mutations can occur in any of the N_B sites in the entire genome. At the first replication cycle, the R_0 daughter cells produced by the single infected cell will each differ from the infecting strain at exactly m positions with probability given by

$$\mathbb{P}(\text{mutations} = m) = \binom{N_B}{m} \eta^m \Big(1-\eta\Big)^{N_B - m},$$

where η is a per base mutation rate. The authors [79] showed that the total number of mutations after n replication cycles (assuming that no back mutations), will follow the probability distribution

$$\mathbb{P}(\text{mutations} = m | gen = n) = \binom{nN_B}{m} \eta^m \Big(1-\eta\Big)^{nN_B - m},$$

a convolution of n binomial distributions which is also a binomial distribution. The Hamming distance (HD_0) is defined as the number of base differences from the founder strain, assumed to coincide with the number of mutations and therefore it follows the same distribution:

$$\mathbb{P}(HD_0 = d | gen = n) = \binom{nN_B}{d} \eta^d \Big(1-\eta\Big)^{nN_B - d}. \tag{2.2.1}$$

In addition to comparing any given sequence to its founder, all sequence pairs in a sample can be used to calculate their relative Hamming distance, where the distribution of the intersequence Hamming distance (HD_I) distribution is

$$\mathbb{P}(HD_I = d|gen = n) = \binom{2nN_B}{d}\eta^d\Big(1-\eta\Big)^{2nN_B-d}. \tag{2.2.2}$$

Based on the calculated Hamming distance from the founder strain and the intersequence Hamming distance between all possible sequence pairs, the authors defined the following measures of diversity at any generation n :

1. Divergence as the average Hamming distance per base from the founder strain and using equation 2.2.1, it can be estimated as the mean of the binomial distribution divided by the number of bases, i.e. $n\eta$.

2. Diversity as the average intersequence Hamming distance per base between sequence pairs and by using equation 2.2.2 is given by $2n\eta$.

3. Sequence identity as the proportion of sequences identical to the founder strain sequence, using equation 2.2.1 and setting d to zero, we have $(1-\eta)^{nN_B}$.

4. Expected maximum Hamming distance, see [79]

All these four measures of diversity depend only on the number of generations and the authors [79] argued that the number of transcriptional events that have occurred along a lineage are important in determining viral diversity and not the number of cells infected at each generation. Monte Carlo based simulations can be used to calculate the defined indicators of viral diversity.

The simulation starts at generation zero with one infected cell with a single HIV-1 sequence N_B bases long. The founder sequence is generated randomly with base

frequencies for [A C G T] given by [0.373 0.193 0.241 0.192]. At every generation each infected cell infects R_0 other cells synchronously. Mutations occur during infection and the occurrence of the base substitutions are chosen randomly from N_B bases. The probability that base i is replaced by base j is given by a 4×4 transition matrix deduced from a simple parametric model of nucleotide substitution by Jukes and Cantor [69], i.e. all nucleotides are equally likely to undergo substitution and given that a substitution has taken place, any other nucleotide is equally likely to be a replacing nucleotide (uniform replacement). Lee et al. [79] used the maximum likelihood General Time Reversible (GTR) model of substitutions. At each generation exactly N_s sequences are sampled with replacement and the Hamming distance distribution is constructed. Multiple runs are performed with Hamming distance frequencies computed at each generation step averaged over all iterations giving the mean field measures of diversity given by the closed form equations.

We assume a genome with $N_B = 2600$ bases, a base substitution rate of $\eta = 2.16 \times 10^{-5}$ per base per replication [79] and R_0 of 2. Each run consists of 1000 replicates with the maximum number of generations given by 50. At each generation, $N_s = 30$ nucleotide sequences were chosen randomly from the population and are used to calculate the metrics. When the total population exceeds 10^4, we allow 10^4 cells (selected at random from a uniform distribution) to multiply and sample another 10^4 from $10^4 R_0$ new cells to contribute to the next generation. The simulated results, showing the dependance of the metrics of diversity on the number of generations, are given in figure 2.4 (the simulations match the formulas). The results still coincide with the ones obtained by Lee et al. [79], when they assumed a GTR model of substitutions and a reproductive ratio (R_0) of 6.

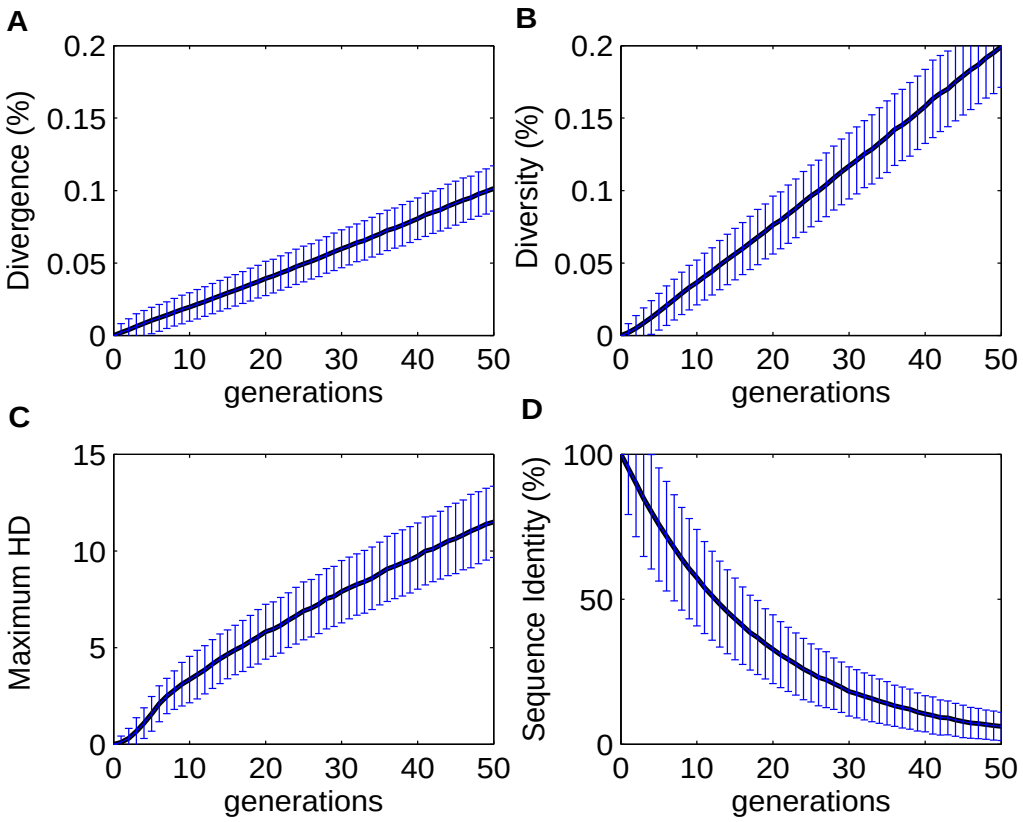

Figure 2.4: Monte Carlo simulations of the synchronous infection model. Dynamics of (A) divergence - average hamming distance per base from the founder strain, (B) diversity - average inter sequence hamming distance per base between sequence pairs, (C) maximum hamming distance and (D) percentage identity - proportion of sequences identical to the founder strain, for sequences of length 2600, and from 1000 simulations where n is the generation. The vertical bars are the standard errors.

A Critical Review of The Number of Transmission Events

To expand the analysis of the synchronous model with full viral genome, we allow multiple infections by distinct types to initiate the infection process. For simplicity, we assume two very distinct founder sequences with different fitness values (i.e. different reproductive ratios). The reproductive ratios of the two founder strains are R_{01} and

R_{02} such that $R_{02} = (1 - f_2)R_{01}$, where f_2 is the growth disadvantage of the second founder strain. We allow the two founder strains to evolve as described previously (Monte Carlo based simulation) and at each generation n, we draw a sample of N_s sequences with a probability of picking a descendant of founder strain i given by

$$\frac{\left(R_{0i}\right)^n}{\left(R_{01}\right)^n + \left(R_{02}\right)^n}, \qquad i = 1.2. \tag{2.2.3}$$

and construct the intersequence Hamming distance distribution. In the single scenario we consider here, we assume that infection starts with two founder strains with different reproductive rates $R_{01} = 4$ and $R_{02} = 2$. At the time of infection, the Hamming distance between the two sequences is fixed at 50. At certain time points, within a period of 20 generation, we sample $N_s = 30$ sequences and plot the histograms of the observed intersequence Hamming distance frequencies, see figure 2.5 and figure 2.6.

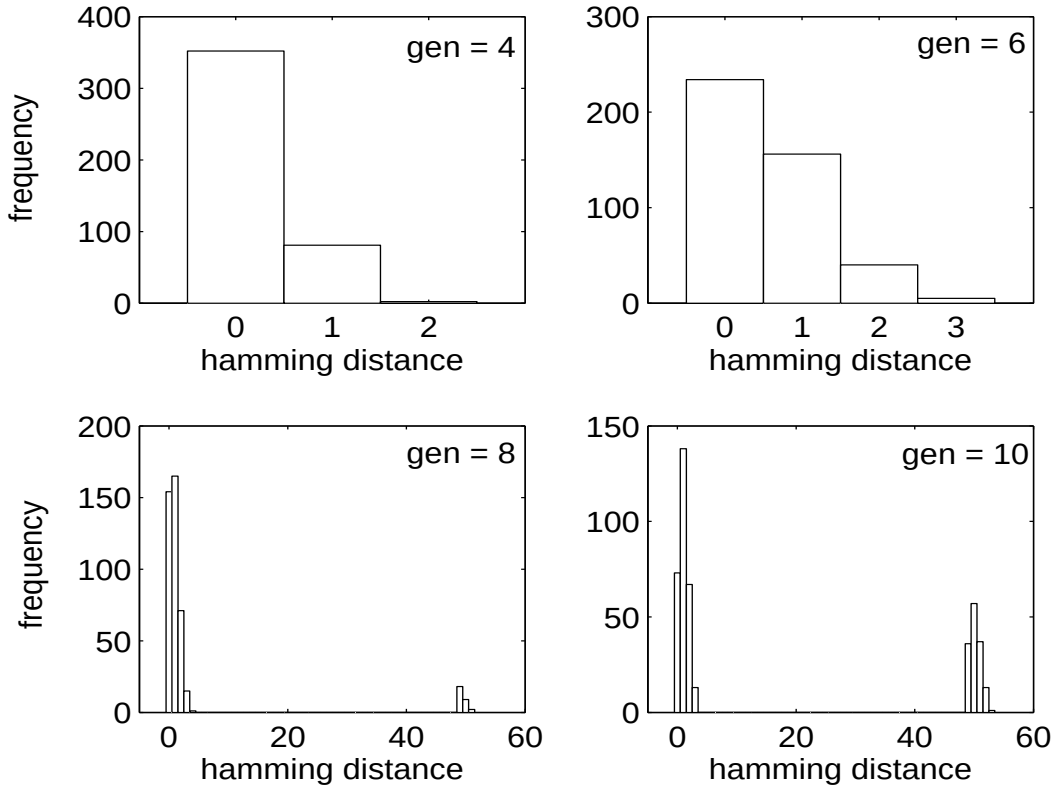

Figure 2.5: Observed intersequence hamming distance frequencies. At the specified generation we randomly draw 30 sequences (from a uniform distribution) and compute the intersequence hamming distance, continued in figure 2.6.

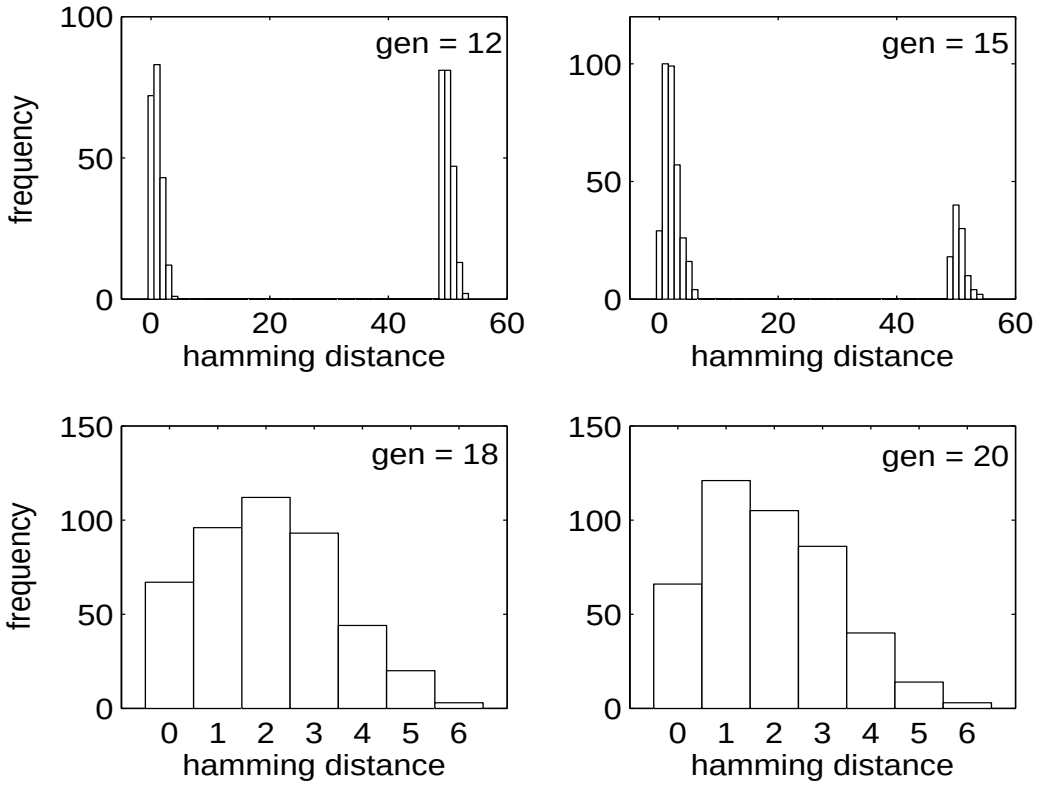

Figure 2.6: Continuation of figure 2.5 of the observed intersequence hamming distance frequencies.

Sampling at generation 18 (figure 2.6 shows the distribution of the intersequence Hamming distance), we get sequences with the maximum Hamming distance of 6 which is consistent with that of an infection started by a single founder strain (see figure 2.4 where the maximum Hamming distance at generation 18 is around 6). This is expected because at generation 18, the probability of selecting the fitter strain (strain with an R_0 of 4) is almost 1 and that of selecting a less fitter strain is nearly 0. In our simple model, we have only incorporated differential fitness and the model is silent about the origin of this fitness difference. Effects of selection pressure due to the

immune system can greatly influence the population frequencies such that random samples of genomes from populations seeded with multiple genotypes may resemble those of single-genome infections. Due to innate differential fitness and selection by immune system pressure, wrong deductions about the number of transmission events may be made. In this simple example, analysis of the extent of viral diversity, some time after infection by multiple founder strains, will resemble those of individuals infected by a single strain because the fittest strain will be the dominant species.

Probability Generating Function Approach

In this framework, instead of considering the entire genome (all N_B bases), we choose a particular segment of the genome. For illustration purposes, we consider a single-point mutation that occurs in a particular position in the viral genome, i.e. we consider an artificial viral genome with a single site, changes at the other remaining sites are deemed irrelevant. In this scenario, we only have two types of infected cells of relevance, the initially infecting strain (wild type) and a population of cells infected with a virus carrying a sequence with a base change at the site of interest, i.e. the single point mutant. We extend the size of the genome segment to three bases in chapter 3. Branching processes have a recursive structure that makes it amenable to analysis by generating functions [59]. Definitions and properties of generating functions are given in Appendix A.

The population of the virus is modelled as a two-type process where the types are 0 (wild-type infected cells) and 1 (mutant infected cells). The set of types is $T = \{0, 1\}$. Independently of each other, each wild-type infected cell gives birth at a rate η to a mutant infected cell and at rate $(1 - \eta)$ to a wild-type infected cell. Similarly, a mutant infected cell gives birth at a rate η to a wild-type infected cell

and at a rate $(1-\eta)$ to a mutant infected cell. In our notation, superscripts will denote the generation number and subscripts the type of the cell (0 for wild-type and 1 for the mutant). The transition matrix is given by

$$\begin{array}{c} \\ P_0 \\ P_1 \end{array} \begin{array}{c} \begin{array}{cc} P_0 & P_1 \end{array} \\ \begin{pmatrix} 1-\eta & \eta \\ \eta & 1-\eta \end{pmatrix} \end{array}, \tag{2.2.4}$$

where the number of wild-type and single point mutant infected cells are given by P_0 and P_1, respectively. The offspring distribution for the wild-type and mutant infected cells are: $p_0(k_0,k_1) \sim \text{Bin}(R_0, 1-\eta)$ and $p_1(k_0,k_1) \sim \text{Bin}(R_0,\eta)$, respectively. Here $p_0(k_0,k_1)$ is the probability that the wild-type cell will give birth to k_0 wild-type cells with probability $1-\eta$ and k_1 mutant cells with probability η, assuming that at death each cell gives birth to R_0 cells (i.e. a binomial distribution). Using, equation A.0.7 (Appendix A), we can derive the wild-type infected cell offspring probability generating function (pgf) as:

$$\begin{aligned} g_0(s_0,s_1) &= \sum_{k_0=0}^{\infty}\sum_{k_1=0}^{\infty} p_0(k_0,k_1) s_0^{k_0} s_1^{k_1}; \\ &= \sum_{k_0=0}^{\infty}\sum_{k_1=0}^{\infty} \binom{R_0}{k_0} (1-\eta)^{k_0}\eta^{k_1} s_0^{k_0} s_1^{k_1}; \\ &= \sum_{k_0=0}^{\infty} \binom{R_0}{k_0} \Big((1-\eta)s_0\Big)^{k_0} \Big(\eta s_1\Big)^{(R_0-k_0)}, \qquad (\text{where } k_1 = R_0 - k_0); \\ &= \Big((1-\eta)s_0 + \eta s_1\Big)^{R_0}, \end{aligned} \tag{2.2.5}$$

where at the last step we have used the binomial theorem. Similarly, the probability generating function for mutant infected cells can be shown to be

$$g_1(s_0,s_1) = \Big(\eta s_1 + (1-\eta)s_1\Big)^{R_0}. \tag{2.2.6}$$

Assuming that the population is started from a single wild-type infected cell, i.e. the total population initial conditions $\{P_0(0), P_1(0)\} = \{1, 0\}$, we have

$$\begin{aligned} G_0^n(s_0, s_1) &= g_0\Big(G_0^{n-1}(s_0, s_1), G_1^{n-1}(s_0, s_1)\Big); \\ &= \Big((1-\eta)G_0^{n-1}(s_0, s_1) + \eta G_1^{n-1}(s_0, s_1)\Big)^{R_0} \end{aligned} \tag{2.2.7}$$

and

$$\begin{aligned} G_1^n(s_0, s_1) &= g_1\Big(G_0^{n-1}(s_0, s_1), G_1^{n-1}(s_0, s_1)\Big); \\ &= \Big(\eta G_0^{n-1}(s_0, s_1) + (1-\eta)G_1^{n-1}(s_0, s_1)\Big)^{R_0}, \end{aligned} \tag{2.2.8}$$

assuming that each infected cell gives rise to exactly R_0 new cells of generally all types at generation n, with initial conditions $G_i^0(s_0, s_1) = s_i$ for $i = 0, 1$. Here

$$G_0^n(s_0, s_1) = \mathbb{E}\Big(s_0^{P_0(n)} s_1^{P_1(n)} \Big| P_0(0) = 1, P_1(0) = 0\Big)$$

is the probability generating function of the population started by a single wild-type infected cell and

$$G_1^n(s_0, s_1) = \mathbb{E}\Big(s_0^{P_0(n)} s_1^{P_1(n)} \Big| P_0(0) = 0, P_1(0) = 1\Big)$$

is the probability generating function of the population started by a single mutant infected cell, where $n \geq 0$, $s_0, s_1 \in [0, 1]$, $P_0(n)$ is the number of wild-type infected cells and $P_1(n)$ the number of mutant infected cells at generation n. We can calculate the following indicators of viral diversity in this framework:

1. Probability that a single mutant has never occurred. To calculate this probability, we use the following trick: Compute $G_0^n(1, 0)$ in the model with type transition matrix given in equation 3.2.1 but with state 1 (mutant) made an

absorbing state, i.e.

$$\begin{array}{c} \\ P_0 \\ P_1 \end{array} \begin{array}{c} \begin{array}{cc} P_0 & P_1 \end{array} \\ \begin{pmatrix} 1-\eta & \eta \\ 0 & 1 \end{pmatrix} \end{array}, \tag{2.2.9}$$

where the last row of the matrix is reset to (0 1). The modified process will go to state 1 for the first time exactly as the process would, but will stay there. Denoting $S_0(n) = G_0^n(1,0)$ and also $S_1(n) = G_1^n(1,0)$, we have the following recursive equations

$$\begin{aligned} S_0(n) &= \Big((1-\eta)S_0(n-1)\Big)^{R_0}; \\ S_1(n) &= \Big(S_1(n-1)\Big)^{R_0}, \end{aligned} \tag{2.2.10}$$

with initial conditions $S_0(0) = 1$ and $S_1(0) = 0$. This implies that $S_1(n) \equiv 0$, such that the probability of the event in question (mutant has never occurred) is given by

$$\begin{aligned} S_0(n) &= \Big(1-\eta\Big)^{\sum_{i=1}^{n} R_0^i}; \\ &= \Big(1-\eta\Big)^{\frac{R_0}{R_0-1}\Big(R_0^n-1\Big)}. \end{aligned} \tag{2.2.11}$$

2. A related question of the mean time to the occurrence of a particular single point mutant is given by

$$\begin{aligned} \mathbb{E}(W_T) &= \sum_{n=0}^{\infty} S_0(n); \\ &= \sum_{n=0}^{\infty} \Big(1-\eta\Big)^{\frac{R_0}{R_0-1}\Big(R_0^n-1\Big)}. \end{aligned} \tag{2.2.12}$$

The median time to the appearance of a particular single point mutant is given by solving the equation $S_0(n) = 0.5$ for n. Thus the median time is

$$n_m = \frac{1}{\ln\, R_0} \ln\left(1 - \frac{(R_0-1)\,\ln\, 2}{R_0\,\ln\,(1-\eta)}\right). \tag{2.2.13}$$

3. The probability that a mutant infected cell is not currently present in the population. This metric is precisely given by $\mathcal{P}_0(n) = G_0^n(1,0)$ which can be obtained from the equations

$$\begin{aligned} \mathcal{P}_0(n) &= \Big((1-\eta)\mathcal{P}_0(n-1) + \eta\mathcal{P}_1(n-1)\Big)^{R_0}; \\ \mathcal{P}_1(n) &= \Big(\eta\mathcal{P}_0(n-1) + (1-\eta)\mathcal{P}_1(n-1)\Big)^{R_0}, \end{aligned} \tag{2.2.14}$$

with initial conditions $\mathcal{P}_0(0) = 1$ and $\mathcal{P}_1(0) = 0$. This system of equations can be easily solved numerically.

4. The expected number of infected cells present at generation n. For illustration purposes, we consider the simplest case when $R_0 = 2$. Denoting the matrix of expected cell counts $M(n) = \Big(M_{ij}(n)\Big)$,

$$\begin{aligned} M_{ij}(n) &= \mathbb{E}\Big(P_j(n)\Big|P_k(0) = \delta_{ik}, k = 0,1\Big); \\ &= \frac{\partial}{\partial s_j} G_i^n(s_0,s_1)\Big|_{s_0=s_1=1}, \end{aligned} \tag{2.2.15}$$

the expected number of type j offspring of a single type i cell in generation n and δ_{ik} is the Kronecker delta. The expected total number of cells present at a particular time n is

$$\begin{aligned} P_T(n) &= \mathbb{E}\Big(P_0(n) + P_1(n)\Big|P_0(0) = 1, P_1(0) = 0\Big); \\ &= \Big(\frac{\partial}{\partial s_0} + \frac{\partial}{\partial s_1}\Big) G_0^n(s_0,s_1)\Big|_{s_0=s_1=1} \end{aligned} \tag{2.2.16}$$

The expected number of mutant infected cells at a particular time is

$$\begin{aligned} m(n) &= \mathbb{E}\Big(P_1(n)\Big|P_0(0) = 1, P_1(0) = 0\Big); \\ &= \frac{\partial}{\partial s_1} G_0^n(s_0,s_1)\Big|_{s_0=s_1=1} \end{aligned} \tag{2.2.17}$$

Differentiating the pgfs of the process, we obtain

$$\begin{aligned} M(n) &= 2\begin{pmatrix} (1-\eta)\frac{\partial G_0^{n-1}(1,1)}{\partial s_0} & \eta\frac{\partial G_1^{n-1}(1,1)}{\partial s_1} \\ \eta\frac{\partial G_0^{n-1}(1,1)}{\partial s_0} & (1-\eta)\frac{\partial G_1^{n-1}(1,1)}{\partial s_1} \end{pmatrix}; \\ &= 2\begin{pmatrix} 1-\eta & \eta \\ \eta & 1-\eta \end{pmatrix}\begin{pmatrix} \frac{\partial G_0^{n-1}(1,1)}{\partial s_0} & 0 \\ 0 & \frac{\partial G_1^{n-1}(1,1)}{\partial s_1} \end{pmatrix}; \\ &= \mu M(n-1), \qquad n = 1, 2, \cdots; \\ &= \mu^n, \end{aligned} \tag{2.2.18}$$

where μ is the expected offspring matrix

$$\mu = 2\begin{pmatrix} 1-\eta & \eta \\ \eta & 1-\eta \end{pmatrix}, \tag{2.2.19}$$

and $M(0) = I$ is the identity matrix derived from the initial conditions:

$$\begin{aligned} \mathbb{E}\Big(P_0(0)\Big|P_i(0) = \delta_{0i}\Big) &= 1, \qquad \mathbb{E}\Big(P_1(0)\Big|P_i(0) = \delta_{1i}\Big) = 1; \\ \mathbb{E}\Big(P_0(0)\Big|P_i(0) = \delta_{1i}\Big) &= 0, \qquad \mathbb{E}\Big(P_1(0)\Big|P_i(0) = \delta_{0i}\Big) = 0. \end{aligned}$$

Matrix μ is diagonalizable if there is a matrix, say V, such that $V^{-1}\mu V = D$ is a diagonal matrix. Then, as the matrix product is associative

$$\mu^n = VD^nV^{-1}. \tag{2.2.20}$$

The two eigenvalues of the matrix μ are 2 and $2(1-2\eta)$ and the matrix of the corresponding eigenvectors is given by

$$V = \begin{pmatrix} 1 & -1 \\ 1 & 1 \end{pmatrix} \tag{2.2.21}$$

and its inverse given by

$$V^{-1} = \frac{1}{2}\begin{pmatrix} 1 & 1 \\ -1 & 1 \end{pmatrix}, \tag{2.2.22}$$

such that

$$\begin{aligned} \mu^n &= \begin{pmatrix} 1 & -1 \\ 1 & 1 \end{pmatrix}\begin{pmatrix} 2^n & 0 \\ 0 & (2(1-2\eta))^n \end{pmatrix}\begin{pmatrix} \frac{1}{2} & \frac{1}{2} \\ -\frac{1}{2} & \frac{1}{2} \end{pmatrix} \\ &= \begin{pmatrix} 2^{n-1} + 2^{n-1}(1-2\eta)^n & 2^{n-1} - 2^{n-1}(1-2\eta)^n \\ 2^{n-1} - 2^{n-1}(1-2\eta)^n & 2^{n-1} + 2^{n-1}(1-2\eta)^n \end{pmatrix}. \end{aligned} \tag{2.2.23}$$

The expected total number of infected cells is given by

$$P_T(n) = 2^n,$$

the expected number of mutant cells at generation n is

$$m(n) = \frac{2^n}{2}\Big(1 - (1-2\eta)^n\Big),$$

and the expected number of wild-type infected cells at generation n is

$$w(n) = 2^{n-1} + 2^{n-1}(1-2\eta)^n,$$

for $n = 0, 1, 2, \cdots$. Numerical simulations are carried out to compare to the derived formulas and results are shown in figure 2.7. The two solutions (probability generating function framework and stochastic simulations) are in perfect agreement.

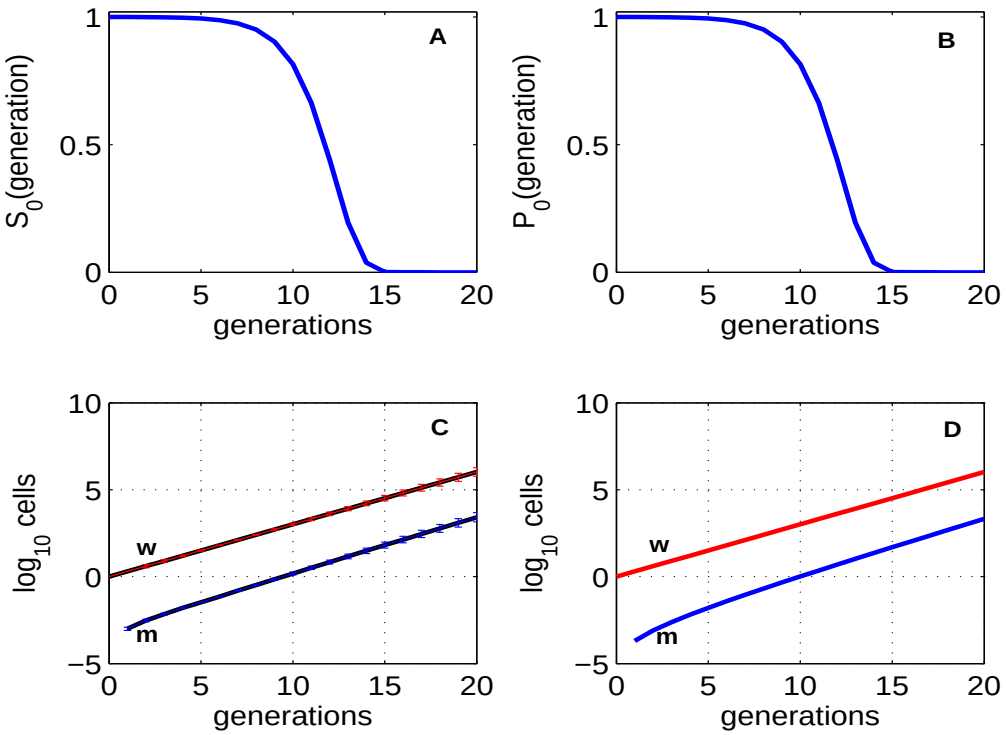

Figure 2.7: The probability that the mutant has never occurred (A) and (B) the probability that the mutant is not currently present in the population. (C) Average cell counts (wild-type (w) and mutant (m)) of 1000 runs of the branching process, started by a single wild-type infected cell (with 95% confidence intervals) and (D) the expected cell counts given by the formulas for $R_0 = 2$, mutation rate $\eta = 10^{-4}$. The simulations and the formulas give the same result.

In general, if each infected cell produces R_0 cells at the time of death, the mean offspring matrix is

$$\mu = R_0 \begin{pmatrix} 1-\eta & \eta \\ \eta & 1-\eta \end{pmatrix}, \tag{2.2.24}$$

such that the two eigenvalues are given by R_0 and $R_0(1-2\eta)$. Similarly, the

expected number of infected cells at every generation is given by the matrix

$$\mu^n = \begin{pmatrix} \frac{1}{2}R_0^n + \frac{1}{2}(R_0(1-2\eta))^n & \frac{1}{2}R_0^n - \frac{1}{2}(R_0(1-2\eta))^n \\ \\ \frac{1}{2}R_0^n - \frac{1}{2}(R_0(1-2\eta))^n & \frac{1}{2}R_0^n + \frac{1}{2}(R_0(1-2\eta))^n \end{pmatrix}. \tag{2.2.25}$$

The expected total number of infected cells is given by

$$P_T(n) \;=\; R_0^n, \tag{2.2.26}$$

the expected number of mutant cells at generation n is

$$m(n) \;=\; \frac{R_0^n}{2}\Big(1-(1-2\eta)^n\Big), \tag{2.2.27}$$

and the expected number of wild-type infected cells at generation n is

$$w(n) \;=\; \frac{R_0^n}{2}\Big(1+(1-2\eta)^n\Big), \tag{2.2.28}$$

for $n = 0, 1, 2, \cdots$.

2.3 Viral Diversity Measures

In order to assess aspects such as the number of transmission events and resistance evolution in HIV infections, various diversity indicators can be clinically measured. Different questions require different diversity measures. Diversity measures are important and they can act as signals of epidemiological and clinical conditions. Among these various indicators some may be very informative especially if a clinical condition variation is a function of a metric indicator, e.g. appearance of particular mutations (metric) can result in drug failure (clinical condition). We compare the different

metrics that can be computed using different tools and suggest those that might be of clinical or epidemiological significance, i.e. those metrics that can be related to prognosis.

From the two methodologies used to compute diversity outlined in the previous sections, i.e. tracking individuals in the population (sequence evolution) and the use of probability generating functions, a variety of diversity measures can be calculated. Computing viral diversity indicators for each individual cell, diversity metrics such as hamming distance distributions, average diversity, average divergence and sequence identity do not depend on the virus reproductive rate, but depend on time only. Asking questions about particular mutants in the probability generating function framework, we can calculate diversity metrics such as the probability that a particular mutant has never occurred or the probability of its non-existence in the population. These diversity indicators which are readily calculated in the probability generating function framework depend on both time and viral replication rate. Figure 2.8 shows how different metrics depend on time and the number of new infected cells.

Instead of asking questions about probabilities of particular events or Hamming distance distributions, alternatively we can ask questions about the mean and median times to the occurrence of particular mutants in both paradigms. We have already demonstrated how the mean and median waiting times are calculated in the probability generating function framework and now we use the full viral genome evolution model (i.e. Monte Carlo Simulations only) to calculate the mean and median times to the appearance of a particular single point mutation and compare these to the closed form solutions obtained in the probability generating function framework.

Our numerical scheme is as follows: we assume that the mutation probability per

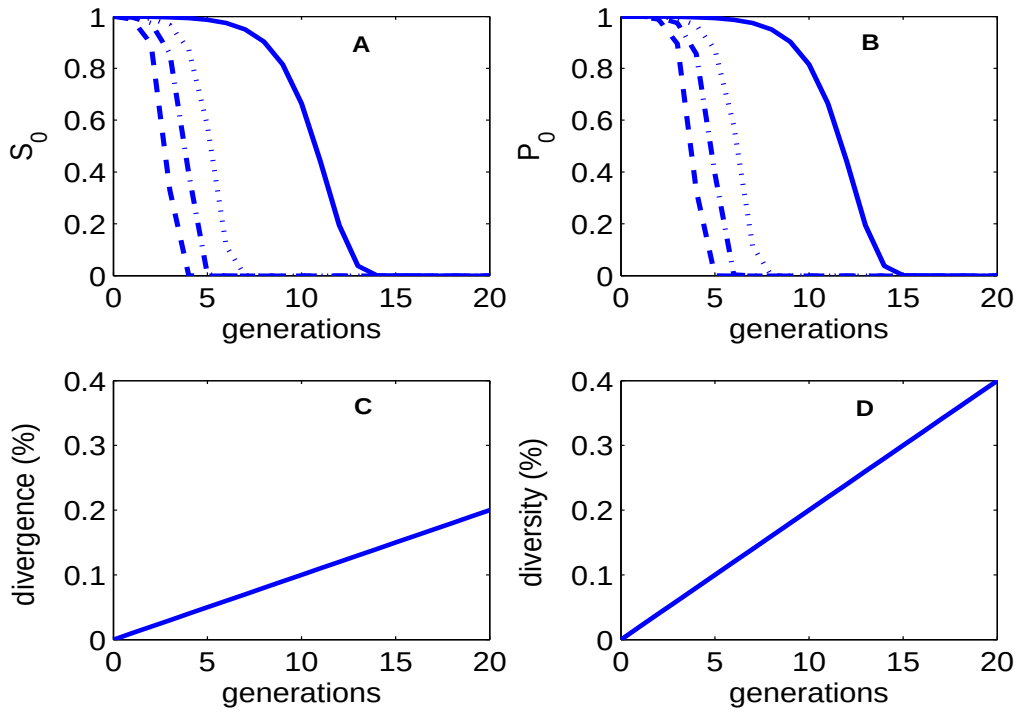

Figure 2.8: The dependence of diversity metrics on time and virus replication rate. The probability that a particular single point mutant A: has never occurred and B: is currently absent for varying virus replication rates., i.e. R_0 decreases from left to right ($R_0 = 10$ - dashed line, $R_0 = 6$ - dashed and dotted line, $R_0 = 4$ - dotted line and $R_0 = 2$ - continuous line). C: Average divergence, $n\eta$. D: Average diversity, $2n\eta$, where n is the generation number.

base is $\eta = 10^{-4}$ and sequences are of length $N_B = 175$. We generate the founder sequence with weights [A C G T] given by [0.373 0.193 0.241 0.192], respectively. Our substitution model is the Jukes and Cantor model [69]. We also assume that the relevant single point mutation occurs when a base at a specific position X changes to a particular base, for example, say C is the current base at X and the relevant mutation occurs when base C changes to base G at position X. This can be achieved straight away or through intermediate bases, A or/and T. The substitution rate is

modified such that the probability that sequence i with base C at position X changes to sequence j with base G at position X is given by $\mathbb{P}(i \to j) = \frac{1}{3}\eta$ (the new mutation rate in the closed form equation). We also assume that any changes at other remaining sites other than that at site X in the sequence are regarded as not important, and hence there is no differential fitness among infected cells carrying these sequences.

We start the simulation with one wild-type cell and when total population exceeds 10^6, we allow 10^6 cells (selected at random from a uniform distribution) to multiply and sample another 10^6 from $10^6 R_0$ new cells to contribute to the next generation. For each value of R_0, we run the model 1000 times and calculate the mean and median times. The dependence of the mean and median times to appearance of a particular single point mutant on replication rate is shown in Table 2.2 and figure 2.9. The table and figure made counting only those simulations where the mutant appeared in the population.

Table 2.2: Mean and median generations to the appearance of a particular single point mutant calculated from the closed form probability generating function equations (cf) (i.e. equations 2.2.12 and 2.2.13, respectively) and Monte Carlo simulations of the synchronous model (sim). SE is the standard error that will give 95% confidence intervals.

R_0	2	3	4	5	6	7	8	9	10
median (cf)	13.34	8.68	6.96	6.04	5.45	5.03	4.72	4.47	4.27
median (sim)	14	9	7	7	6	6	5	5	5
mean (cf)	13.54	8.99	7.31	6.41	5.83	5.43	5.12	4.86	4.67
mean (sim)	13.43	9.04	7.31	6.42	5.84	5.44	5.16	4.89	4.66
SE	0.11	0.07	0.06	0.05	0.05	0.04	0.04	0.04	0.04

Using the sequence evolution modelling framework to calculate calculate different indicators of diversity, we observe that different metrics behave differently. In this case mean and median times to the appearance of particular mutations depend on both the

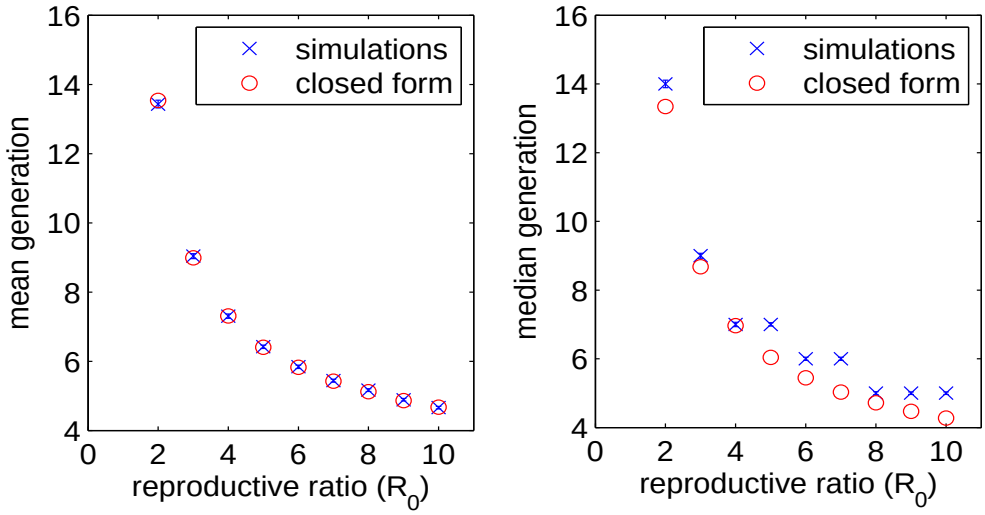

Figure 2.9: Mean and median generations to the occurrence of a single point mutation as given by the closed form solutions of the probability generating functions (i.e. equations 2.2.12 and 2.2.13, respectively) and Monte Carlo simulations of the full viral genome model, including 95% confidence intervals.

number of generations and the number of infected cells at each generation (whereas Hamming distance distributions depend only on the number of transcriptional events). For these measures (mean and median times to the occurrence of particular genomes), the probability generating function technique and the Monte carlo simulations of the full viral genome framework coincide. We conclude that choosing measures of diversity to compute is very important as different metrics behave differently. Perhaps the presence or absence of a particular variant (especially therapy defeating variants) is prognostic. It is important to choose measures that correlate to the probable outcome. Experiments can be performed to test whether there are correlations of clinical outcomes and diversity measures.

2.4 Conclusion

We have demonstrated that deterministic models are appropriate to investigate evolution of common mutants. In environments where rare higher order mutations may appear, deterministic models cannot explain appropriately the evolution of these rare mutations. We develop a deterministic model with a few assumptions that allow for a pseudo-stochastic component in chapter 4. The Poissonian waiting time is used to refine the estimate for the impact of both transient and chronic treatment on strain selection. The model is then extended to allow for non-exponential death rates and for the transient survival of new genomes.

For discrete time models, we considered a simple synchronous model of viral evolution and used two fundamentally similar frameworks to compute viral diversity measures. The sequence evolution framework developed by Lee et al. [79] was successful in assessing the degree of viral diversity during the early phase of infection. However, the effect of assumptions such as differential fitness and selection pressure can significantly affect the overall conclusions. The probability generating function paradigm offers the ability to efficiently compute important indicators of viral diversity without simulating the full range of individual level scenarios. Because of the computational efficiency and the fact that important measures of viral diversity that can be computed from this paradigm depend on both time and virus replication rate, we use this methodology in chapter 3 to model early events of HIV infection and assess the impact of therapeutic interventions on the course of infection.

2.5 Summary of Implications for the Biomedical Field

Components of virus-host interactions are sufficiently complex that intuition alone is insufficient to understand the dynamics of such interactions [9]. Mechanistic models attempt to explain real events, observed or not. Selection of modelling techniques should be influenced by the essence of the problem to be investigated to avoid misapplication such as using deterministic models to capture the dynamics of rare mutants that exist as small sub-populations. Models need not be necessarily complex. Sensible model building that incorporates realistic size and timescales, where possible, avoiding having to estimate numerous microscopic properties such as molecular avidities can be very useful. Models with realistic assumptions can be experimental and analytical tools. For example models have helped elucidate high viral turnover in HIV infected individuals [120] and through coupling a mathematical model of HIV diversification and single genome amplification (SGA) sequencing techniques, transmitted HIV *envelope* sequences have been identified [71] . This work also showed that there is a high barrier to infection, with approximately 80% of heterosexual infections apparently started by a single virus, and that within 8 days of infection escape mutants for envelope-directed CTLs appeared in the viral population. Also, models developed in this work suggest that new measures of viral diversity, which correlate to prognosis, should be sought, and monitored in clinical trials for vaccines for example.

Chapter 3

Modelling the Impact of Acute Infection Dynamics on the Accumulation of HIV-1 Mutations

3.1 Introduction

The extent of virus replication and immunopathological events during primary infection may be important determinants of the subsequent course of HIV disease [58]. Despite advances in elucidating the structure of HIV, its genetics and its mechanisms of replication and survival in host immune system cells, the course of primary infection (the dynamics, timing and specificity of the immune response and the creation and establishment of cellular reservoirs of virus) is only partially understood. In sexual transmission, early events in HIV infection at the mucosal surface are critical to the initiation and propagation of the disease [56].

Recent advances, through coupling data analysis and mathematical modelling, have allowed the identification and characterization of the nature of the transmitted virus. Results indicate that HIV-1 quasispecies that arise following a mucosal infection are apparently consistent with a single transmitted strain [1, 71, 79]. The

evidence of a high barrier to infection has created the enthusiasm and re-energized the interest in targeting the early infection period with preventative or therapeutic interventions such as vaccines [124] or pre-exposure prophylaxis (PrEP) [70]. Therapeutic vaccines can prime the immune system to develop antibodies and cytotoxic T lymphocytes (CTLs) against the virus such that they are readily available to block or control infection by attenuating virus replication. PrEP can block the early amplification process (when infected resting cells pass the virus to activated cells which are critical for the infection process to start) after the virus has permeated through the mucosa [56] or restrict viral expansion by reducing the reproductive rate of the virus, preventing chronic infection.

The main clinical benefit of intervention at the early phase of HIV-1 infection is to block infection or contain early viral spread in the case of a breakthrough infection. There are undesirable consequences of undeterred viral replication during early infection, for example, 1) massive depletion of the CD4+ T-cell population, in particular within the gut-associated lymphoid tissue (GALT) [14, 96, 100] and 2) probable early establishment of viral reservoirs [37]. The establishment of viral reservoirs is a likely barrier to eradication of the virus [20]. Also, undeterred viral replication during early HIV infection seems associated with amplified transmission probability per sex act, and the timing of this peak in infectiousness means that patients are unlikely to know their HIV status at the time of this peak. Massive depletion of the CD4+ T-cell population is harmful for the patient: e.g. the risk of tuberculosis (TB) disease seems to be much higher in acutely infected people than in HIV negative people [26].

Existing analysis and modelling of early infection is largely driven by the kind of questions being addressed. For example, models of random mutations have been used

successfully to assess viral diversity as an indicator of the number of infection events or founder strains [71, 79]. According to these models, in homogenous infections, i.e. infections initiated by a single founder strain, the hamming distance (the number of bases at which any two sequences differ) distributions are essentially Poisson distributions. Models of sequence evolution have also been used to assess viral diversity during the chronic phase [80, 132]. Using recent acute HIV-1 infection data and a codon model of sequence evolution, a group of researchers found evidence of positive selection which appeared to be driven by cytotoxic T lymphocyte responses [154].

Also, population dynamic type models, mainly ordinary differential equations, have been used to study viral dynamics of early HIV-1 and SIV infections. Some of these models have been used to estimate viral growth rates, basic reproductive numbers and post peak decay rates [87, 114, 128]. Such models have also been used to understand the role of early immune responses in HIV infection [6, 47, 141]. These models have helped to define the challenge that immune responses and therapeutic interventions have to overcome to defeat HIV early in infection. However, these models make specific assumptions about many intra-cellular processes, such as cell entry rates and lifetime distributions, that are not directly observable.

As an alternative to the use of diversity, divergence, sequence identity and maximum hamming distance as correlates of the number of transmission events, we propose a new metric of diversity which may relate to prognosis. Whilst every possible single point mutation in the viral genome may occur in each generation, we are interested in computing the probability of appearance of particular mutations in the viral genome, i.e. we can ask about the probability that a particular mutant has never occurred or is currently present. Viral genetic changes can result in increased virulence, increased

cell tropism, escape from host immune/drug pressure [32, 84, 140] and may consequently lead to treatment failure [67]. One study has reported that low pre-treatment diversity (diversity defined by pairwise comparisons of nucleotide substitutions per site) is also associated with control of viremia during subsequent treatment interruption and low viral replication capacity [68]. Accumulation of quasispecies can also result in alterations in receptor usage, in particular CCR5 and CXR4, and this switch in receptor usage is correlated with a faster progression of the disease [84, 132]. Also these new mutations are likely to be archived in latently infected cells and are unlikely to be eliminated by HIV-1 immune responses and antiretroviral therapy, even after treatment intensification [31].

Previously, some authors calculated the expected frequency of resistant virus and showed that the likelihood of generating resistant mutants during treatment is less than the likelihood that such mutants are present before treatment is initiated [13, 112, 127]. A simple calculation of waiting times to the appearance of mutants before and during treatment shows that it is highly unlikely that new mutants appear during suppressive therapy (see chapter 4). Unabated viral replication results in a continuous accumulation of variants which may persist at very low frequencies. The pre-existing minority mutations which may not be detected by standard bulk sequencing genotypic assays in both drug-naive and drug-experienced persons, e.g. thymidine analogue mutations (TAMS), have shown to be significantly associated with virologic failure [67, 101].

A birth and death process model of viral growth [125] was used to assess the probability of appearance of resistant mutants. In their framework, the authors calculated the total number of replications until a specific mutant first appeared. From direct

simulations in [125], results show that common mutants (one point and two point mutants) were likely to appear early during acute infection and three point mutants may emerge around the peak of viremia but disappeared at the set point. However, calculating the number of replication cycles may not be a good metric if immune effects are considered because immune control impact can change the absolute time until appearance of a specific mutant but not the number of replication cycles. In this model [125], the number of infected cells changes by one at a time. This assumption is unlikely suited for virus proliferation as noted in [57].

In this chapter, we use a multi-type Galton-Watson branching process (GWBP) in a varying deterministic environment. In our branching process model, the number of offspring is time dependent (in discrete non-overlapping generations). Multi-type branching processes have been used to calculate the risk of escape that comes from pre-existence of resistant mutations held in a mutation-selection equilibrium for a population of organisms challenged by a biomedical intervention [64, 65], mutation accumulation in mitochondrial DNA and the polymerase chain reaction [75, 117]. The Galton-Watson process has a simple recursive structure that makes it amenable to analysis by generating functions, hence we can derive ensemble level probabilities of diversity without the need for calculating many population level 'realizations'.

Our model differentiates from previous studies [64, 65, 125] in that it parameterizes the dynamics through an effective reproductive number of offspring per individual. This makes it relatively straightforward to model changes between scenarios corresponding to interventions, whose impact on the course of infection can then be heuristically described. By contrast, previous authors have tended to define specific microscopic dynamics, such as exponential growth, or mass action, with particular

rate constants that have not been reliably measured. We can tune our effective reproductive number over a period of several weeks/months post infection to obtain realistic initial viremic peaks and set points, without having to unpack the underlying combination of target cell depletion and immune system responses, as it is only the infected cell population which we need to model in order to quantify opportunities for evolution.

The main focus here is calculating probabilities of appearance and the likelihood of existence of genomes which potentially arise from infections initiated by a single strain. We explore how the dynamics of early infection affects the accumulation of mutations which lay the seeds for long term evolution of drug resistance and immune system evasion. These models may be useful to test the biological effectiveness of early interventions (PrEP or vaccines) in the case of a breakthrough infection. There is concern that PrEP or imperfect vaccines may lead to clinically disadvantageous selective pressures during HIV transmission. The details of how a topical exposure becomes a systemic infection are beyond the scope of this analysis. In the case of a drug or vaccine naive infectious partner, it may be that the relevant mutations are absent, or present only in trace quantities, so that to first order there is little selective pressure affecting what, for the purposes of the present analysis, is the founding strain or wild-type, defined by a narrow view of a small portion of the viral genome.

3.2 A Model of Viral Diversity

In our model, we consider an infection that is started by a single infected cell carrying a particular sequence with a certain number of bases. We focus on a small segment of the viral genome where changes or mutations at these particular sites are relevant and

lead to key variants. Any changes at the other remaining sites are deemed irrelevant in our model. The mutation rate per nucleotide is given by a parameter η. The branching process model is as follows: one infected cell initiates the process. On replication, each cell produces new cells; the type of each new daughter cell may or may not be the same as that of the parent cell, i.e. infected cell populations evolve as a pure stochastic process with random choices for the type of offspring.

3.2.1 Single Mutation

We start by considering a single-point mutation that occurs in a particular position in the viral genome, i.e. our artificial viral genome has a single site. In this scenario, we only have two types of infected cells of relevance, i.e. the initially infecting strain (wild type) and a population of cells infected with a virus carrying a sequence with a base change at the site of interest (single point mutant). The mutation matrix with transition probabilities is given by:

$$\begin{array}{c} \\ P_0 \\ P_1 \end{array} \begin{array}{c} \begin{array}{cc} P_0 & P_1 \end{array} \\ \begin{pmatrix} 1-\eta & \eta \\ \eta & 1-\eta \end{pmatrix} \end{array}, \tag{3.2.1}$$

where the number of wild-type and single point mutant infected cells are given by P_0 and P_1, respectively. This process is a two-type Galton-Watson process (see Appendix for details). We assume that the two types have different replication rates and the mean number of offspring for each type may change from generation to generation, i.e. the two effective reproductive numbers are $R_0(n)$ and $R_1(n)$ for the wild-type strain and mutant, respectively. The effective reproductive number is the average number of new infections caused by one infected cell at a given time/context in a population that is not necessarily wholly susceptible. In our notation for probability generating

functions (pgfs), superscripts will denote the generation number and subscripts the type of the cell (0 for wild-type and 1 for the mutant).

The offspring distributions for the wild-type and mutant infected cells at every generation are binomial, i.e. $p_0(k_0,k_1) \sim \text{Bin}(R_0(n), 1-\eta)$ and $p_1(k_0,k_1) \sim \text{Bin}(R_1(n),\eta)$, respectively, where $p_i(k_0,k_1)$ is the probability that a cell of type $i=0,1$ has k_0 offspring of type 0 and k_1 of type 1. Using equation A.0.7, the pgf for the wild-type infected cell offspring at generation n is given by

$$\begin{aligned} g_0^n(s_0,s_1) &= \sum_{k_0=0}^{\infty}\sum_{k_1=0}^{\infty} p_0(k_0,k_1)s_0^{k_0}s_1^{k_1}; \\ &= \sum_{k_0=0}^{\infty}\sum_{k_1=0}^{\infty} \binom{R_0(n)}{k_0}(1-\eta)^{k_0}\eta^{k_1}s_0^{k_0}s_1^{k_1}; \\ &= \sum_{k_0=0}^{\infty} \binom{R_0(n)}{k_0}\Big((1-\eta)s_0\Big)^{k_0}\Big(\eta s_1\Big)^{R_0(n)-k_0}; \\ &= \Big((1-\eta)s_0+\eta s_1\Big)^{R_0(n)}, \end{aligned} \tag{3.2.2}$$

where $k_1 = R_0(n) - k_0$ and at the last step we have used the binomial theorem. Similarly, the pgf for the mutant infected cell offspring is given by

$$g_1^n(s_0,s_1) = \Big(\eta s_0+(1-\eta)s_1\Big)^{R_1(n)}. \tag{3.2.3}$$

Assuming that the population is started from a single wild-type infected cell, we have the process initial conditions given by $\{P_0(0)=1, P_1(0)=0\}$. We can use the iteration

$$G_i^n(\mathbf{s}) = G_i^{n-1}\Big(g_0^n(\mathbf{s}), g_1^n(\mathbf{s})\Big), \qquad n=2,3,\cdots \tag{3.2.4}$$

for $i=0,1$, where $\mathbf{s}=(s_0,s_1)$, to derive the pgf specifying the distribution law of the number of cells at every generation. The marginal laws for subsets P_i can be obtained by setting respective arguments of the pgf equal to 1 [75]. The derived marginal pgf

constructs can then be used to calculate probabilities of interest. The marginal pgf of mutant infected cells in a process initiated by a single wild-type infected cell is given by $G_0^n(1, s_1)$, such that the probability that a mutant infected cell is not currently present at generation n in the population is precisely given by $\mathcal{P}_0(n) = G_0^n(1, 0)$. To calculate the probability that a single point mutant has never occurred, we use the following trick: we compute $G_0^n(1, 0)$ in the model with type transition matrix given in equation 3.2.1 but with state 1 (mutant) made an absorbing state, i.e. where the last row of the matrix is reset to (0 1). The modified process will go to state 1 for the first time exactly as the process would, but will stay there. Letting $S_0(n) = G_0^n(1, 0)$ with the initial condition $S_0(0) = 1$, we have the sequence

$$\begin{aligned}
S_0(1) &= \Big((1-\eta)\Big)^{R_0(1)}; \\
S_0(2) &= \Big((1-\eta)(1-\eta)^{R_0(2)}\Big)^{R_0(1)}; \\
S_0(3) &= \Big((1-\eta)\Big((1-\eta)(1-\eta)^{R_0(3)}\Big)^{R_0(2)}\Big)^{R_0(1)}; \\
S_0(4) &= \Big((1-\eta)\Big((1-\eta)\Big((1-\eta)(1-\eta)^{R_0(4)}\Big)^{R_0(3)}\Big)^{R_0(2)}\Big)^{R_0(1)}; \\
\vdots &= \vdots
\end{aligned} \tag{3.2.5}$$

and so on, such that the probability that the mutant has never occurred is given by

$$S_0(n) = \Big(1-\eta\Big)^{\sum_{i=1}^{n}\prod_{j=1}^{i} R_0(j)}, \tag{3.2.6}$$

which has boundary conditions $S_0(0) = 1$ and $S_0(\infty) = 0$. The exponent is the total wild-type infected cell population size after n generations. Equation 3.2.6 is the "survival" function ("survival" means no mutant present). Let a non-negative random variable T represent the number of generations until there is a mutation, then the cumulative distribution function, which gives the probability that the mutation has

occurred by generation n, is given by $\Pr(T \leq n) = 1 - S_0(n)$. Thus the density is given by $f(n) = S_0(n-1) - S_0(n)$. The expected time (generation) to the appearance of a single point mutant is given by:

$$\begin{aligned} \mathbb{E}(W_T) &= \sum_{n=0}^{\infty} n f(n); \\ &= \sum_{n=1}^{\infty} \Big(1-\eta\Big)^{\sum_{i=1}^{n} \prod_{j=1}^{i} R_0(j)}. \end{aligned} \tag{3.2.7}$$

3.2.2 Multiple Mutations

For higher order mutations, we choose a small portion of the viral genome with three sites where we assume a founder strain (wild-type), the possibility of three single-point and three double-point mutants, and also the possibility of multiple mutations which lead to a three point mutant that is reachable by different pathways (see Appendix C for the three point mutation network matrix). This is just one example of a phylogenetic tree; any tree can be easily accommodated in our framework by modifying the mutation matrix. We are using the minimum number of mutations within which we can describe the interplay between common mutations, unviable intermediate mutations, and 'compensatory' mutations. It will be interesting to apply this approach to high quality clinical data, demonstrating how mutations accumulate to provide increasing resistance [67, 101, 129, 136].

From system C.0.5 in Appendix C, the result that is relevant to our setting is the joint pgf of the numbers of cells of all types, present at generation n in the process initiated by a single wild-type infected cell given by $G_0^n(\mathbf{s})$, where $\mathbf{s} = (s_0, \cdots, s_7)$. In our notation, {0} represents wild-type infected cells, {1,2,3} three single point mutant infected cells, {4,5,6} three double point mutant infected cells and {7} triple point

mutant infected cells. We can derive recurrent equations for:

1. the marginal joint pgf of the numbers of all single point mutant infected cells as $G_0^n(\mathbf{s})|_{s_j=1,j\neq\{1,2,3\}}$, such that the probability that no single point mutant infected cells are present at generation n is given by

$$\mathcal{P}_0^{sp}(n) = G_0^n(\mathbf{s}), \tag{3.2.8}$$

   using substitutions $\mathbf{s} = (1, 0, 0, 0, 1, 1, 1, 1)$.

2. the marginal joint pgf of the number of all double point mutant infected cells as $G_0^n(\mathbf{s})|_{s_j=1,j\neq\{4,5,6\}}$, where the probability that no double point mutant infected cells are present at generation n is given by

$$\mathcal{P}_0^{dp}(n) = G_0^n(\mathbf{s}), \tag{3.2.9}$$

   using substitutions $\mathbf{s} = (1, 1, 1, 1, 0, 0, 0, 1)$.

3. the marginal pgf of triple point mutant infected cells as $G_0^n(\mathbf{s})|_{s_j=1,j\neq 7}$, where the probability that no triple point mutant infected cells are present at generation n is given by

$$\mathcal{P}_0^{tp}(n) = G_0^n(\mathbf{s}), \tag{3.2.10}$$

   using substitutions $\mathbf{s} = (1, 1, 1, 1, 1, 1, 1, 0)$.

3.3 Early Infection Scenarios

The effective reproduction number is of great importance in facilitating quantitative assessment, in real time, of the impact of intervention strategies on the course of disease progression [53]. In order to explore the impact of intervention early in infection

(such as effects of vaccines or PrEP) on the probability of diversity, we choose various profiles of the effective reproduction number and calculate the probability that particular mutants are currently absent from the population. We assume that the effective reproduction number is given by the following continuous piecewise linear function:

$$R(n) = \begin{cases} R_0 & \text{if } n < n_g \\ \dfrac{(R_0 - R_m)(n_p - n)}{n_p - n_g} & \text{if } n_g \leq n < n_p \\ R_m & \text{if } n_p \leq n < n_s \\ 1 & \text{if } n \geq n_s \end{cases} \tag{3.3.1}$$

schematically shown in figure 3.1. Here R_0 is the basic reproductive ratio, defined

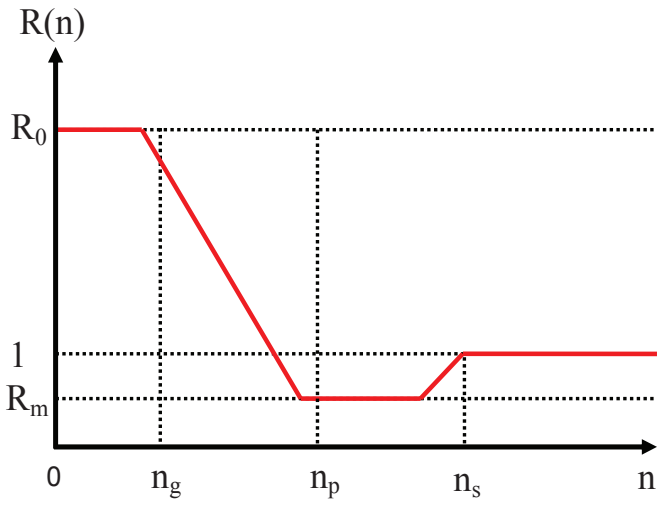

Figure 3.1: A generic profile of the effective reproductive number. Parameters: $n_g - 1$ is the initial number of generations when infected cells replicate undeterred, $n_p - 1$ is the number of generations taken to reach the maximum number of infected cells (peak) and n_s is the number of generations it takes for the infected cell population to settle at steady-state, with each productively infected cell producing on average a single new infected cell. Varying n_g and R_0 we can mimic the effects of a vaccine and PrEP strategies.

as the number of new infections caused by one infection in an extremely susceptible

population, i.e. at the beginning of infection [4]. We have $R(n) \leq R_0$, with the upper bound and n is the generation number. This offspring production function gives three stages in the infection process, i.e. exponential growth up to generation $n_p - 1$ (time to attain peak viral levels), decline from generation n_p up to generation $n_s - 1$ (time to reach set point) with a minimum offspring production of R_m and finally the infection incidence remains approximately constant at set-point starting from generation n_s.

We obtain the following dynamics from this function: an exponential expansion soon after infection until generation $n_g - 1$, (we call this the period of unrestrained growth) which may be attributed to the unlimited availability of target cells and the absence of immunological control. Subsequently, immune control becomes activated, together with the gradual depletion of the target cell pool hence the decline in the number of offspring produced. There is an attenuated viral expansion up to generation $n_p - 1$. During the period between n_p and n_s generations, we have $R(n) < 1$, i.e. the chain reaction is subcritical due to immune system control and/or loss of target cells. We can vary the four parameters in this simple function to mimic aspects such as: the time the immune system comes into effect, the period at which the immune system can suppress viremia, the time to reach peak and set-point, and the height and width of the viremia peak. Using the offspring effective reproductive function, the number of infected cells at generation n is given by:

$$P(n) = \lfloor P(n-1)R(n) \rfloor, \qquad \text{for} \quad n \geq 1, \tag{3.3.2}$$

where $\lfloor x \rfloor = \max\{m \in \mathbb{Z} | m \leq x\}$ is the floor function where $\mathbb{Z}$ is the set of integers. This slight modification of the total number of infected cells in each generation allows us to retain the integer counts of infected cells. Unless stated in the scenarios, we assume that all types of infected cells have the same number of offspring at generation

n - i.e. no differential fitness among variants.

Also, we can relax the assumption that there is no differential fitness among variants and explore the impact of intermediate mutants fitness bottleneck on the probability of viral diversity. We let the growth disadvantage of mutant i relative to the wild-type be given by $f_i = 1 - R_{0i}/R_0$, for $i = 1, 2, 3$ representing single point, double point and triple point mutants, respectively. R_0 is the basic reproduction rate of the wild-type strain. Now the effective reproduction number for the mutants will be given by $R_{0i}(n)$ and we assume that there is no differential fitness at steady state. At steady state each infected cell produces one new cell. For illustration purposes, we assume that the reproductive ratios of the wild-type and the triple point mutants are equal, i.e. $R_{03} = R_0$. Therefore, this investigates the effect of intermediate mutants' fitness bottleneck on the evolution of a higher order mutant.

To investigate the effects of biomedical interventions, we choose a base scenario that may correspond to the standard course of disease progression and then explore perturbations that influence viral diversity. Our parameters are assigned values to produce realistic population sizes and timescales observed clinically. The inspiration is to produce different phases of viral growth after a breakthrough infection, i.e. a viremic peak of a couple of weeks, viral load to decline and to stabilize at equilibrium (stages of early HIV infection [36]). With these different parameter values, we can explore important regimes of classes of models which are consistent with important overall features of the system. This analysis captures regimes of impact, on diversity, of PrEP and vaccine strategies.

Our base scenario is generated by the effective reproduction number profile given by the following parameters: $R_0 = 6$, $n_g = 8$, $n_p = 20$ and $n_s = 28$. In all the figures,

we assume a per base mutation probability (η) of 3×10^{-5} [92]. The profile, explicit stochastic simulations and recurrent equation solutions for probability of diversity (equations 3.2.8, 3.2.9 and 3.2.10) are shown in figure 3.2. In this figure, we are comparing solutions derived from the use of pgfs, which capture likelihoods of existence of particular genomes, against full explicit stochastic simulations. Figure 3.2(B) is a single run of the full branching process. Simulations and recurrent equation solutions are in good agreement, where single and double point mutations are overwhelmingly likely to appear early and most of the times (about 80%), the triple point mutant does not appear around the peak viral load (similar to results obtained by Ribeiro and Bonhoeffer [125]). This illustrates that using pgf equations rather than explicit simulations, we can efficiently obtain answers to key questions about viral evolution.

Therapeutic interventions may provide inhibition from the very onset of viral entry (e.g. PrEP) or attenuate viral load during the course of infection (e.g. vaccine) and may significantly change the course of disease progression. We investigate the impact of these intervention programmes by calculating viral diversity on either side of our 'threshold', i.e. base scenario. Our models capture well known semi-quantitative aspects of HIV infection such as the magnitude and duration of early viremia which itself parameterizes opportunities for mutation. Using several model scenarios that we regard as clinically relevant, we demonstrate various regimes of 'response' of evolution to 'intervention' in a framework in which a modest number of assumptions create the scenarios.

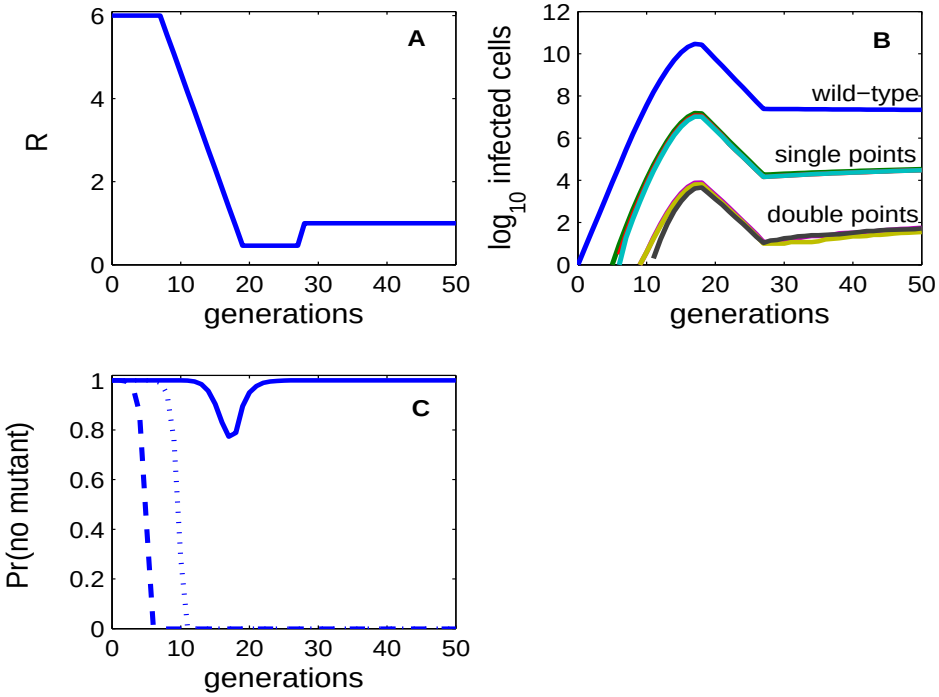

Figure 3.2: A comparison of pgf recurrent equation solutions and explicit stochastic simulations. A : Viral reproduction rate profile when $R_0 = 6$, $n_g = 8$, $n_p = 20$, $n_s = 28$. B: A single realization of the 8-type branching process generated by profile in panel A, showing the dynamics of wild-type, three single point mutant and three double point mutant infected cell populations. We assume a per base mutation probability of $\eta = 3 \times 10^{-5}$. C: The probabilities of non-existence of i) single-point mutants ($\mathcal{P}_0^{sp}$ - dashed curve), ii) double point mutants ($\mathcal{P}_0^{dp}$ - dotted curve) and iii) triple point mutant ($\mathcal{P}_0^{tp}$ - solid line). There is no differential fitness among variants, i.e. all viral strains have the same effective reproduction number profile given in panel A. Panels A and C make up panel B in both figures 3.3 and 3.4.

3.3.1 Vaccine Effects

We assume that a hypothetical vaccine intervention's impact can resemble trends that have been observed in SIV vaccinated animal models, i.e. it causes the attenuation of viral load that results in reduced peak and set-point. Clinical trial data on

SIV animal models has shown that there is a significant difference between viral load growths, peak viremia and early viral set point of vaccinated and unvaccinated animals [81, 151]. In general unvaccinated animals had fast growth, high peak viremia and often high early viral set-point compared to the vaccinated animals. A vaccine can prime and/or boost immune function of an individual that can limit the rate of viral replication. To mimic the effects of vaccine-induced immunity using our framework, we vary the time of unrestrained viral growth (n_g) and explore its impact on diversity, see figure 3.3. Reducing n_g in our base case to 1 (which resembles an ever ready vaccine-induced immune control at infection), significantly increases the chances of extinction of even common (single point and double point) mutants later during chronic infection. Delaying viral control, i.e. increasing n_g in our model, results in a higher likelihood of mutation accumulation and persistence.

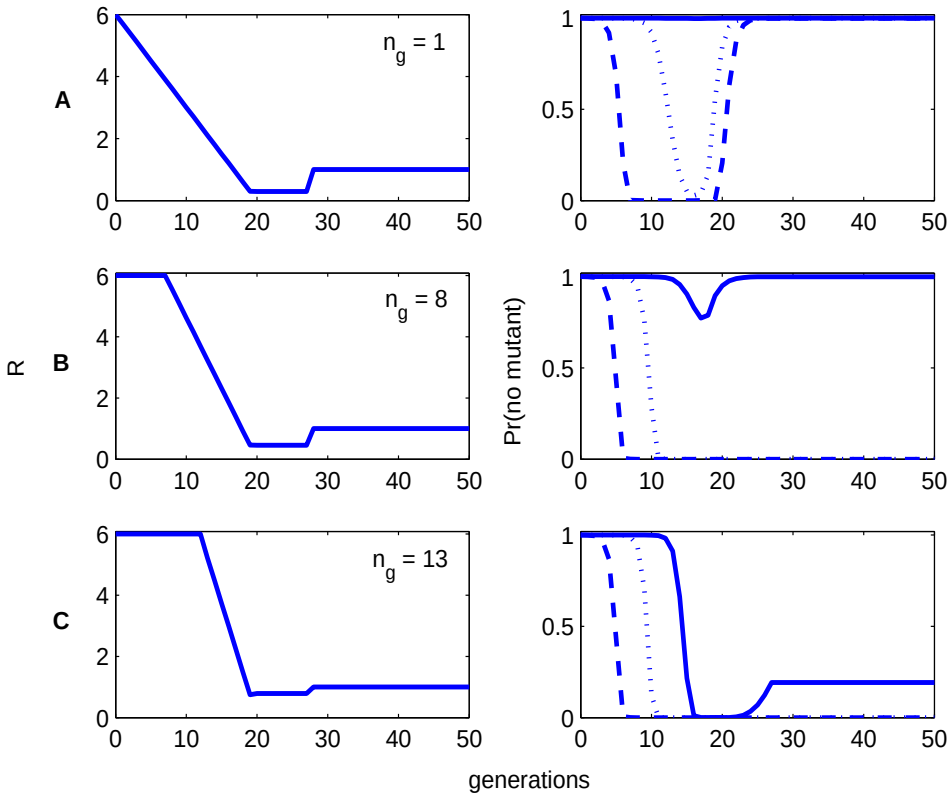

Figure 3.3: The effects of varying the time of unrestrained replication (n_g) on the probability of mutations being currently absent from the population. In each panel, we show the attenuated viral replication profile and the corresponding viral diversity, i.e. probability of non-existence of i) single-point mutants ($\mathcal{P}_0^{sp}$ - dashed line), ii) double point mutants ($\mathcal{P}_0^{dp}$ - dotted line) and iii) triple point mutant ($\mathcal{P}_0^{tp}$ - solid line). The other parameters are fixed: $R_0 = 6$, $n_p = 20$, $n_s = 28$ and the per base mutation rate is $\eta = 3 \times 10^{-5}$. A: effects of early intervention, B: baseline scenario and C: effects of late intervention.

3.3.2 PrEP Effects

PrEP is one of the options currently being tested as part of the efforts to identify additional tools to reduce the risk of HIV acquisition. The rationale of this approach is to inhibit HIV replication from the moment of infection and this may help to avert

chronic or persistent infection. Drugs such as tenofovir disoproxil fumarate which can be used on its own or in combination with emtricitabine taken daily are candidates for oral preventative drugs. PrEP trials in macaques [44] and humans [121] reported evidence of efficacy. We vary the virus's basic reproduction ratio, R_0, and assess its impact on accumulation of mutations. Figure 3.4 shows PrEP scenarios varying in effectiveness and the associated impact on viral diversity. Effects that reduce the amplification process early (reducing virus's reproduction rate) significantly reduce viral fitness and consequently reduce viral diversity. Unabated and rapid replication (high virus reproduction rate) soon after infection quickly leads to high diversity.

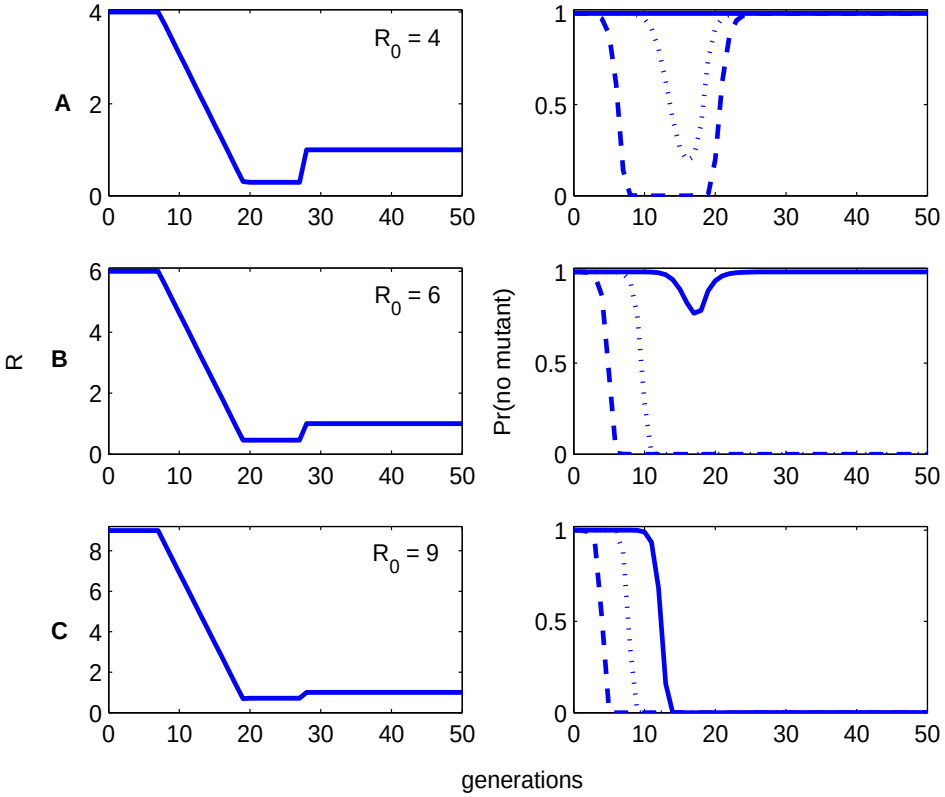

Figure 3.4: The effects of varying the basic reproductive number (R_0) on the probability of mutations being currently absent from the population. In each panel, we show the attenuated viral replication profile and the corresponding viral diversity, i.e. probability of non-existence of i) single-point mutants ($\mathcal{P}_0^{sp}$ -dashed line), ii) double point mutants ($\mathcal{P}_0^{dp}$ -dotted line) and iii) triple point mutant ($\mathcal{P}_0^{tp}$ -solid line). The other parameters are fixed: $n_g = 8$, $n_p = 20$, $n_s = 28$ and the per base mutation rate is $\eta = 3 \times 10^{-5}$. A: effects of reduced reproductive number, B: baseline scenario and C: effects of high reproductive number.

Incorporating differential fitness among variants in both vaccine and PrEP scenarios, we explore the impact of intermediate mutants fitness bottleneck on the probability of non-existence of the triple point mutant during the chronic state of infection. For illustration purposes, we choose the worst case scenarios in both the vaccine and PrEP strategies (i.e. figure 3.3(C) and figure 3.4(C)). As shown in the two contour

plots (figure 3.5 and figure 3.6), high fitness costs for early events are important in reducing diversity later on. High fitness cost for single point mutants significantly reduces viral diversity (measured as the probability that there is no triple-point mutant at chronic stage, i.e. at generation 50) compared to high fitness costs for double point mutants.

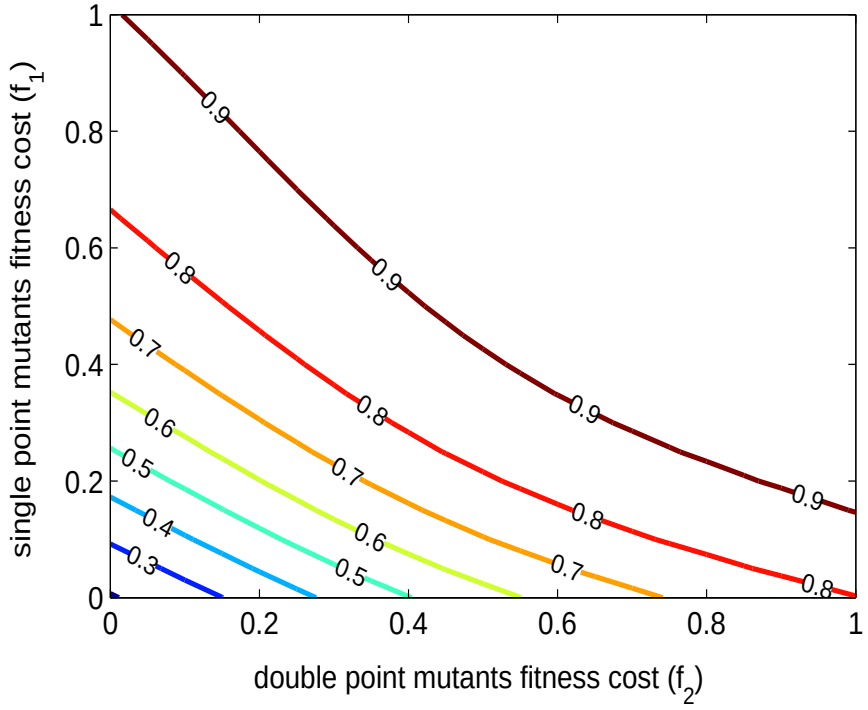

Figure 3.5: A contour plot for the probability of non-existence of a triple point mutant at generation 50 as a function of intermediate mutants fitness costs (for scenario 3.3 (C)). We assume that the reproductive ratios of the wild-type and triple point mutants are equal, therefore this investigates the effect of intermediate mutants' fitness bottleneck on the evolution of a higher order mutant.

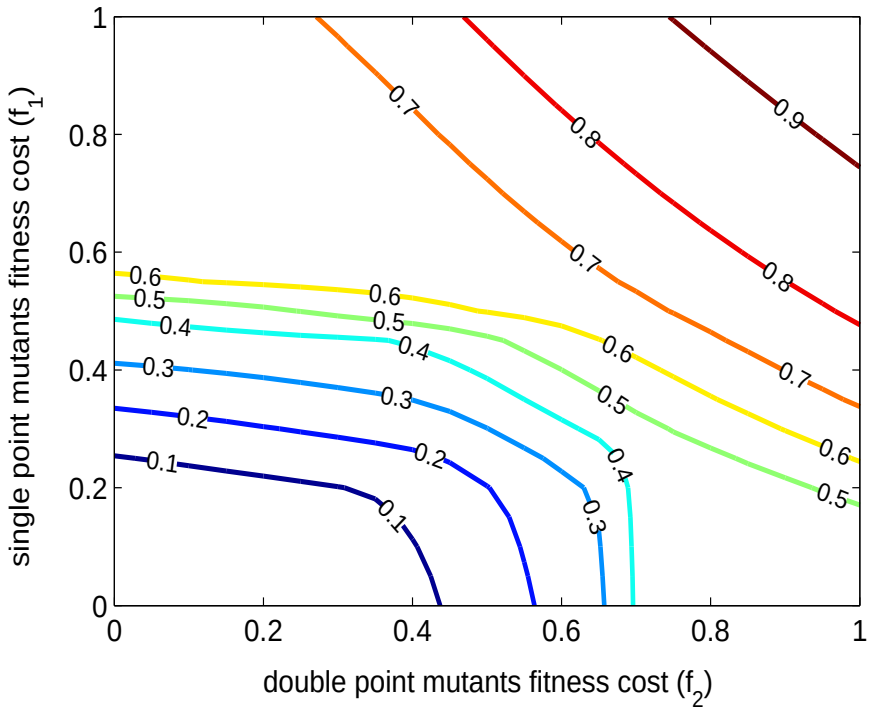

Figure 3.6: A contour plot for the probability of non-existence of a triple point mutant at generation 50 as a function of intermediate mutants fitness costs (for scenario 3.4 (C)). We assume that the reproductive ratios of the wild-type and triple point mutants are equal, therefore this investigates the effect of intermediate mutants' fitness bottleneck on the evolution of a higher order mutant.

3.4 Conclusion

Using a simple model, we have calculated viral diversity (defined as the probability of existence of particular mutants) under various scenarios. It is useful to identify and characterize particular mutations that can evolve during the early stages of infection. We relate the exploration to the effects of interventions on mutation accumulation and have shown that early intervention has a profound impact on the evolution of

the virus. This is another dimension to investigate whether the unrestrained growth of virus during early infection generates sufficient diversity which may relate to prognosis.

An ever ready intervention at the time of infection may not prevent the occurrence of single point and double point mutations but has a very significant impact on their persistence, i.e. attenuating the founder virus results in reduced diversity. Delaying viral control guarantees the persistence of common mutants but does not necessarily mean higher order mutations (e.g. triple point mutants) will occur or will persist if they appear. Further delay of viral control will result in a higher likelihood of mutation accumulation and persistence. Our scenarios include 1) the effect of a vaccine on the immune system (i.e. a vaccine that can prime the immune system to develop antibodies or CTLs against the virus) being present at the very beginning of infection or immune response that gradual develops and 2) therapy that inhibits infection of target cells. We would also like to mention that there is also a danger of drug resistance if individuals continue to take PrEP drug after they became infected with HIV, they could develop resistance forms of the virus because of suboptimal suppression.

Branching process models have also been used to estimate the probability of success or failure of a biomedical intervention basing on assumptions that mutation rates are small, mutations exist in mutation-selection equilibrium and all intermediate mutants carry subcritical fitness costs [64, 65]. These studies characterized the efficacy of interventions in terms of a critical population size, typically relying either on substantial simplifying assumptions which make it possible to derive closed form solutions

[64, 65] or complex models which involve explicit simulation of the infection dynamics [125]. In the present approach, there is no need to perform explicit simulations, yet we can calculate what appear to be the crucial indicators of diversity, within a model that captures known semi-quantitative aspects of HIV infection such as the magnitude and duration of early viremia - which itself parameterizes opportunities for mutation.

Our analysis is a new way to study replication/viral diversity where the number of offspring per individual is given by an effective reproductive number function. This allows us to model the impact of interventions on the course of infection, without having to make specific assumptions about many microscopic details. Within this framework, we explored scenarios demonstrating the interplay between common, intermediate and rare mutations, by calculating statistical indicators of diversity. This method obtains impressive efficiency by making use of recursion relations for ensemble level probability generating functions without the need for calculating many population level 'realizations'.

An HIV vaccine is still years ahead, therefore treatment is one of the immediate therapeutic remedies at our disposal. The brighter side is that current drug profiles are favorable (dosing convenience, e.g. multi-pills in one and improved safety profiles) and patients can now easily adhere to prescriptions but there is evidence that pre-existence of mutations before therapy is a crucial part of the long term prognosis [67, 86]. At the rate at which diversity increases, by the time patients start treatment (at the late stage of infection, usually after 5 to 10 years if treatment is initiated during symptomatic phase), a lot of mutations could have been generated and probably archived too.

Early treatment might help retard accumulation of resistance and therefore might cut into the opportunity for viral replication to produce treatment defeating variants. Also, studies have shown that early treatment reduces the size of the latent viral reservoir [89, 137]. Initiation of treatment early is also associated with the preservation of the immune function [63], a benefit to the patient which can increase the probability of cure as well as decreased transmission within the population. Reducing the number of mutants in the viral population may help increase treatment efficacy and options for patients. If treatment should be started to benefit from low prevalence of mutants, "universal treat and test" approach [50] might be a good idea although "hit hard and early" tactic [62] would be the best.

This simple analysis supports both proponents of "hit hard and early" and "universal test and treat" in that early treatment-induced control of viremia will help reduce viremia of homogenous population therefore reducing chances of further mutation accumulation. Waiting for years to initiate treatment gives the virus enough time to accumulate compensatory mutations which will reduce treatment efficacy later on. This is in line with the clinical assumption that the window of opportunity is from transmission to peak viremia and after that it becomes a point of no return [99, 153].

Although such analysis may be probably too simplistic for the complex dynamics of HIV, we have shown that including, even conservative assumptions such as equal fitness for all variants, there is still a chance that higher order mutants generated early in infection might eventually go to extinction. There is an overwhelming likelihood that variants generated early in infection and are present in low quantities will go to extinction during viral decline due to either limited target cell population or immune

control provided that it is cross reactive. The branching process construct incorporates a fair amount of the complexity of the stochastic reality. In our scenarios, we chose an arbitrary tipping point between the good and the bad regimes, and our model seems heuristically sensible. Our model captures realistic overall population sizes and timescales characterizing the typical course of infection. It remains to be seen if our framework can be quantitatively accurate if applied to detailed clinical/experimental scenarios from careful studies.

There are some limitations to our approach. We have modelled populations with discrete and non-overlapping generations, whereas in HIV dynamics, individual infected cells die and reproduce at random times. Also, as noted previously by Iwasa et al. 2003 [64], multi-type branching processes describe accumulation of mutations in independent lineages, so that the model is unable to describe recombination, which can be crucial in viral evolution. Nevertheless, this analysis captures regimes of impact, on diversity, of some topical intervention strategies.

3.5 Summary of Implications for Public Health

According to the analysis in this chapter, there may be substantial clinical benefits for patients who are on PrEP but happen to be infected, as it appears that the initial drug levels can substantially impede viral replication and hence long term prospects for viral evolution. This could be investigated further by following up patients infected during studies and monitoring their viral diversity over longer periods of time, such as in the recent (IPreX) trial (Grant et al. [51]).

Chapter 4

Chronic and Transient Antiretroviral Therapy Selecting for Common HIV-1 Mutations Substantially Accelerates the Appearance of Rare Mutations

4.1 Introduction

The rapidity of human immunodeficiency virus (HIV) replication, combined with its high reverse transcriptase error rate [41], leads to rapid viral evolution, in particular the emergence of drug resistance. Treatment that is unable to sufficiently inhibit viral replication allows the appearance and/or selection of drug-resistant strains. Further accumulation of resistant variants may limit therapeutic efficacy and jeorpadize subsequent treatment options.

A single dose nevirapine (NVP) regimen for prevention of mother to child transmission (PMTCT) is a well known example of a suboptimal regimen that inevitably, if

temporarily, exerts selective pressure in favour of resistant strains. This is still a major concern in developing countries where a prophylactic regimen of single dose NVP is widely used for PMTCT [74]. Given the high frequency of mutation, some minority resistant mutants are always preexisting, albeit in trace quantities, at the moment therapy is initiated. Because of the long half-life of single dose NVP, with blood levels detectable up to 2-3 weeks after exposure [25, 107], the duration of sub-therapeutic NVP concentrations may present a significant hazard of developing resistance for the mother. There is a risk of treatment failure after single dose NVP exposure, if the treatment includes a non-nucleoside reverse transcriptase inhibitor (NNRTI) [39]. The question arises whether, and to what extent, a transient treatment-induced boost to an otherwise marginal subpopulation results in increased risk of accumulation of further resistance mutations that could potentially increase the risk of subsequent NNRTI-based treatment failure.

In the search for better PMTCT regimens, improved efficacy has been demonstrated for a number of short course regimens for PMTCT in resource-limited settings. For example, 1) use of single dose NVP with additional short course of zidovudine/lamivudine during 3-7 days postpartum [97], 2) addition of single dose NVP to zidovudine short course during the antenatal period [88] and, recently, 3) use of intrapartum single dose of combined tenofovir/emtricitabine taken after antenatal short course of zidovudine plus intrapartum single dose NVP [18]. These regimens improve on single dose NVP either in efficacy for PMTCT or reduction of NVP resistance in the mother, or both. However they appear suboptimal in that they select for NNRTI-resistant strains and therefore increase the mothers' risk of virologic failure for subsequent NNRTI-based therapy. For example, in the MASHI study[88] a

total of 218 women started post partum NVP-based therapy after they had received zidovudine from 34 weeks of gestation through delivery. Of these, 112 had received single dose NVP, whilst the rest had received a placebo during labour. After 6 months of post partum treatment with a NVP-based regimen, women without prior NVP exposure were less likely to have virologic failure compared to women who had received intrapartum NVP. Strikingly, of women who started NVP-based therapy within 6 months, 41.7% from the single dose NVP group, but none from the control group, had virologic failure.

In-vivo mathematical models have been useful in exploring the evolution of drug resistance, suggesting that significant evolution can occur during treatment or before initiation of treatment [3, 12, 13, 126, 130, 134, 155]. Based on the models, the authors argued that chances of resistance evolving during treatment are small compared to chances of resistance evolving before suppressive therapy. However these studies did not explore, in any dynamically consistent framework, the emergence/accumulation of multiple mutations in a possibly non constant environment. In this chapter, we extend these standard models to explicitly investigate the consequences of population dynamical effects amongst common resistant mutants. We show how the deterministic dynamics of the common mutants affects the time taken to produce the rarer mutants.

We start from an ordinary differential equation (ODE)-type model of in-vivo viral replication in the deterministic regime, applicable to cell populations that are large enough for statistical fluctuations to be relatively small (wild-type and common mutant strains). We explicitly add expressions for Poisson rates for the occurrence of rare mutations. Using standard survival analysis, we compute, as a function of time, the probability of avoiding a mutation event. Furthermore, we introduce an additional

timescale to the 'survival function' to capture the time over which cells infected by an unfit genome persist before being ecologically overwhelmed. This 'survival function' is a continuous state variable that is incorporated into the system of ODEs without much complexity.

We apply our modelling framework to clinically inspired scenarios. Firstly, we explore the quasi steady state that corresponds to chronic treatment in the presence of two viral populations. We characterize treatment regimes in which rates of appearance of rare mutants are either increased or decreased. Secondly, inspired by regimens used for PMTCT in resource limited countries, we investigate the transient behaviour of the model under a short perturbation of the fitness parameters, such as occurs during a short course of suboptimal therapy. Transient therapy significantly increase the hazards of rare mutations. Thirdly, we explore the interaction between a monotherapy short course and subsequent ongoing antiretroviral therapy (ART). Appendix D deals with details of mutation combinatorics.

4.2 The Model

We develop a hybrid deterministic-stochastic model of healthy and infected T cell populations. Our analysis starts with a standard multi-strain model of in-vivo viral replication that distinguishes cells infected with one of N_{S} viral strains. These kinds of models have been used to try to understand viral evolution in the context of immune response and antiretroviral therapy [3, 5, 13, 125, 126]. For our purposes, we add a new self-consistent stochastic element to the standard deterministic model of viral evolution. Uninfected T cells are produced at rate S_{T} and die at rate μ_{T}. Virus-producing cells, infected with strain i, are counted under P_i and have a mean

lifetime of $1/\mu_{\rm P}$. Mass-action (perfect mixing) contact between infected and healthy cells produces new infected cells, with a rate constant k_i. The probability of error free transcription is given by f and ϵ_{ij} is the probability of a particular mutation, that is strain i arising out of strain j from a reverse transcription error. This leads to the base model equations:

$$\begin{aligned} \frac{dT(t)}{dt} &= S_{\rm T} - T(t)\sum_{i=1}^{N_{\rm d}} k_i P_i(t) - \mu_{\rm T} T(t) \qquad (4.2.1) \\ \frac{dP_i(t)}{dt} &= f k_i P_i(t) T(t) + \sum_{\substack{j=1 \\ j\neq i}}^{N_{\rm d}} \epsilon_{ij} k_j P_j(t) T(t) - \mu_{\rm P} P_i(t), \quad i = 1, \cdots, N_{\rm d} \end{aligned}$$

where $N_{\rm d}$ is the number of strains which are modelled by a deterministic process, i.e. those strains which are assumed to be present with sufficiently large populations for deterministic models to be sensible. We address the incorporation of rare strains shortly.

Physiologically, HIV transmission occurs either by cell-free viral particles released by infected cells, or by direct cell-to-cell contact. It has been demonstrated that cellular contacts drastically enhance productive viral transfer compared to what is observed with free virus infection [135]. Our model, like previously published models of in-vivo HIV dynamics, does not have free virions. Even if free virions are physiologically important, including them for the present purposes would not change any of our conclusions as the dynamical effects appear only at very short time scales. In our basic model, k_i is a composite fitness parameter that captures the effective cell-to-cell transmission efficiency via all mechanisms. Antiretroviral therapy with currently known drugs does not affect virion or infected-cell survival, but interferes with some stage of the viral replication cycle, i.e. reduces the values of the fitness parameter k_i. This basic model also does not explicitly incorporate the dynamics of immune

system response such as clonal expansion of effector cells or feedback linking viral and infected-cell clearance rates to the healthy cell population. Our base parameter values are given in Table 4.1.

Table 4.1: Model parameters

Symbol	Description	Value	Source
μ_{T}	natural healthy cell death rate	0.02 day^{-1}	[11]
μ_{P}	productively infected cell death rate	0.5 day^{-1}	[24]
S_{T}	supply rate of target cells	2×10^8 cells day^{-1}	Estimated
k_i	viral strain infectivity	varies	Estimated
ϵ_{21}	single-point mutation rate	2.5×10^{-5}	Appendix D
f	probability of error free transcription	0.37	Appendix D

Since it is not possible to measure all of these parameters directly in-vivo, some of these values are hypothetical, but they give rise to reasonable dynamics. We assume a universal, single-point-mutation rate, where the substitution rate of any base is of the order 10^{-4} [109]. The derivation of any particular ϵ_{ij} follows directly from combinatorial arguments outlined in the Appendix D .

Latently infected cells may be responsible for ongoing viral production in treated individuals, and their presence will introduce a longer timescale into a model. To capture effects of long-lived cells, we can consider the following model:

$$\begin{aligned}
\frac{dT(t)}{dt} &= S_{\mathrm{T}} - T(t)\sum_{i=1}^{N_{\mathrm{d}}} k_i P_i(t) - \mu_{\mathrm{T}} T(t) \\
\frac{dP_i(t)}{dt} &= fFk_i P_i(t)T(t) + \sum_{\substack{j=1 \\ j\neq i}}^{N_{\mathrm{d}}} \epsilon_{ij} k_j P_j(t)T(t) + aL_i(t) - \mu_{\mathrm{P}} P_i(t), \qquad i = 1, \cdots, N_{\mathrm{d}} \\
\frac{dL_i(t)}{dt} &= f(1-F)k_i P_i(t)T(t) - aL_i(t), \qquad i = 1, \cdots, N_{\mathrm{d}}.
\end{aligned} \tag{4.2.2}$$

Error free infected cells either become productive or latent. A fraction F of infected cells become virus producing. The others become latent and, on average, take time $1/a$ to reactivate to become virus-producing cells. For simplicity, we assume that latently infected cells have a much longer lifetime than their activation time. Note that for $F = 1$, we obtain system 4.2.1. By adjusting F (it cannot be very realistically estimated directly from data) we can vary the importance assigned to the presence of latently infected cells, without changing the equilibrium values of healthy and virus-producing infected cells. The model assumes that latently infected cells do not mutate at either infection or activation and are merely infected cells with integrated provirus that is transcriptionally silent [21, 23]. For our purposes, only a small fraction of cells become latent therefore incorporating mutation of these cells would not significantly change our conclusions. We do not attempt to capture fine physiological details of latently infected cell dynamics, but rather the concept that these cells can be the source of new productively infected cells and hence give rise to slower dynamics than a model with just virus producing infected cells.

Our main goal is to model rare mutation events which are characterized by waiting times rather than continuous processes. We consider scenarios in which the initial populations of these rare mutations are zero, and we would like to model the waiting time to their appearance. In this regime, the appearance of rare mutant strains i ($N_{\mathrm{d}} < i \leq N_{\mathrm{S}}$) should be modelled as a nonhomogenous Poisson process with intensity

$$\lambda_i(t) = T(t)\sum_{j=1}^{N_{\mathrm{d}}}\epsilon_{ij}k_jP_j(t), \quad \text{for} \quad i = N_{\mathrm{d}}+1, \cdots, N_{\mathrm{S}}, \tag{4.2.3}$$

which captures mutations from all the deterministically modelled strains. (Recall that N_{S} is the total number of strains.) According to standard survival analysis, the

probability of there being no rare mutant of type i, at time t, given that there was none at time 0, is

$$\Lambda_i(t) = \exp\left(-\int_0^t \lambda_i(\tau)d\tau\right). \tag{4.2.4}$$

The phylogenetic relationships amongst all strains, and the initial conditions, determine the number of continuously and stochastically modelled strains. We adopt the following computational procedure:

1. Initially run the deterministic model with populations for N_{d} strains, and survival functions for avoiding the $N_{\mathrm{S}} - N_{\mathrm{d}}$ rare mutants.

2. Draw a uniformly distributed random variable $R_i \in [0, 1]$ for each possible rare mutation event.

3. When Λ_i reaches R_i the appearance of mutant i occurs.

4. If the mutant appears into an environment in which it is fit enough to thrive, pause the simulation.

5. Add one cell of the new rare mutant.

6. Resume running the new deterministic model with $N'_{\mathrm{d}} = N_{\mathrm{d}} + 1$ strains.

This piecewise deterministic model is hardly more complex than a purely deterministic model. The abrupt changes to the evolving process transforms the ODE system into differential equations involving impulse effects (impulsive differential equations) [78]. The difference between our computational approach and previously considered schemes of which we are aware, is that in our scheme, mutation hazards are derived from explicit deterministic model state variables, and also, they depend on mutational

pathways, whereas, for example, in Nowak *et al* [111], the probability of generating a new mutant is proportional to the total virus population.

Note that in the computational procedure just outlined, we have only explicitly modelled the consequences of those rare genomes which have a fitness above a critical value. Of course, the appearance of low fitness mutations is also possible. We now propose that genomes with sub-critical fitness, which do not give rise to explicitly modelled populations, survive, presumably in trace quantities, for a typical time (which we call Δ) before they are driven to extinction. If there is an environmental shift during this persistence period, such as initiation of therapy that strongly suppresses the other genomes, this one can then begin to thrive and grow in the same manner as any mutation which arises into an initially favourable environment. If the perfect-mixing model is assumed to be valid on all size scales, this new timescale would simply be the lifetime of the infected cell bearing the new genome, as an unfit variant will be unlikely, under a fully stochastic treatment, to produce daughter cells. However, it is far from certain that this simple view captures the dynamics surrounding rare mutations. A small local cluster of cells bearing the new genome may have a good chance of arising from the seminal mutation, but then be almost certain to be overwhelmed ecologically within a typical time as mixing or directly competing with fitter variants occurs. Since we do not know what this time may be, we simply note the crucial role it plays in our modified survival analysis. Now, instead of simply considering the probability that the mutant has never occurred since time 0, as in equation 4.2.4, we consider the probability that a rare mutant has not occurred in the most recent time interval of size Δ, i.e.

$$\Lambda_{\Delta}(t) = \exp\left(-\int_{t-\Delta}^{t} \lambda(\tau) d\tau\right). \tag{4.2.5}$$

This new state variable is just the probability that the relevant mutant genome is absent at time t. The smallest physically feasible value of Δ is the lifetime of an infected cell (as noted above for the case where the rare mutant produces no daughter cells from the seminal mutation) and the largest feasible value is greater than the expected survival time of the infected individual (if the genome is significantly banked into a latently infected cell population) i.e. essentially infinite for practical purposes. It is particularly relevant when we model environmental shifts, such as the start or end of an antiretroviral (ARV) regimen. We will demonstrate scenarios in which the presence or absence of a 'currently unfit' genome, at the moment of initiation of therapy, can have an impact on rates of treatment failure.

4.3 Chronic Treatment

We now apply, to clinically inspired scenarios, the survival analysis of the model presented in the previous section. The particular model implementations are in certain respects simplistic preliminary work, but they demonstrate the kinds of questions that can be seriously investigated within this framework. We use a model with two continuously variable strains (wild-type and common mutant) and a waiting time for the appearance of the third strain (rare mutant). In the absence of treatment, the wild-type strain is dominant and the mutant subpopulation is present in trace quantities, of the order of the mutation rate.

We are interested in modelling mutations that occur rarely i.e. those that do not typically exist at most points in time. Consider a mutant which differs from the wild-type by three single-point mutations (say M1, M2 and M3) and from a common mutant (M1) by two-point mutations (M2 and M3). We assume that strains bearing

just M2 or M3, or any two of M1, M2 and M3 are highly fitness compromised i.e. the M1 M2 M3 (P_3) are all compensatory mutations. We use this particular phylogeny to illustrate the application of our method. Adding a rare mutant to a two-strain deterministic model as strain $i = 3$ gives the Poisson rate

$$\lambda_3(t) = T(t)\Big(\epsilon_{31}k_1P_1(t) + \epsilon_{32}k_2P_2(t)\Big), \tag{4.3.1}$$

which shows how a rare mutant variant can arise through a number of pathways, such as sequential single-point mutations or simultaneous higher-order mutations.

First, we consider a quasi steady state scenario corresponding to chronic treatment, then we model a short course of monotherapy, followed, after some delay, by initiation of chronic therapy. Important interactions between the two regimens are captured by the newly introduced state variable Λ_Δ.

We start by analyzing the steady-state dynamics of the two continuously modelled strains in the absence of a rare mutant. The choice of parameter F, which introduces latently infected cells, does not affect this analysis. An approximate, much simpler, equilibrium solution can be derived directly from the exact equations 2.1.9 by setting ϵ_{21}^2 and other higher-order terms to zero, where ϵ is replaced by ϵ_{21}:

$$\begin{aligned}
\bar{T} &= \frac{\mu_{\mathrm{P}}}{fk_1} + O(\epsilon_{21}^2) \\
\bar{P}_1 &= \frac{\mu_{\mathrm{T}}}{k_1}(R'_{01} - 1)\left(1 - \frac{\epsilon_{21}k_2}{f(k_1 - k_2)}\right) + O(\epsilon_{21}^2) \\
\bar{P}_2 &= \frac{\epsilon_{21}\mu_{\mathrm{T}}}{f(k_1 - k_2)}(R'_{01} - 1) + O(\epsilon_{21}^2),
\end{aligned} \tag{4.3.2}$$

where the wild-type is the fitter strain ($k_1 > k_2$). The basic reproductive ratio of

strain i is given by

$$R'_{0i} = \frac{f S_{\mathrm{T}} k_i}{\mu_{\mathrm{P}} \mu_{\mathrm{T}}} \qquad i = 1, 2. \tag{4.3.3}$$

We are interested in modelling the regime where R'_{0i} is always greater than one in the absence of therapy, since our main focus is on persistent infection. Note that

$$\bar{P}_2 = \frac{\epsilon_{21} k_1}{f(k_1 - k_2)} \bar{P}_1 + O(\epsilon_{21}^2). \tag{4.3.4}$$

The less-fit strain is present in trace quantities that will be very difficult to detect by standard clinical assays, even if the fitness difference is marginal. This is a modified version of the usual population genetics phenomenon that two species in a single niche do not coexist even with very similar fitness; one dominates and drives the other to extinction. The non-extinction of the less-fit quasispecies observed in this case results from the high mutation rate, which leads to waiting times between mutation events that are very small compared to the lifetimes of productively infected cells, so that the subdominant species persists in significant quantities. Given realistic orders of magnitude for infected cell populations (10^8) and lifetimes (a day), and the mutation rates between strains that differ by a single base mutation (10^{-5}) [24, 55], certain minority populations (single-point and double-point mutations relative to a dominant wild type) are large enough to be modelled deterministically.

The mean waiting time to the occurrence of a rare mutation according to the Poisson rate (equation 4.3.1) before treatment (evaluated at the pre-treatment equilibrium state) is given by

$$\langle \tau_w \rangle = \left[\bar{T} \Big(\epsilon_{31} k_1 \bar{P}_1 + \epsilon_{32} k_2 \bar{P}_2 \Big) \right]^{-1} \approx \left[\frac{S_{\mathrm{T}}(R'_{01} - 1)}{R'_{01}} \left(\epsilon_{31} + \frac{(\epsilon_{32} - \epsilon_{31}) \epsilon_{21} k_2}{f(k_1 - k_2)} \right) \right]^{-1}. \tag{4.3.5}$$

It is important to understand how fundamentally different this result (and reality)

is from a what can be obtained in a model which treats all strains deterministically. Mathematically, it is perfectly sensible to define a model with any number of deterministically strains, as per the basic model above, and to try to capture the 'rare' mutants by using suitably small mutation rates. When a purely deterministic model runs from an initial condition in which the fitter strain is absent, this absent strain is immediately produced continuously. The new strain then grows according to its fitness advantage (see figure 4.1). Thus, the time taken for it to reach some proportion

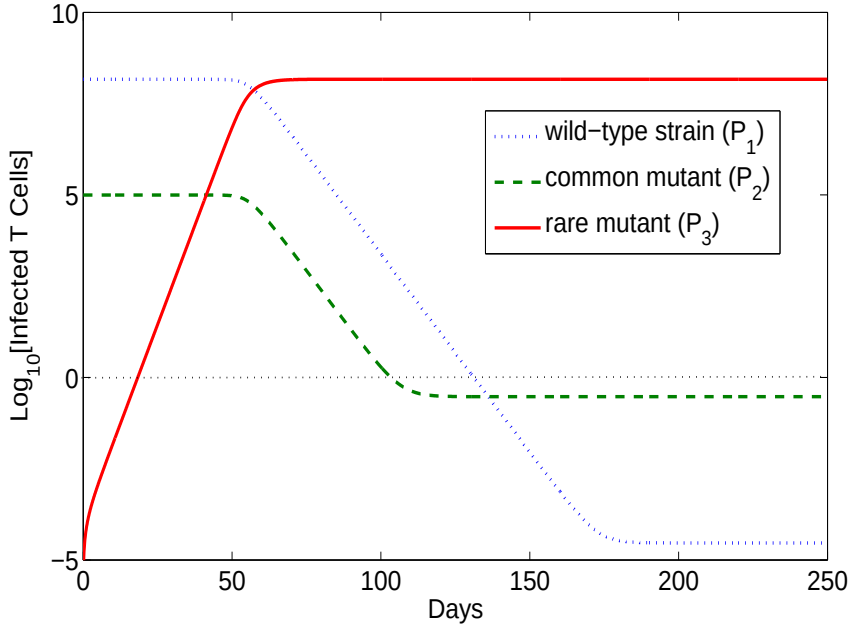

Figure 4.1: Growth of a rare mutant strain (i.e. with no waiting time) in the deterministic model. The initial value of the rare mutant (P_3) is zero whereas viral strains: wild-type (P_1) and common mutant (P_2) begin their dynamics from the steady state. The rare mutant is immediately produced continuously and grows according to its fitness advantage. The time required to attain one cell infected by this rare mutant is of the order of weeks. In these simulations, the differential fitness parameters are given by $(k_3, k_2, k_1) = (2k_1, 0.9k_1, k_1)$ where $k_1 = 2 \times 10^{-8}$; that is, the environment favours the rare mutant to outgrow existing viral variants.

of the total infected cell population is deterministic, and substantially dominated by

the dynamical interaction of the two strains. The time required to attain one cell infected by the new strain ($P_3 = 1$) can be derived by solving $P_3(t) = 1$ from an initial value of $P_3(0) = 0$, and using the dynamical equation

$$\begin{aligned} \frac{dP_3(t)}{dt} &= fk_3P_3(t)T(t) + T(t)\Big(\epsilon_{31}k_1P_1(t) + \epsilon_{32}k_2P_2(t)\Big) - \mu_{\rm P}P_3(t) \\ &= \tilde{\lambda}_3 + \mu_{\rm P}(\gamma - 1)P_3(t) \end{aligned} \tag{4.3.6}$$

where

$$\tilde{\lambda}_3 = \frac{S_{\rm T}(R'_{01} - 1)}{R'_{01}}\left(\epsilon_{31} + \frac{(\epsilon_{32} - \epsilon_{31})\epsilon_{21}k_2}{f(k_1 - k_2)}\right) \quad \text{and} \quad \gamma = \frac{k_3}{k_1} > 1. \tag{4.3.7}$$

This implements the assumption that the other cell populations are not significantly perturbed from their initial values over the time it takes to produce one cell of the rare mutant. Then

$$\langle \tau_1 \rangle = \frac{1}{\mu_{\rm P}(\gamma - 1)} \ln\left(1 + \frac{\mu_{\rm P}(\gamma - 1)}{\tilde{\lambda}_3}\right). \tag{4.3.8}$$

For the chosen parameter values (Table 4.1), the time required to attain one cell infected by the new strain is of the order of weeks (see figure 1). On the other hand, the explicitly modelled mean waiting time ($\langle \tau_w \rangle$) to the occurrence of the new mutation according to the constant Poisson rate $\tilde{\lambda}_3$ is of the order of years. It seems to us that the latter is a reasonable model of rare events and the former is fundamentally flawed.

We now return to the stochastic waiting time model, which at the pre-treatment equilibrium state, has a waiting time to the occurrence of a rare mutant of the order of years for the chosen parameter values given in Table 4.1. We are interested in the impact of long term treatment on these waiting times. Let treatment efficacy on

strain i be denoted by $\xi_i \in [0, 1]$, so that the infectivity parameter during treatment is $k_i' = \xi_i k_i$. In figures 4.2 and 4.3, we show the surface plots of the waiting times to the occurrence of rare events as a function of drug efficacy on viral strains. Less effective selection pressure or treatment that successfully suppresses both viral subpopulations results in increased waiting times or even guarantees the non-occurrence of rare mutations. Suboptimal treatment that suppresses the wild-type strain but barely affects the common mutant leads to dramatic reduction in waiting times to the occurrence of rare mutations. On the other hand, treatment that affects the common mutant but allows continuation of wild-type strain replication, increases the waiting time to the occurrence of a rare mutant.

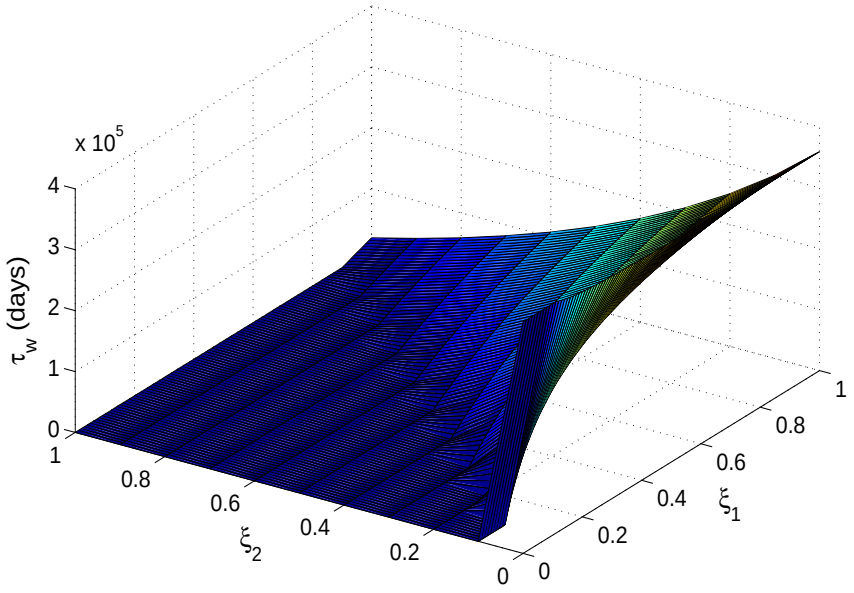

Figure 4.2: Surface plot showing the waiting times to the occurrence of rare mutations as a function of drug efficacy on viral strains (ξ_i) for $k_2 = 0.9k_1$ where $k_1 = 2 \times 10^{-8}$. The point $((\xi_1, \xi_2) = (0, 0))$ represents potent treatment that results in viral elimination.

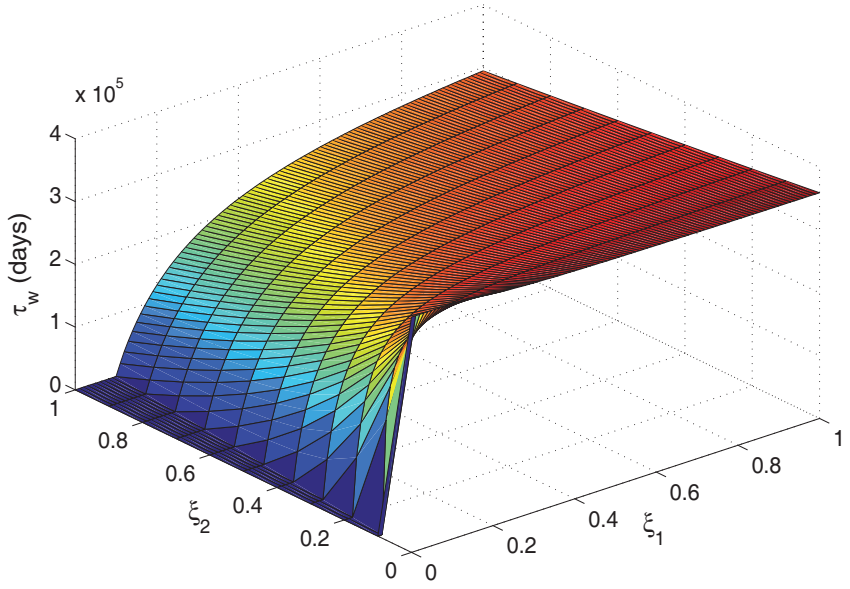

Figure 4.3: Surface plot showing the waiting times to the occurrence of rare mutations as a function of drug efficacy on viral strains (ξ_i) for $k_2 = 0.1k_1$ where $k_1 = 2 \times 10^{-8}$. The point $((\xi_1, \xi_2) = (0, 0))$ represents potent treatment that results in viral elimination.

A key result is that waiting times are significantly smaller when the common mutant is only marginally less fit, than when there is a large fitness cost. Note that these plots describe a relationship between 'clinical' parameters (waiting times) and pharmacological parameters (drug efficacies) which are difficult to determine in-vivo. On the other hand, quantitation of plasma HIV RNA can be performed to determine viral populations which in turn can be used as alternative parameters to calculate the waiting times to the occurrence of rare mutations. We demonstrate this by introducing parameters which express treatment effectiveness at the level of changes in the equilibrium viral loads. Let the treated equilibrium values of the wild-type and the mutant-strain-infected cell populations, relative to the pre-treatment wild-type

infected cell level, be given by

$$F_w = \frac{\bar{P}_1(k_1', k_2')}{\bar{P}_1(k_1, k_2)} \qquad \text{and} \qquad F_m = \frac{\bar{P}_2(k_1', k_2')}{\bar{P}_1(k_1, k_2)}, \tag{4.3.9}$$

respectively. Recalling that in the untreated state, the viral load is strongly dominated by the wild type ($\bar{P}_1(k_1, k_2)$), this notation facilitates comparisons between the treated and untreated states, both in terms of overall viral suppression, and selection between strains.

Disruption of the pre-treatment equilibrium state ($F_w = 1$ and $F_m \ll 1$) by therapy leads to different possible effects on the "benchmark" (pre-treatment) waiting time. The limiting case scenarios of interest are

1. Therapy suppresses the mutant subpopulation ($F_m \to 0$) but allows the dominant wild-type strain to replicate relatively unhindered ($F_w \approx 1$); this increases the waiting times to the occurrence of a new strain. In other words, even though the total viral load is barely affected, there is a benefit in terms of impaired viral evolution.

2. Treatment is optimal against the wild-type strain ($F_w \to 0$) but barely affects the common mutant i.e.

$$F_m \to \frac{k_1}{k_2}\left(\frac{R_{02}' - 1}{R_{01}' - 1}\right), \tag{4.3.10}$$

   where R_{0i}' is strain i reproductive ratio. This leads to a dramatic reduction in waiting times to the appearance of rare mutations, i.e. the much more rapid emergence of the rare mutant.

3. Treatment is optimal; that is, treatment that successfully suppresses both viral subpopulations ($(F_w, F_m) \to (0, 0)$). This essentially guarantees the non-occurrence of rare mutations.

4.4 Transient Nevirapine Monotherapy

We use our piecewise deterministic model to explore the consequences of transient increases in the relative frequency of common mutations (such as K103N) on the occurrence of rarer mutations, during and after short-course monotherapy. To obtain curves resembling the K103N decay data shown in figure 4.4 [90], we incorporate a population of latently infected (i.e. long-lived and non-virus-producing) cells [22, 115] that are activated to productively infected cells on a timescale of 2 to 3 weeks, by setting $F = 0.9$.

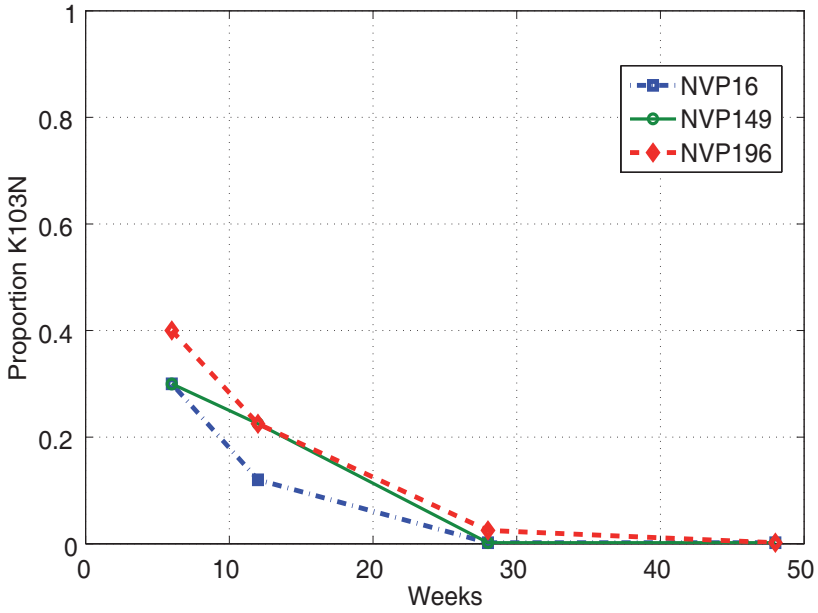

Figure 4.4: Relative fractions of K103N variants in maternal plasma viral RNA after single dose nevirapine for three individual women (NVP16, NVP19 and NVP196). We read data off a chart published in [90]. In this study, the relative abundance of K103N declined to undetectable levels by 12 months [90]

First we explore the effect of a single short course of highly selective treatment on waiting times to the appearance of rare mutations. Initiating suboptimal therapy

results in dramatic increase of the common resistant mutant (K103N) population and an equally dramatic decrease in the wild-type strain (K103) population. When pressure of therapy is discontinued, the common mutant population declines to pre-treatment levels. At every time point during and after short course therapy, we evaluate the cumulative probability of a rare mutation having occurred. Figure 4.5 illustrates the transient increase and decline in the proportion of a common mutant, and figure 4.6 shows the corresponding cumulative probabilities of observing a rare mutant. We compare the cumulative probability under transient treatment to the case in which therapy is not given at all. For the chosen parameters, the probability of observing a rare mutation, within a year in the absence of therapy, is negligible. However, transient therapy dramatically increases this probability.

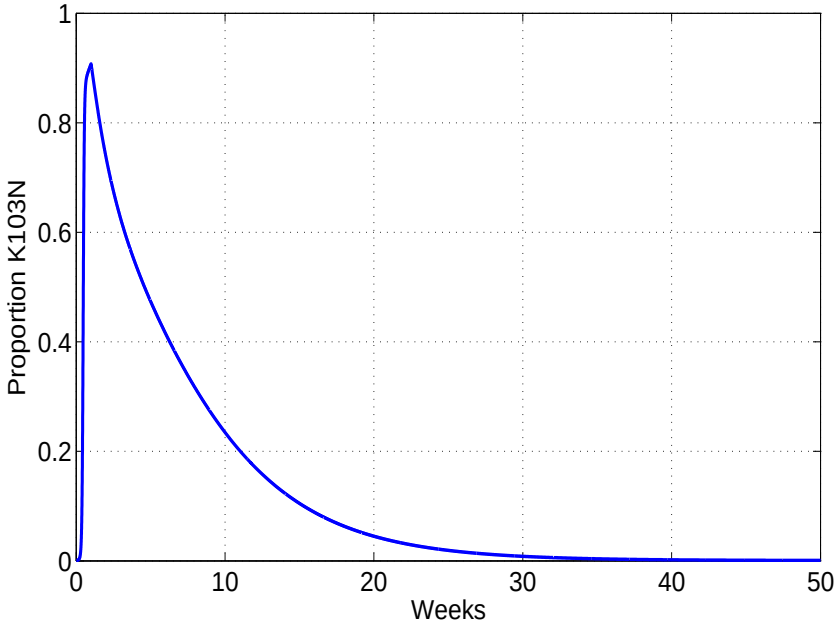

Figure 4.5: Relative frequency of K103N during and after 7 days of idealized treatment. Short-course highly selective therapy results in dramatic increases in pre-existing resistant viral variants. Withdrawal of therapy results in a slow decline of the subpopulation. We assume that 10% of infected cells become long-lived infected cells and are activated after 2 weeks i.e. we set $F = 0.90$ and $a = 1/14$.

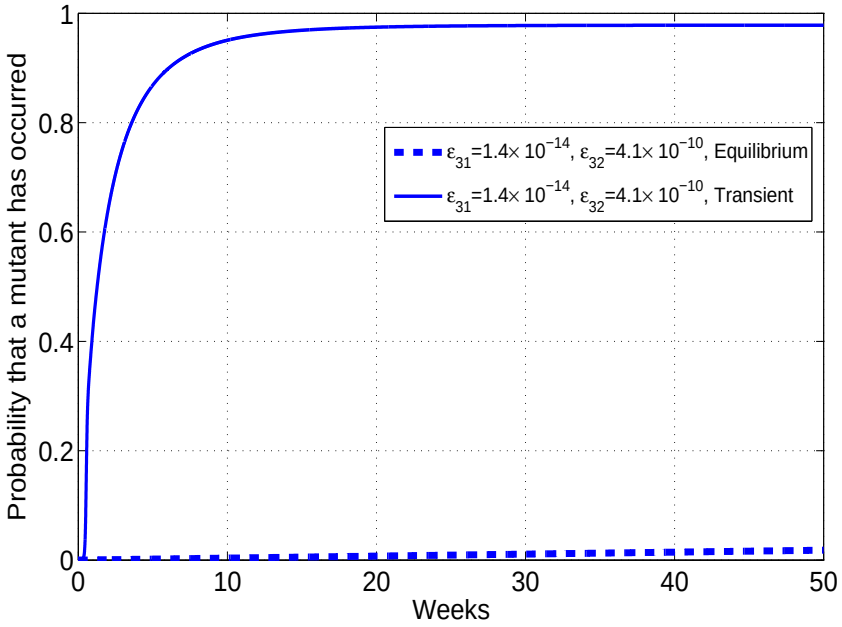

Figure 4.6: The cumulative probabilities of observing a new mutation in the absence (Equilibrium) and presence (Transient) of drug pressure. Model choices which produce a transient of a magnitude and duration shown in figure 4.5 lead to significant acceleration of viral evolution. In the absence of selective pressure chances of observing a new mutant are negligible.

Next we explore the interaction between a monotherapy short course and subsequent continuous therapy, as was investigated in the MASHI study. We evaluate the probability that a rare mutant is currently present at time t, given various possible values of the rare mutant persistence timescale Δ (see figure 4.7). For values of Δ less than 60 days, the probability of a rare mutant being present, at some point more than 6 months after the single dose of NVP, is small ($< 5\%$) i.e. cells infected by the new genome are unlikely to be present, and hence pose a low residual risk if the mother is put on treatment more than six months after single dose Nevirapine for PMTCT. This is not inconsistent with the clinical findings from the MASHI study [88]. The

reality is presumably more complex than what our model can capture, but little is known about the persistence of unfit mutants. It has been observed that resistant genomes may persists, even at undetectable level, for prolonged periods [17, 35]. It makes sense that initiating therapy in the presence of a therapy defeating mutant, or an immediate precursor to such a mutant (even at levels too low for detection by typical assays), will reduce chances for treatment success.

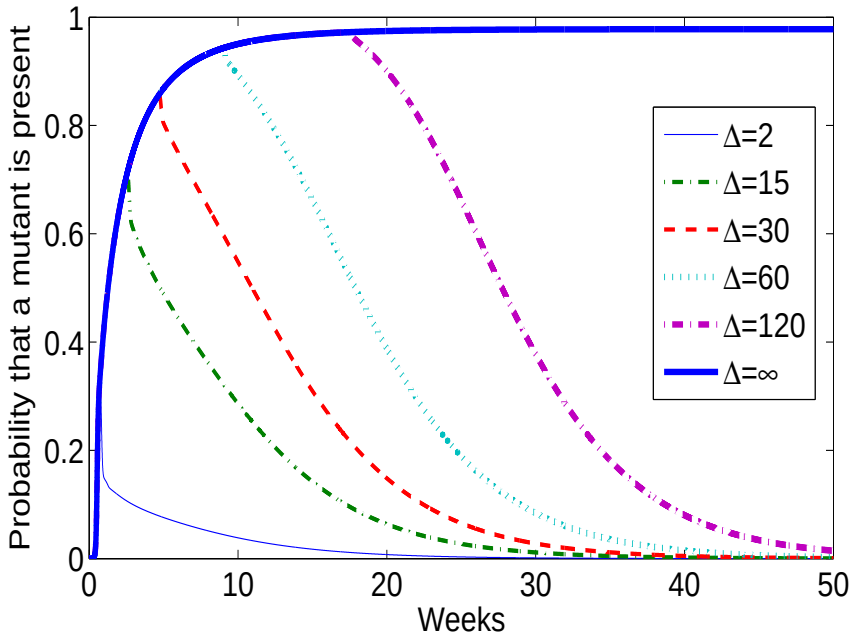

Figure 4.7: The probability of there existing a mutant which persists for a time Δ after a seminal mutation, plotted as a function of time from a brief period of selective pressure (such as single dose NVP). Plots are shown for a number of values Δ ranging from 2 days to 350 (taken as ∞) days. The other parameter values are as in figure 4.5.

4.5 Conclusion

We have considered a number of more-or-less standard deterministic multi-strain models of in-vivo viral dynamics, which are tunable to produce scenarios like a chronic ARV regimen, and a short course of monotherapy. We have adjoined a stochastic component to these models, in the form of a 'sliding window' survival analysis, which substantially expands the possible analyses of rare strain dynamics within the framework of ordinary differential equations.

We have considered scenarios which capture the concepts of a dominant wild-type strain, a relatively unimpaired 1 base mutant, a number of unviable 2 base mutants, and the possibility of compensatory mutations which lead to a treatment defeating 3 base mutant that is reachable by different pathways, *which have different relative importance at various stages during transient dynamics.* Different phylogenies, together with different chosen fitness parameter values, will result in different numbers of deterministically and stochastically modelled strains and pathways, all of which can immediately be accommodated into our general model.

The transient increases in common subpopulations of cells infected by mutant genomes produced by the short course of antiviral therapy affects waiting times to the appearance of rare mutations, conceived as differing more from the wild type than from the deterministically modelled primary mutant. Over a range of model choices which produce a transient of the order (size and duration) of that known to occur under nevirapine monotherapy used for PMTCT, there is significant acceleration of viral evolution - even from just the short course alone. This effect is suspected, but not unambiguously observed, from clinical studies.

A further important set of questions arises about the risks associated with initiation of chronic therapy (HAART) a short while after the suboptimal transient regimen like for PMTCT. Our newly proposed additional timescale Δ, representing the persistence of a new genome in an infavourable environment has a substantial impact on the rates of treatment failure.

These models demonstrate that even transient subpopulations of common mutants which appear to fade are associated with accelerated appearance of rarer mutations. Further work which should be performed includes 1) variations on these models which are designed to capture precise genetic differences (and hence realistic pathways and mutation rates) between sets of quasispecies being directly observed in studies utilising highly sensitive assays, and 2) biological investigation into the dynamics of small populations of new mutants (the theme of chapter 5), which these models summarise into the timescale Λ_Δ.

4.6 Summary of Implications for Public Health

Results in this chapter show that even relatively brief, and fully reversed, increases in subpopulations of common mutants are associated with accelerated appearance of further rarer mutations. The accelerated appearance of new genomes in patients on failing therapy highlights a potential risk for public health. The analysis highlights an important point of biology which is difficult to observe, and on which experimental evidence would be instructive. Specifically, it is likely that rare mutations carrying potentially serious properties like multiple drug resistance occur from time to time, but that these variants are created largely in unfavourable environments where they do not thrive, so that they usually become extinct in a short time. Knowledge of

how long these transient subpopulations of new genomes persist would help guide expectations for studies trying to link patterns of treatment, viral load, etc. to longer term outcomes like regimen failure. These issues will need to be investigated in the long run as more and more clinicians and their patients face complex decisions about regimen choice and switch.

Chapter 5

Modelling the Persistence of Drug Resistant Mutations After Cessation of Suboptimal Therapy

5.1 Introduction

This chapter reflects on how the the previous chapter might be extended. In chapter 4, we showed how suboptimal therapy may accelerate the appearance of higher order rarer mutations. However, we did not investigate in a dynamically consistent way whether the new cell harboring the rare mutant will die before infecting other cells or before infecting enough other cells for it to be fixed, i.e. the persistence of mutants. The absolute time it takes for subcritical minority variants to eventually go to extinction is not known. Initiating therapy in the presence of a therapy defeating mutant, even at levels too low for detection by typical assays, will reduce chances for treatment success. Since we do not know what this time may be, in the previous chapter, we simply noted the crucial role it plays in the modified survival analysis. In reality, the new rare mutant has to compete with existing strains, i.e. its persistence depends on its characteristics such as viability and replication ability.

In clinical practice, resistance tests are performed at baseline and also on patients who are failing therapy. However, there is a big danger of misinterpreting resistance tests, due to failure in minority mutation detection, such that clinicians may end up administering regimens that may fail to suppress viremia. In treatment naive patients, mutations that are not detected at baseline may subsequently emerge during the early weeks of therapy [102]. In patients on failing regimens, newly emergent mutations may not be detected because they may not replicate to levels that are detectable. Administering therapy in the presence of these undetectable minority species increases the risk of continued selective pressure which may result in development of additional mutations.

The persistence of transmitted or primary drug resistance has been assessed [10, 15, 29, 43, 85, 119] and results have shown that primary resistance persists over a prolonged time-period even in cases where mutants have impaired replicative competence. Secondary resistance (developed in response to antiretroviral treatment) is usually lost at a rapid rate [10]. However, little is known about typical persistence times of these small populations.

Here, we investigate the persistence of secondary resistance that develops after a short course treatment. We perform numerical simulations of the hybrid model developed in the previous chapter. Our framework allows us to assess the role of stochasticity and its interplay with nonlinearity. This framework is appropriate for modelling small populations as ODEs cannot incorporate high heterogeneity, because small populations become important and important events become random. To better understand the relationship between fitness cost and persistence times, we vary the new genome's replicative ability and determine the likelihood of persistence of this

new genome lineage in the face of competition from existing strains after its initial appearance. The replacement or mutual co-existence of strains is strongly influenced by competition. The only form of competition in our model is the infection of healthy target T cells.

5.2 The Model

From the deterministic model developed in chapter 4 given by system of equations 4.2.2, we can derive a full stochastic model, i.e. a Markov jump process. The schema for this process, which specifies the probability of the system transitioning to each of the possible states, is given in Table 5.1. Recall that the model assumes, for simplicity, that latently infected cells do not mutate at either infection or activation and are merely infected cells with integrated provirus that is transcriptionally silent [21, 23]. The sojourn times in each state of the process follow an exponential distribution, thus stochastic events are timed by an exponential clock with a parameter

$$\begin{aligned}\Omega &= \sum_{\text{Jumps}} (\text{Rate})\,; \\ &= S_{\text{T}} + \mu_{\text{T}} T + \sum_{i=1}^{N_s} \Big(f k_i P_i T + \mu_{\text{P}} P_i + a L_i \Big) + \sum_{\substack{i=1 \\ j \neq i}}^{N_s} \epsilon_{ji} k_i P_i T, \end{aligned} \tag{5.2.1}$$

a sum of all allowed jump rates (see Table 5.1). This parameter is an average of an exponential distribution and is used to generate the next jump time. Also, the type of the next jump is random in this stochastic process. Assuming that both jumps and jump times are random is convenient because even in theory we don't know when the next event (e.g. infection of a target cell, death of an infected or uninfected cell, etc) will occur, nor even what it will be.

Table 5.1: Stochastic process schema showing allowed jumps and jump rates

Event	Jump	Rate
Supply of target T cells	$T \to T+1$	S_{T}
Target T cell death	$T \to T-1$	$\mu_{\mathrm{T}} T$
Infection of T cells by strain i :		
(a) error free transcription :		
(i) productive infection	$T \to T-1$ and $P_i \to P_i+1$	fFk_iP_iT
(ii) latent infection	$T \to T-1$ and $L_i \to L_i+1$	$f(1-F)k_iP_iT$
(b) mutation into strain j (for $j \neq i$)	$T \to T-1$ and $P_j \to P_j+1$	$\epsilon_{ji}k_iP_iT$
Activation of strain i latently infected cell	$L_i \to L_i-1$ and $P_i \to P_i+1$	aL_i
Strain i productively infected cell death	$P_i \to P_i-1$	$\mu_{\mathrm{P}} P_i$

One standard way of analyzing this problem is to use Gillespie's algorithm [45] but because some of our processes involve large numbers (billions of cells), this method becomes inefficient as it searches for the next event (maybe in less than a nanoday) [72, 149]. Although efficient methods have been developed that involve either grouping together processes that occur in fast succession (τ - leap methods) [16, 46, 123], application of quasi-steady-state theory [122], or averaging over first reactions [60],

purely stochastic simulations of such systems remain computationally expensive.

We adopt a strategy that models processes with a large number of cells (fast rates) in a deterministic way whilst keeping small populations as stochastic processes (i.e. minority populations become random). Mixed frameworks have been proposed to simulate biochemical systems [2, 54, 73, 138, 147]. They are mainly based on a prediction correction type heuristics for the realization of the stochastic part. The main concept is to first calculate the time (waiting time) in which a stochastic event should occur. During the waiting time to the next jump, the ODE component of the process is kept evolving [2]. Our populations are divided into compartments. Small populations evolve in a discrete compartment and we call this compartment D whilst large populations are in a continuous compartment called C simulated by ODEs, i.e. our compartments are:

$$\{T, P_1, P_2, L_1, L_2\} \in C \quad \text{and} \quad \{P_3, L_3\} \in D.$$

In our mixed method, the dynamics of healthy T cells, wild-type and common mutant infected cells is given by the sum of all fast rates or simply by a set of ODEs given in chapter 4 (equation 4.2.2) whilst the stochastic schema for the discrete populations P_3 and L_3 is given in Table 5.2. We write the mutations' fitness parameter as $k_i = (1 - f_i)k_1$ for $i = 2, 3$ and f_2, f_3 are fitness costs for the common and rare mutant, respectively. To simulate our system, we use the direct hybrid method [2]. This method explicitly calculates which event occurs next and when it occurs. At the beginning, the system is set to the initial state. An exponential random number with a mean of one is drawn to prepare for the numerical integration of the ODE system. The time to a discrete event is determined by the cumulative hazard function that depends on the state of the system. If a discrete event has been generated, the next

event to occur is randomly chosen and the state variables are updated accordingly. This procedure continues until the entire trajectory is computed. The pseudo-code is given in Appendix E.

Table 5.2: Stochastic process schema showing allowed jumps and jump rates for small populations (or for slow rates)

Event	Jump	Rate
Infection of T cells by strain i :		
(a) error free transcription :		
(i) productive infection	$T \to T-1$ and $P_3 \to P_3+1$	fFk_3P_3T
(ii) latent infection	$T \to T-1$ and $L_3 \to L_3+1$	$f(1-F)k_3P_3T$
(b) mutation into strain P_3 $(i=1,2)$	$T \to T-1$ and $P_3 \to P_3+1$	$\epsilon_{3i}k_iP_iT$
Activation of latently infected cell	$L_3 \to L_3-1$ and $P_3 \to P_3+1$	aL_3
Productively infected cell death	$P_3 \to P_3-1$	$\mu_{\mathrm{P}}P_3$

We have explained in principle how hybrid simulations can be done (an example is given in the next section). To determine approximately persistence of new genomes does not require explicit modelling of the stochastic process of population eradication. We now demonstrate that, in practice, population numbers for infected cells are typically large enough to be modelled deterministically for heuristic conclusions about

magnitudes of persistence times, i.e. "deterministic extinction". A scenario in which we can model stochastic persistence explicitly is the radioactive decay process. We assume that a constant per-item decay rate is given by the parameter λ, and we calculate the mean time it takes to reach 0 items, starting from an initial population of P. This mean decay time is given by

$$\mathbb{E}[\tau_0] = \frac{1}{\lambda} \sum_{n=1}^{P} \frac{1}{n}.$$

We can calculate the number of cells at $\mathbb{E}[\tau_0]$, in the deterministic version of the model, as

$$P(\mathbb{E}[\tau_0]) = Pe^{-\lambda \mathbb{E}[\tau_0]}. \tag{5.2.2}$$

The coefficient of variation (the ratio of the standard deviation to the mean) is calculated as:

$$c_v = \frac{\sqrt{\text{var}}}{\mathbb{E}[\tau_0]}, \tag{5.2.3}$$

where the numerator is the standard deviation (square root of the variance). The variance of the decay time is given by:

$$\text{var} = \frac{1}{\lambda^2} \sum_{n=1}^{P} \frac{1}{n^2}.$$

We show the dependence of the expected number of cells at the expected time to decline to zero and the coefficient of variation with the initial population size in figure 5.1. The number of cells evaluated at the expected decay time rapidly approaches an asymptote with a value close to one half and the coefficient of variation, for a population that starts at a size of at least 100 is somewhat less than 20%, but declines slowly with initial population size. Evidently, the intrinsic uncertainty in persistence in the stochastic process dominates over any error made in using the deterministic

model to estimate expectation values. In this example, it was not difficult to calculate the stochastic result, but in the HIV applications which follow, there is not a single decay rate, so the fully stochastic model is considerably more complex. We will model a fading subpopulation deterministically.

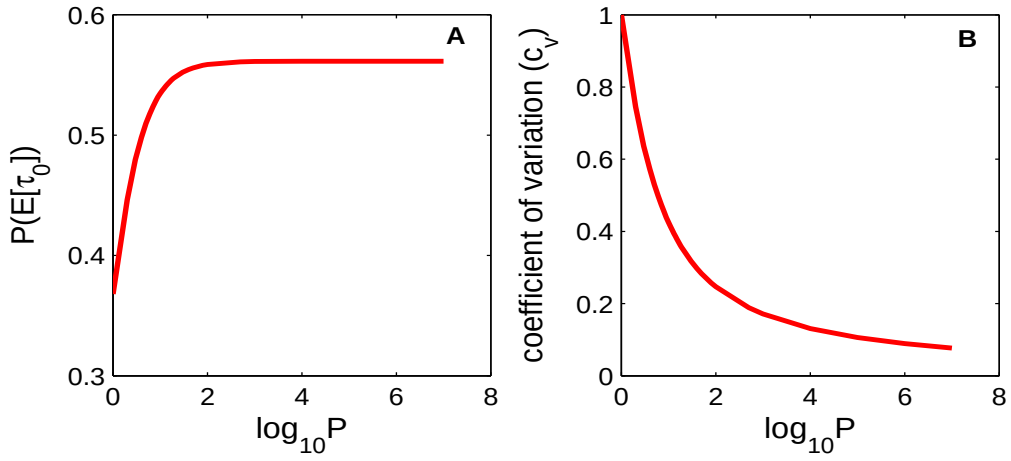

Figure 5.1: A: The number of cells at the expected decay time, i.e. "deterministic extinction". B:The coefficient of variation as a function of the initial population size.

5.3 Persistence of Rare Mutations

First, we present simulations of the hybrid model that resemble the single dose NVP case presented in chapter 4, where we have assumed a 10% fitness cost ($f_2 = 0.1$) for the common mutant strain and a 5% fitness cost ($f_3 = 0.05$) for the rare mutant that appears as a result of suboptimal suppression. The dynamics of all populations started from an infected equilibrium state with two strains (see equation 2.1.9) are shown in figure 5.2. We assume treatment is administered for 7 days. For these parameter values, the mean time to appearance of a rare mutant is 0.54 ± 0.005 weeks (with a probability of appearance within a year of 0.9998 after 10^4 runs).

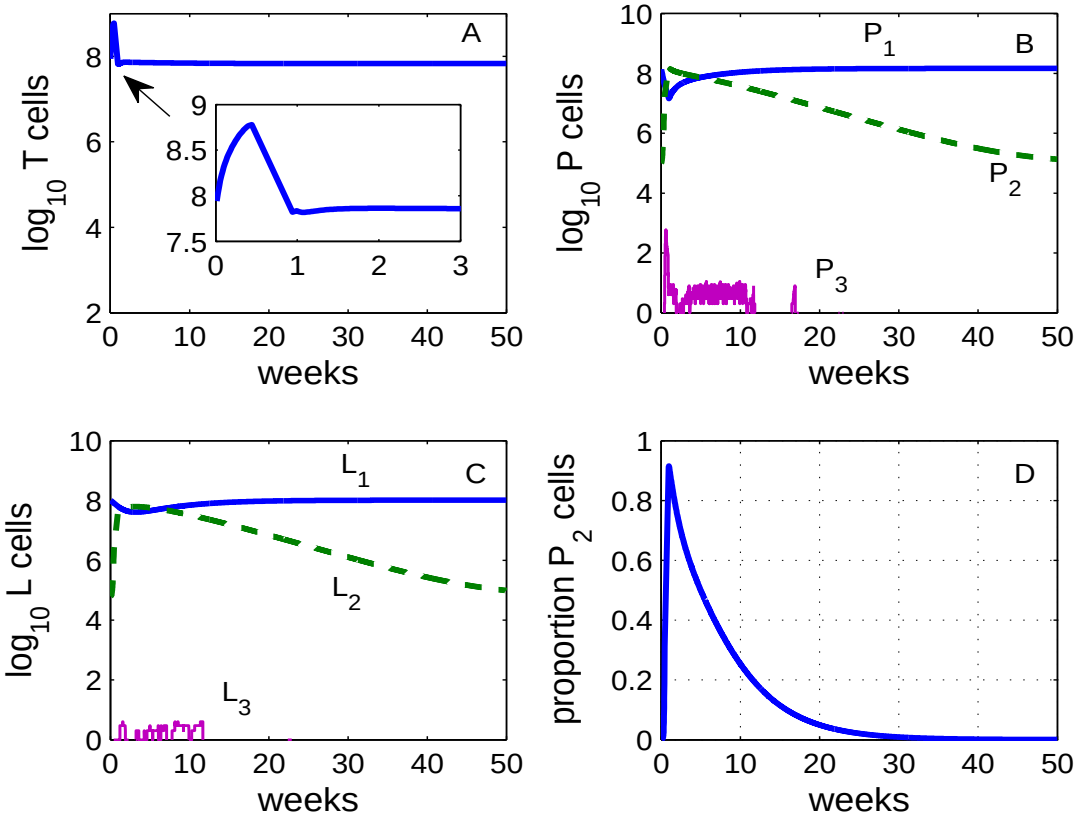

Figure 5.2: A single realization showing the dynamics of infected cell populations for a scenario such as NVP given previously. A: uninfected T cells, B: productively infected cells, C: latently infected cells and D: proportion of P_2 cells. Here $f_2 = 0.1$, $f_3 = 0.05$, $k_1 = 2 \times 10^{-8}$, we assumed 7 days of idealized treatment and simulations are started at the two strain equilibrium state.

Now we investigate the typical time until a small cluster of cells infected by the new genome persist before disappearing. Using the survival function for the appearance of a rare mutant given by equation 4.2.4 (see figure 5.3(A)), we can calculate the distribution of times to first occurrence of a rare mutant, i.e. the probability that a rare mutant first appears in any interval [a b] is given by $\Lambda(a) - \Lambda(b)$. For short term treatment, we calculate the probability that a rare mutant will appear in sub-intervals

between 0 and 7 days. These intervals for the time to first appearance of the rare mutant are broken down as in Table 5.3. A new rare genome with a subcritical fitness cost that appears in the absence of selective pressure persists for a while or even make occasional offspring and finally go to extinction. We want to assess persistence time of subcritical genomes that appear, survive for a short time in the presence of pressure that favours them and then go to extinction after the removal of selective pressure.

Table 5.3: The probability that a new rare mutant will appear in a given interval, using the survival function given by equation 4.2.4.

Interval	[0 1]	[1.01 2]	[2.01 3]	[3.01 4]	[4.01 5]	[5.01 6]	[6.01 7]	[$\geq$ 7.01]
prob (%)	0.02	0.11	1.84	19.24	11.35	5.21	4.65	57.58

In figure 5.3(B), we show the dynamics of wild-type, common mutant and rare mutant infected cells. We assume that prior to treatment we have only two strains (wild-type and common mutant) and after starting treatment, the new genome (rare mutant) appears after 0.5 days. Recall that the new genome is only rare in the absence of suboptimal therapy. In this case, the new genome carries a 10% fitness cost relative to the wild-type strain. Under drug influence the environment is favourable for the rare mutant (it is fitter than the wild-type strain) so it grows to fairly large populations such that we can use the deterministic model to compute "deterministic extinction" times. In this scenario, the appearance of the rare mutant is stochastic and its growth and decay are treated deterministically.

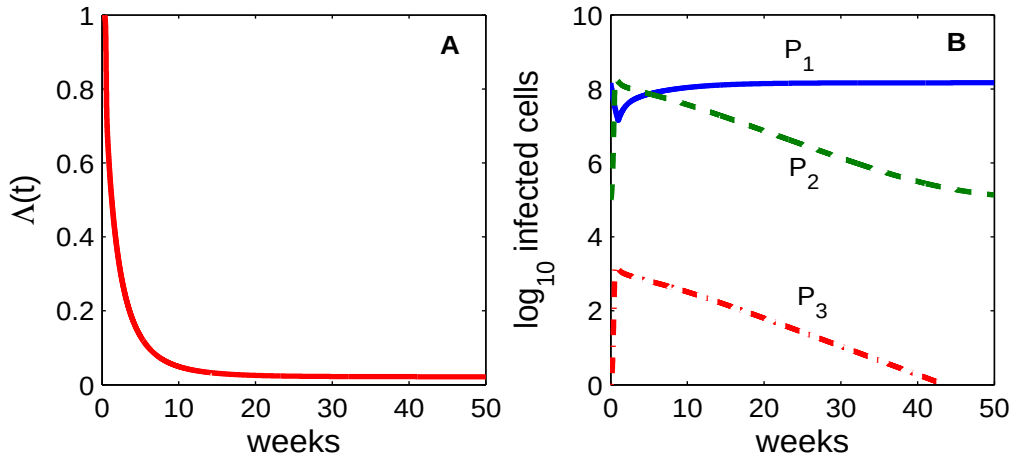

Figure 5.3: A: Survival function, $\Lambda(t)$, up to 350 days and B: The dynamics of all infected cell populations (wild-type (P_1), common mutant (P_2) and rare mutant (P_3)) when treatment is administered for 7 days. Here $f_2 = f_3 = 0.1$, $k_1 = 2 \times 10^{-8}$, and simulations are started at the two strain equilibrium state. The rare mutant is allowed to appear after 0.5 days.

Now we vary the replicative disadvantage of the new genome and time of appearance and assess the typical time it takes to decay to a single cell. In our simulations, we introduce a new rare mutant at the middle of each interval and allow it to grow deterministically and assess the time it takes for its population to reach a single cell ("deterministic extinction" time). Now, we can ask questions such as: what is the probability that a cluster of cells infected by the new genome exist in the population at 6, 12 and 18 months for varying fitness cost parameter?

For illustration purposes, we assume that a rare genome carries either a 5%, 10% or 50% fitness cost relative to the wild-type strain. For each of these replicative competencies, we assess the persistence of the new genome that appears at the centre of these intervals [0 1], [1.01 2], [2.01 3], [3.01 4] and [4.01 5]. We let the rare mutant population size decline to a value near one, see figure 5.4 which shows the dynamics of

the rare mutant infected cell population. Through eye-balling, we note the population size of rare mutant infected cells at different time points (6, 12 and 18 months for our scenario) after suboptimal treatment and determine persistence through stochastic averaging over initial conditions, i.e. use the probability distribution of appearance given by the intervals (see Table 5.3) to evaluate the likelihood of persistence, see Table 5.4.

After 18 months, only mutants that emerge at the centre of either intervals [0 1] or [1.01 2] (and if the mutants carry a 5% fitness cost relative to the wild-type strain) will be still present in the population. Thus the probability that a rare mutant with a 5% fitness cost will exist after 18 months is approximately given by 0.1%, which is calculated from the sum of respective probabilities of appearance in intervals [0 1] and [1.01 2], i.e. 0.02% + 0.11% rounded off to 1 decimal point. Similarly, assuming a rare mutant with a 10% fitness cost, there is a 2% probability that it will persist beyond 6 months (since genomes that appear at the centre of three intervals [0 1], [1.01 2] and [2.01 3] will be still present). A new genome with a 50% growth disadvantage is guaranteed to die out quickly.

From this ad hoc approach of using initial stochastic conditions to predict intrinsic population decay rates, i.e. extinction probabilities, we observe that there is a complicated relationship between persistence time and the time at which the new genomes appear. Small population persistence is determined by both replication competence and the environment.

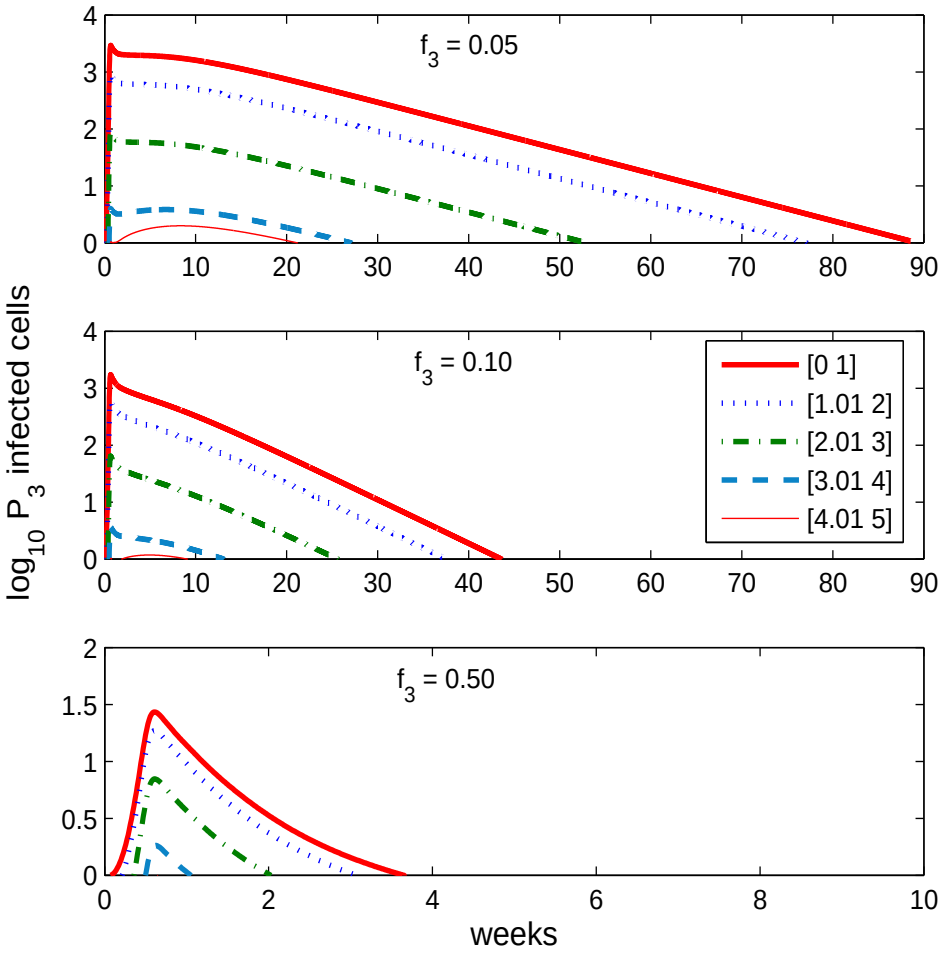

Figure 5.4: Dynamics of the rare mutant with 5%, 10% and 50% fitness cost relative to the wild-type strain that gets produced at the centre of the intervals [0 1], [1.01 2], [2.01 3], [3.01 4] and [4.01 5]. The other parameter values are as in figure 5.2.

Table 5.4: The probability that rare mutant infected cells exist at 6, 12 and 18 months as a function of growth disadvantage and time of occurrence (these are approximate values).

Rare mutant fitness cost(f_3)	6 months	12 months	18 months
0.05	21%	2%	0.1%
0.10	2%	0%	0%
0.50	0%	0%	0%

5.4 Conclusion

Numerical simulations of the hybrid model confirm the significant acceleration of viral evolution from just the short course treatment. We have performed full simulations incorporating assumptions on the replicative competence of the new genome to assess persistence of secondary resistance after short course treatment. Varying the rare genome's replicative ability and the time to appearance, we have determined the period at which the new genome lineage will be sustained in the face of competition from existing strains after the initial appearance of a single cell with a new genome.

In terms of the interaction between a short course and subsequent continuous therapy, model results have shown that the disappearance of a rare mutant carrying a 10% fitness cost or more relative to the founder at some point more than 6 months after selective therapy is highly likely (there is a 2% likelihood of persistence for rare genomes with such replicative competence). This is comparable to the small probabilities of a rare mutant being present derived using the modified survival analysis previously. Administering therapy in the presence of these undetectable minority species increases the risk of continued selective pressure which may result in

development of additional mutations.

These results are also important in the setting of HIV-1 suboptimal chronic treatment. It is not known whether the benefits of continued treatment with a failing regimen outweigh those of interrupting failing therapy. Maintaining suboptimal treatment may have immunological and virological benefits, e.g. stable immune cells and viral load despite limited control of viral replication [28, 104]. However, long term exposure to incomplete viral suppression may lead to the development of additional mutations and continued exposure to drug toxicities [91, 104]. There may be benefits of discontinuing failing therapy in spite of viral rebound, such as loss of resistance mutations [28, 66, 95]. Some studies on patients with previous treatment failures and multidrug-resistant virus indicated that in some patients a shift to complete wild-type population may occur upon discontinuation of all treatments [30] and that treatment re-initiation in patients who had interrupted treatment may achieve durable virus population suppression [27, 104]. In patients failing first line regimens, it may be beneficial to give drug holidays before administering a second line or salvage regimen to allow the minority variants to eventually die out.

In our models, the only form of competition is infection of target cells. It remains to be seen if this form of competition alone is sufficient to block or enable the formation of quasi-species. Another issue is whether the evolution of new genomes is a function of population sizes of existing strains alone or is due to intrinsic randomness in retroviral reproduction caused by the varying activation of target cells or both. However, as a starting point, our framework is heuristically sensible, it demonstrates the interplay of deterministic evolution with stochastic averaging over initial conditions.

5.5 Summary of Implications for Public Health

It is very difficult, or impossible, to observe small subpopulations of virions and infected cells by standard laboratory assays, so there is little direct data on these populations. Mathematical modelling, after making particular assumptions, may be the only recourse available to develop intuition on the dynamics of these undetectable populations. This might not yield precise estimates but at least qualitative results such as distinguishing fast from slow decay rates of subpopulations with no selective advantage. The analysis in this work shows that there is a complex relationship between occurrence time and persistence of new variants. We might not have obtained credible estimates of persistence times but the model shows that subcritical genomes have a high chance of going to extinction. Clinical studies of molecular evolution guided by modelling of this kind may shed light on how best to manage patients seen to be on failing regimens, helping shed light on such options as quick switching, what regimen to switch to, whether to have drug holidays between regimens, or perhaps even interim regimens.

Chapter 6

Conclusion

In this chapter, we take stock of what we have achieved in this thesis and suggest areas of extension. The aims of the thesis were to develop and test appropriate models of viral evolution, and then use these models to investigate the impact of acute infection dynamics on the accumulation of mutations, the effect of suboptimal therapy on the appearance of rare higher order mutations and the persistence of new variants after suboptimal treatment. We tried to ensure that the models remain close to the biology, so that the models will be fairly transparent and comprehensible to experimentalists. On the other hand, a "kitchen sink", approach where just about every known physiological or immunological detail is incorporated, was avoided, since the aim was to gain some insight into overall system behaviours.

6.1 The Results

We demonstrated that while ODE models may be adequate for modelling mutations of HIV as some variants may be produced many times a day, they are inappropriate

to model the generation of rare mutants, as they have no explicit waiting time to the occurrence of rare mutants. The sequence evolution framework developed by Lee et al.[79] was successful in assessing the degree of viral diversity during the early phase of infection. However the effect of assumptions such as differential fitness and selection pressure can significantly affect the overall conclusions. Viral diversity measures are important as they can act as signals of epidemiological and clinical outcomes. We suggest that diversity indicators that correlate to prognosis need to be sought in experiments and clinical trials.

Transient effects of therapeutic interventions early in infection, that confer a fitness cost to early viruses, can significantly reduce the extent of diversity later during the chronic state of infection. This stands in contrast to the concern that early selective pressure may increase the probability of later existence of drug resistance mutations, for example. These models may be useful to illustrate the impact of vaccines and PrEP on viral evolution in the case of breakthrough infection.

Scenarios with a transient change in relative fitness of strains, of a magnitude and duration such as is known to occur under NVP monotherapy, exhibit significantly accelerated viral evolution compared to no-treatment scenarios. Total viral load suppression (which results in reduced overall viral replication) but with transient/temporary increases (order of weeks) of common minority mutants can lead to acceleration of rarer mutations appearance. Experimental data on the persistence of small subpopulations of rare mutants, in unfavourable environments, should be sought, as this affects the risk of subverting later regimens.

Simulations of the hybrid model shows that some unfit drug resistant viruses, even those carrying only a small fitness cost relative to the wild-type strain, would

not persist indefinitely in the absence of selective pressure. This suggests that discontinuing failing therapy for a certain period may give patients a better opportunity for viral suppression with subsequent regimens. The idea is to understand the effects of suboptimal therapy and its interruption on patient management.

6.2 Future Directions

The topics discussed within this thesis leave considerable scope for further research and development. Perhaps the most fruitful avenue would not be by developing more nuanced or sophisticated mathematical models, but by working more closely with specific data sets. For example, we constructed a model scenario inspired by data about NVP containing regimens, by choosing a particular phylogeny to explore the effects of a suboptimal regimen on the common and rare resistant mutants. It captures the concepts of a primary, relatively unimpaired mutant, a number of unviable 2 base mutants, and the possibility of compensatory mutations which lead to a treatment defeating 3 base mutant that is reachable by different pathways which have different relative importance at various stages during transient dynamics. While we do not claim that this is a truly faithful representation of the relevant physiology, realistic trees can be chosen, and they can be immediately accommodated into our general framework. Recently, the advent of new sequencing technologies, vast amounts of HIV-1 clinical data have become available for analysis. The mathematical modelling presented in this thesis can be extended and coupled with statistical methods to understand and predict the dynamics and control of HIV-1 infection.

6.3 Strengthening Multidisciplinary Collaborations

In this thesis we have attempted to answer specific questions on viral evolution during acute infection and suboptimal treatment using mathematical models. Perhaps our models have generated more questions than answers, but these appear to be important questions for the management of patients infected with HIV, so that viral evolution can be limited. The complex interplay between laboratory, clinical and mathematical disciplines suggests that communication and active collaboration across these fields should be enhanced, to develop new concepts in HIV/AIDS pathogenesis, and understand their implications for patients.

Appendix A

Generating Functions

Generating functions are a useful tool for calculating probabilities and expectations. Any sequence of real numbers can be transformed into several kinds of "generating functions", in this case a power series. Let us consider a positive count (Z_+) random variable X, i.e. a discrete random variable taking non-negative values, such that $p_k = \mathbb{P}(X = k)$. We can write $X \sim \{p_k\}_{k\geq 0}$ and say that $\{p_k\}$ is the distribution of X [75].

Definition A.0.1. (Definition of the probability generating function)[75]. The probability generating function G_X of a Z_+-valued random variable is a function $G_X(s) = \mathbb{E}(s^X) = \sum_{k=0}^{\infty} p_k s^k$ for those values of the parameter s for which the sum converges. For a given sequence, there exists a radius of convergence such that the sum converges absolutely if $|s| < 1$ and diverges if $|s| > 1$, i.e. the symbolic argument $s \in U \equiv [0, 1]$.

The following properties are true for the power series, $G_X(s)$:

$$G_X(1) = 1, \qquad \text{and} \qquad G_X(0) = p_0.$$

We can recover the coefficient p_k by calculating the kth derivative of $G_X(s)$ at $s = 0$, i.e

$$p_k = \frac{G_X^{(k)}(0)}{k!}$$

The kth factorial moment of X is $\mu_k = G_X^{(k)}(1)$ such that the first derivative of the series evaluated at $s = 1$ is the expectation of the random variable X. If X and Y are two independent Z_+-valued random variables, then we have $G_{X+Y}(s) = G_X(s)G_Y(s)$.

Proof.

$$\begin{aligned} G_{X+Y}(s) &= \mathbb{E}(s^{X+Y}); \\ &= \mathbb{E}(s^X)\mathbb{E}(s^Y) \qquad \text{(independence)}; \\ &= G_X(s)G_Y(s). \end{aligned} \tag{A.0.1}$$

□

If N is a discrete random variable with probability generating function G_N. If $X_1, X_2, \cdots, X_N$ are independent count random variables and identically distributed, with a common probability generating function G_X such that $N, X_1, X_2, \cdots, X_N$ are independent count random variables, then $S_N = X_1 + \cdots + X_N$ has a probability generating function $G_{S_N}(s) = G_N(G_X(s))$ [52].

Proof.

$$\begin{aligned}
G_{S_N}(s) &= \mathbb{E}\Big(s^{S_N}\Big) \\
&= \sum_{n=0}^{\infty} \mathbb{E}\Big(s^{S_N}\Big|N=n\Big)\mathbb{P}(N=n) \qquad \text{(conditioning on } N \text{ - see Appendix B)} \\
&= \sum_{n=0}^{\infty} \mathbb{E}(s^{S_n})\mathbb{P}(N=n) \\
&= \sum_{n=0}^{\infty} G_{X_1+\cdots+X_n}(s)\mathbb{P}(N=n) \\
&= \sum_{n=0}^{\infty} \Big[G_X(s)\Big]^n \mathbb{P}(N=n) \\
&= G_N(G_X(s)) \qquad \text{(by definition of } G_N) \qquad \text{(A.0.2)}
\end{aligned}$$

□

This definition of the probability generating function can be generalized to the multivariate case. Suppose that $\mathbf{X} = (X_1, \cdots, X_n) \sim \left\{p_{i_1 i_2 \cdots i_n}\right\}_{i_1, i_2, \cdots, i_n \geq 0}$ is a finite vector of non-negative random variables, or a Z_+^n-valued random variable.

Definition A.0.2. (Definition of the multivariate probability generating function) [75]. The probability generating function $G_{\mathbf{X}}$ of a Z_+^n-valued random variable $\mathbf{X}$ is the function

$$\begin{aligned}
G_{\mathbf{X}}(\mathbf{s}) &= \mathbb{E}\Big(s_1^{X_1} s_2^{X_2} \cdots s_n^{X_n}\Big) \\
&= \sum_{i_1, i_2, \cdots, i_n \geq 0}^{\infty} p_{i_1 i_2 \cdots i_n} s_1^{i_1} s_2^{i_2} \cdots s_n^{i_n}, \qquad \text{(A.0.3)}
\end{aligned}$$

well defined if $\mathbf{s} = (s_1, s_2, \cdots, s_n) \in U_n \equiv [0,1]^n$.

Theorem A.0.1. *(Multivariate probability generating function theorem) [75]. Suppose* $\mathbf{X}$ *is a* Z_+^n*-valued random variable with probability generating function* $G_{\mathbf{X}}$

1. *$G_{\mathbf{X}}$ is non-negative and continuous with all derivatives.*

2. *The marginal laws for subsets of X_i's can be obtained by setting respective arguments of the probability generating function equal to 1, for example,*

$$G_{\mathbf{X}}(\mathbf{s})|_{s_j=1, j\neq i} = G_{X_i}(s_i),$$

etc and $G_{\mathbf{X}}(\mathbf{e}) = 1$, where $\mathbf{e} = (1, \cdots, 1)$.

3. $$\frac{\partial^{k_1+\cdots+k_n} G_{\mathbf{X}}(\mathbf{0})}{\partial s_1^{k_1} \cdots \partial s_n^{k_n}} = k_1! \cdots k_n! p_{k_1 \cdots k_n}.$$

4. $$\mu_{k_1,\cdots,k_n} = \left. \frac{\partial^{k_1+\cdots+k_n} G_{\mathbf{X}}(\mathbf{s})}{\partial s_1^{k_1} \cdots \partial s_n^{k_n}} \right|_{\mathbf{s}=\mathbf{e}}.$$

5. *If $\mathbf{X}$ and $\mathbf{Y}$ are two independent Z_+^n-valued random variables, then*

$$G_{\mathbf{X}+\mathbf{Y}}(\mathbf{s}) = G_{\mathbf{X}}(\mathbf{s}) G_{\mathbf{Y}}(\mathbf{s}).$$

6. *If $\mathbf{Y}$ is a Z_+^n-valued random variable and $\left\{\mathbf{X}_j^{(i)}; i \geq 1\right\}, j = 1, 2, \cdots, n$, are sequences of Z_+^m-valued random variables, then $\mathbf{V} = \sum_{j=1}^{n} \sum_{i_j=1}^{Y_j} \mathbf{X}_j^{(i_j)}$ is a Z_+^m-valued random variable with probability generating function*

$$G_{\mathbf{V}}(\mathbf{s}) = G_{\mathbf{Y}}\left[G_{X_1^{(1)}}(\mathbf{s}), \cdots, G_{X_n^{(1)}}(\mathbf{s})\right], \mathbf{s} \in U_m.$$

Galton-Watson Branching Processes

In a Galton-Watson process, a population of individuals evolves in discrete time. Each $(n-1)$st generation individual produces a random number of offspring in the

nth generation. The state of the process at time n is the number of individuals in the nth generation. For example, consider an organism that lives for exactly one time unit and then dies in the process of giving birth to a family of similar organisms, C, having the distribution $\mathbb{P}(C = k) = p_k; k = 0, 1, 2, \cdots$ [52].

If we let P_n be the number of individuals born at time n (i.e., the size of the nth generation), the evolution of the population is described by the sequence of random variables $P_0, P_1, P_2, \cdots$ (an example of a stochastic process). We assume that $P_0 = 1$, i.e. we start with precisely one organism. Let $g(s)$ be the probability generating function of C (offspring) given by

$$g(s) = \sum_{k=0}^{\infty} p_k s^k,$$

and $G_n(s)$ the probability generating function of P_n given by

$$G_n(s) = \sum_{x=0}^{\infty} \mathbb{P}(P_n = x) s^x.$$

Now we have $G_0(s) = s$, since $\mathbb{P}(P_0 = 1) = 1$ and $\mathbb{P}(P_0 = x) = 0$ for $x \neq 1$. Also $G_1(s) = g(s)$. The population size at generation n is

$$P_n = \sum_{i=1}^{P_{n-1}} C_i,$$

that is, the number of individuals in the nth generation is equal to the number of offspring of all individuals in the $(n-1)$st generation, where C_i is the size of the family produced by the ith member of the $(n-1)$st generation. Any individual in the nth generation of the process can be traced to its parent in the $(n-1)$st generation of the process [52].

Now, since P_n is the sum of a random number of independent and identically distributed (i.i.d.) random variables, we have

$$G_n(s) = G_{n-1}(g(s)) \quad \text{for} \quad n = 2, 3, \cdots \tag{A.0.4}$$

Iterating equation A.0.4, we have

$$\begin{aligned} G_n(s) &= G_{n-1}(g(s)) \\ &= g \circ \cdots \circ g \qquad \text{(n times)} \end{aligned} \tag{A.0.5}$$

that is G_n is a composition (nth iterate) of g. For more general processes, equation A.0.4 (also known as the forward equation) may not be feasible and for Galton-Watson processes, the forward equation leads to the backward equation, i.e. $G_n(s) = g\big(G_{n-1}(s)\big)$ [75]. The single-type Galton-Watson branching process can also be generalized to the multi-type case.

The evolution of a population with multiple variants is a multi-type Galton-Watson process (for further reference see [65, 75, 117]). In this process, each individual is assigned a type from a finite set $T = \{1, \cdots, r\}$, and each individual, say of type $i \in T$ is associated with a random vector $\mathbf{C}_i = (C_{i1}, \cdots, C_{ir})$, where C_{ij} is a random variable that represents the number of offspring of type j born from a type i individual. Given its type, the infected cell reproduces according to a probability distribution. The probability that a type i parent cell produces k_1 children of type 1, k_2 of type 2,$\cdots$, k_r of type r is

$$p_i(k_1, \cdots, k_r) = \mathbb{P}\Big(\mathbf{C}_i = [k_1, \cdots, k_r]\Big), \tag{A.0.6}$$

The ith generating function $g_i(s_1, \cdots, s_r)$ determines the distribution of the number of offspring of various types to be produced by a type i cell

$$\begin{aligned} g_i(\mathbf{s}) &= \mathbb{E}_i\Big(s_1^{k_1} \cdots s_r^{k_r}\Big), \\ &= \sum_{k_1, \cdots, k_r} p_i(k_1, \cdots, k_r) s_1^{k_1} \cdots s_r^{k_r}, \quad |s_1|, \cdots, |s_r| \leq 1; \end{aligned} \tag{A.0.7}$$

such that

$$\mathbf{g}(\mathbf{s}) = \Big(g_1(\mathbf{s}), \cdots, g_r(\mathbf{s})\Big),$$

where $\mathbf{s} = (s_1, \cdots, s_r)$. The multi-type GWBP is a vector-valued, non-negative random process $\mathbf{P}(n) = \Big(P_1(n), \cdots, P_r(n)\Big)$, where $P_i(n)$ represents the nth generation size of type i with $i = 1, \cdots, r$. The vector forms a Markov chain describing the population size and the type structure evolving generation-wise. In general, if

$$\mathbf{P}(n-1) = \Big(P_1(n-1), \cdots, P_r(n-1)\Big),$$

then by summing the number of children generated by parent j of type i in generation $n-1$, the vector-valued population size at generation n is given by

$$\mathbf{P}(n) = \sum_{i=1}^{r} \sum_{j=1}^{P_i(n-1)} \mathbf{C}_i^{(j)},$$

where $\mathbf{C}_i^{(j)}$ is the offspring vector produced by each jth member of the ith type in $(n-1)$st generation. Using the multivariate probability generating function theorem, we have

$$\mathbf{G}^n(\mathbf{s}) = \mathbf{G}^{n-1}(\mathbf{g}(\mathbf{s})), \tag{A.0.8}$$

the generating function of $\mathbf{X}(n)$, where $\mathbf{G}^0(\mathbf{s}) = \mathbf{s}$ and $\mathbf{G}^1(\mathbf{s}) = \mathbf{g}(\mathbf{s})$.

Appendix B

Conditional Expectation

See [52] for more details. If X and Y are discrete random variables with a joint function defined by

$$p_{X,Y}(x,y) = \mathbb{P}(X = x, Y = y),$$

then the marginal probability mass function of X is

$$\mathbb{P}(X = x_i) = \sum_y \mathbb{P}(X = x_i, Y = y),$$

and that of Y is

$$\mathbb{P}(Y = y_i) = \sum_x \mathbb{P}(X = x, Y = y_i).$$

The conditional expected value of X given $Y = y_j$ is defined as:

$$\begin{aligned} \mathbb{E}(X|Y = y_j) &= \sum_i x_i \mathbb{P}(X = x_i|Y = y_j) \\ &= \sum_i x_i \frac{\mathbb{P}(X = x_i, Y = y_j)}{P(Y = y_j)}, \qquad \forall y_j \ (j = 1, 2, \cdots) \end{aligned} \tag{B.0.1}$$

Since $\mathbb{E}(X|Y)$ is a function of Y, we can write down its mean as

$$\begin{aligned}
\mathbb{E}[\mathbb{E}(X|Y)] &= \sum_j \mathbb{E}(X|Y=y_j)\mathbb{P}(Y=y_j) \\
&= \sum_j \sum_i x_i \mathbb{P}(X=x_i|Y=y_j)\mathbb{P}(Y=y_j) \qquad \text{(from equation B.0.1)} \\
&= \sum_j \sum_i x_i \frac{\mathbb{P}(X=x_i, Y=y_j)}{\mathbb{P}(Y=y_j)} P(Y=y_j) \\
&= \sum_j \sum_i x_i \mathbb{P}(X=x_i, Y=y_j) \\
&= \sum_i x_i \sum_j \mathbb{P}(X=x_i, Y=y_j) \\
&= \sum_i x_i \mathbb{P}(X=x_i) \qquad \text{(marginal mass function of X)} \\
&= \mathbb{E}(X) \qquad \text{(B.0.2)}
\end{aligned}$$

The result is very useful, it enables us to compute expectations easily by first conditioning on some random variable Y and using

$$\mathbb{E}(X) = \sum_j \mathbb{E}(X|Y=y_j)\mathbb{P}(Y=y_j). \qquad \text{(B.0.3)}$$

Appendix C

8-type Galton-Watson Branching Process

The symmetric mutation matrix ($\mathcal{M}$) for all the pathways is given by:

$$\begin{array}{c} \\ P_0 \\ P_1 \\ P_2 \\ P_3 \\ P_4 \\ P_5 \\ P_6 \\ P_7 \end{array} \begin{array}{c} \begin{array}{cccccccc} P_0 & P_1 & P_2 & P_3 & P_4 & P_5 & P_6 & P_7 \end{array} \\ \begin{pmatrix} (1-\eta)^3 & \eta(1-\eta)^2 & \eta(1-\eta)^2 & \eta(1-\eta)^2 & \eta^2(1-\eta) & \eta^2(1-\eta) & \eta^2(1-\eta) & \eta^3 \\ \eta(1-\eta)^2 & (1-\eta)^3 & \eta^2(1-\eta) & \eta^2(1-\eta) & \eta(1-\eta)^2 & \eta^3 & \eta(1-\eta)^2 & \eta^2(1-\eta) \\ \eta(1-\eta)^2 & \eta^2(1-\eta) & (1-\eta)^3 & \eta^2(1-\eta) & \eta(1-\eta)^2 & \eta(1-\eta)^2 & \eta^3 & \eta^2(1-\eta) \\ \eta(1-\eta)^2 & \eta^2(1-\eta) & \eta^2(1-\eta) & (1-\eta)^3 & \eta^3 & \eta(1-\eta)^2 & \eta(1-\eta)^2 & \eta^2(1-\eta) \\ \eta^2(1-\eta) & \eta(1-\eta)^2 & \eta(1-\eta)^2 & \eta^3 & (1-\eta)^3 & \eta^2(1-\eta) & \eta^2(1-\eta) & \eta(1-\eta)^2 \\ \eta^2(1-\eta) & \eta^3 & \eta(1-\eta)^2 & \eta(1-\eta)^2 & \eta^2(1-\eta) & (1-\eta)^3 & \eta^2(1-\eta) & \eta(1-\eta)^2 \\ \eta^2(1-\eta) & \eta(1-\eta)^2 & \eta^3 & \eta(1-\eta)^2 & \eta^2(1-\eta) & \eta^2(1-\eta) & (1-\eta)^3 & \eta(1-\eta)^2 \\ \eta^3 & \eta^2(1-\eta) & \eta^2(1-\eta) & \eta^2(1-\eta) & \eta(1-\eta)^2 & \eta(1-\eta)^2 & \eta(1-\eta)^2 & (1-\eta)^3 \end{pmatrix} \end{array}, \tag{C.0.1}$$

where the rows and columns are ordered as follows: wild-type strain (P_0), three single-point mutants (P_1, P_2, P_3), three double-point mutants (P_4, P_5, P_6) and a triple-point

mutant (P_7). The pgf of the wild-type offspring is given by:

$$\begin{aligned} g_0^n(s_0,\cdots,s_7) &= \mathbb{E}\Big(s_0^{k_0}\cdots s_7^{k_7}\Big); \\ &= \sum_{k_0=0}^{\infty}\cdots\sum_{k_7=0}^{\infty}\binom{R_0(n)}{k_0,\cdots,k_7}\Big((1-\eta)^3\Big)^{k_0}\cdots\Big(\eta^3\Big)^{k_7}s_0^{k_0}\cdots s_7^{k_7}; \\ &= \Big(\sum_{j=0}^{7}\mathcal{M}(0,j)s_j\Big)^{R_0(n)}, \end{aligned} \tag{C.0.2}$$

where $\mathcal{M}(0,j)$ is the jth element ($j=0,\cdots,7$) of row 0 of matrix (C.0.1); our indexing starts from zero and we have used the multinomial theorem to rewrite the summation. Also the following sum is true, $\sum_{i=0}^{7}k_i = R_0(n)$, at every generation n. Similarly, we can derive the offspring pgfs for all the mutants:

$$\begin{aligned} g_1^n(s_0,\cdots,s_7) &= \Big(\sum_{j=0}^{7}\mathcal{M}(1,j)s_j\Big)^{R_1(n)} \\ \cdots &= \cdots \\ g_7^n(s_0,\cdots,s_7) &= \Big(\sum_{j=0}^{7}\mathcal{M}(7,j)s_j\Big)^{R_7(n)} \end{aligned} \tag{C.0.3}$$

where $R_i(n), i=0,\cdots,7$ is strain i effective reproductive number function such that

$$\mathbf{g}^n(\mathbf{s}) = \Big(g_0^n(\mathbf{s}),\cdots,g_7^n(\mathbf{s})\Big), \tag{C.0.4}$$

where $\mathbf{s}=(s_0,\cdots,s_7)$. We assume that the infection process is started from a single wild-type infected cell, i.e. $\{P_0(0)=1, P_1(0)=0,\cdots,P_7(0)=0\}$. We can use the iteration

$$G_i^n(\mathbf{s}) = G_i^{n-1}\Big(g_0^n(\mathbf{s}),\cdots,g_7^n(\mathbf{s})\Big), \qquad n=2,3,\cdots \tag{C.0.5}$$

to derive the pgfs for the distribution law of the number of cells at every generation.

Appendix D

Mutation Combinatorics

We relate the HIV mutation process parameters ϵ_{ij} and f to an underlying single-point-mutation process. The error rate per site for HIV reverse transcriptase (for any given nucleotide A, C, G and T) is assumed to be 10^{-4} [109], so that the rate of change to any of the three alternatives (for example substitution of A by C, G or T) is given by $\eta = \frac{1}{3} \times 10^{-4}$. The probability that a site within a gene will remain unchanged after reverse transcription (i.e. A $\rightarrow$ A, C $\rightarrow$ C, T $\rightarrow$ T or G $\rightarrow$ G) is given by $(1 - 3\eta)$. Then the probability of a particular mutation (strain $j \rightarrow$ strain i), where i and j differ by precisely m point mutations, given a genome length L (approximately 10^4 bases for HIV) is given by

$$\epsilon_{ij} = (1 - 3\eta)^{L-m}\eta^m \approx (1 - 3\eta)^L\eta^m \equiv f\eta^m, \tag{D.0.1}$$

where $m << L$ and $1 - 3\eta \approx 1$. Note that $f = (1 - 3\eta)^L \approx 0.37$ is the probability of error free replication. For example, we consider particular point mutations at codon 103 of reverse trancriptase gene that are associated with 103K/N viral populations. Given that AAA & AAG code for K and AAC & AAT code for N, the rate of lysine

(K) substitutions by asparagine (N) at this codon is given by

$$\mathbb{P}(\mathrm{K} \to \mathrm{N}) = 2f\eta. \tag{D.0.2}$$

The single point mutation rate at this codon using equation D.0.2 is given by $\epsilon_{21} = 2.5 \times 10^{-5}$. Then, using equation D.0.1, we have $\epsilon_{31} = f\eta^3 \approx 1.4 \times 10^{-14}$ and $\epsilon_{32} = f\eta^2 \approx 4.1 \times 10^{-10}$.

Appendix E

The Direct Hybrid Method

To simulate our system (with the phylogeny given in chapter 4), we use the direct hybrid method [2]:

1. Initialize the system $T(0), P_1(0), P_2(0), P_3(0), L_1(0), L_2(0), L_3(0)$ and set the initial time $t = t_0$;

2. Generate a random variable $\xi \sim \text{Exp}(1)$;

3. Set $g(t/t) = 0$ and solve the system of ODEs starting at time $\tau = t$

$$\begin{aligned}
\frac{dT(\tau)}{d\tau} &= S_{\text{T}} - T(\tau)\sum_{i=1}^{2} k_i P_i(\tau) - \mu_{\text{T}} T(\tau) \\
\frac{dP_i(\tau)}{d\tau} &= fFk_i P_i(\tau)T(\tau) + T(\tau)\sum_{\substack{j=1 \\ j\neq i}}^{2} \epsilon_{ij} k_j P_j(\tau) + aL_i(\tau) - \mu_{\text{P}} P_i(\tau), \quad i = 1, 2 \\
\frac{dL_i(\tau)}{d\tau} &= f(1-F)k_i P_i(\tau)T(\tau) - aL_i(\tau), \quad i = 1, 2 \\
\frac{g(\tau/t)}{d\tau} &= fk_3 P_3(\tau)T(\tau) + T(\tau)\sum_{i=1}^{2} \epsilon_{3i} k_i P_i(\tau) + aL_3(\tau) + \mu_{\text{P}} P_3(\tau) \qquad \text{(E.0.1)}
\end{aligned}$$

   until time $\tau = s$ such that $g(s/t) = \xi$;

4. Generate a discrete random variable with values in D and probabilities (Table 5.2) in order to determine the event to be performed.

5. Make the indicated jump, update the time to $t = s$ and go to step 2.

Bibliography

[1] M. R. Abrahams, J. A. Anderson, E. E. Giorgi, and et al., *Quantitating the multiplicity of infection with human immunodeficiency virus type 1 subtype C reveals a non-poisson distribution of transmitted variants*, J. Virol. **83** (2009), no. 8, 3556–3567.

[2] A. Alfonsi, E. Cances, G. Turinici, B. Di Ventura, and W. Huisinga, *Exact simulation of hybrid stochastic and deterministic models for biochemical systems*, Research Report RR-5435, INRIA **5435** (2004), 1–20.

[3] C. L. Althaus and R. De Boer, *Dynamics of immune escape during HIV/SIV infection*, PLoS Comput. Biol. **4** (2007), no. 7, e1000103.

[4] R. M. Anderson and R. M. May, *Infectious diseases of humans*, Oxford University Press, Oxford.

[5] A. R. Arnaut, M. A. Nowak, and D. Wodarz, *HIV-1 dynamics revisited: biphasic decay by cytotoxic T lymhocyte killing*, Proc. R. Soc. Lond. B **267** (2000), 1347–1354.

[6] B. Asquith, C. T. T. Edwards, M. Lipsitch, and A. R. McLean, *Inefficient cytotoxic T lymphocyte mediated killing of HIV-1 infected cells in-vivo*, PLoS Biol. **4** (2006), no. 4, e90.

[7] B. Auvert, D. Taljaard, E. Lagarde, and et al., *Randomized, controlled intervention trial of male circumcision for reduction of HIV infection risk: The ANRS 1265 trial*, PLoS Med. **2** (2005), no. 11, e298.

[8] D. R. Bangsberg, E. D. Charlebois, R. M. Grant, and et al., *High levels of adherence do not prevent accumulation of HIV-1 drug resistance mutations*, AIDS **17** (2003), 1925–1932.

[9] H. T. Banks and C. Castillo-Chavez (eds.), *Bioterrorism: mathematical modeling applications in homeland security*, Frontiers in Applied Mathematics, vol. 29, SIAM, Philadelphia, 2006.

[10] J. D. Barbour, F. M. Hecht, T. Wrin, and et al., *Persistence of primary drug resistance among recently HIV-1 infected adults*, AIDS **18** (2004), 1683–1689.

[11] R. J. De Boer, D. Homann, and A. S. Perelson, *Different dynamics of CD4+ and CD8+ T cell responses during and after acute lymphocytic choriomeningitis virus infection*, J. Immunol. **171** (2003), no. 8, 3928–3935.

[12] S. Bonhoeffer, R. M. May, G. M. Shaw, and M. A. Nowak, *Viral dynamics and drug therapy*, Proc. Natl. Acad. Sci. USA **94** (1997), 6971–6976.

[13] S. Bonhoeffer and M. A. Nowak, *Pre-existence and emergence of drug resistance in HIV-1 infection*, Proc. R. Soc. Lond. B **264** (1997), 631–637.

[14] J. M. Brenchley, T. W. Schacker, L. E. Ruff, and et al., *CD4+ T cell depletion during all stages of HIV disease occurs predominantly in the gastrointestinal tract*, J. Exp. Med. **200** (2004), 749–759.

[15] B. G. Brenner, J. P. Routy, M. Petrella, and et al., *Persistence and fitness of multidrug-resistant human immunodeficiency virus type 1 acquired in primary infection*, J. Virol. **76** (2002), no. 4, 1753–1761.

[16] K. Burrage, T. Tian, and P. Burrage, *A multi-scale approach for simulating chemical reaction systems*, Prog. Biophys. Mol. Biol. **85** (2004), 217–234.

[17] M. L. Chaix, K. D. Ekouevi, G. Peytavin, and et al., *Impact of nevirapine (NVP) plasma concentration on selection of resistant virus in mothers who received single-dose NVP to prevent perinatal human immunodeficiency virus type 1 transmission and persistence of resistant virus in their infected children*, Antimicrob. Agents Chemother. **51** (2007), no. 3, 896–901.

[18] B. H. Chi, M. Sinkala, F. Mbewe, and et al., *Single dose tenofovir and emtricitabine for reduction of viral resistance to non-nucleoside reverse transcriptase inhibitor drugs in women given intrapartum nevirapine for perinatal HIV prevention: an open label randomised trial*, Lancet **370** (2007), 1698–1705.

[19] Y. K. Chow, M. S. Hirsch, D. P. Merrill, L. J. Bechtel, J. J. Eron, J. C. Kaplan, and R. T. D'Aquila, *Use of evolutionary limitations of HIV-1 multidrug resistance to optimize therapy*, Nature **361** (1995), 650–654.

[20] T. W. Chun, D. Engel, M. M. Berrey, and et al., *Early establishment of a pool of latently infected, resting CD4+ T cells during primary HIV-1 infection*, Proc. Natl. Acad. Sci. USA **95** (1998), no. 15, 8869–8873.

[21] T. W. Chun, D. Finzi, J. Margolick, and et al., *In vivo fate of HIV-1 infected T cells: quantitative analysis of the transition to stable latency*, Nat. Med. **1** (1995), 1284–1290.

[22] T. W. Chun, J. S. Justement, S. Moir, and et al., *Decay of the HIV reservoir in patients receiving antiretroviral therapy for extended periods: implications for eradication of virus*, J. Infect. Dis. **195** (2007), 1762–1764.

[23] T. W. Chun, L. Stuyver, S. B. Mizell, and et al., *Presence of an inducible HIV-1 latent reservoir during highly active antiretroviral therapy*, Proc. Natl. Acad. Sci. USA **94** (1997), 13193–13197.

[24] J. M. Coffin, *HIV population dynamics in-vivo: implications for genetic variation, pathogenesis and therapy*, Science **267** (1995), 483–489.

[25] T. R. Cressey, G. Jourdain, and M. J. Lallemant, *Persistence of nevirapine exposure during the postpartum period after intrapartum single dose nevirapine in addition to zidovudine prophylaxis for the prevention of mother to child transmission of HIV-1*, J. Acquir. Immune Defic. Syndr. **38** (2005), no. 3, 3283–288.

[26] C. L. Daley, P. M. Small, G. F. Schecter, and et al., *An outbreak of tuberculosis with accelerated progression among persons with the human immunodeficiency virus: an analysis using restriction-fragment-length polymorphisms*, N. Engl. J. Med. **326** (1992), no. 4, 231–235.

[27] S. G. Deeks, R. M. Grant, T. Wrin, and et al., *Persistence of drug-resistant HIV-1 after a structured treatment interruption and its impact on treatment response*, AIDS **17** (2003), no. 3, 361–370.

[28] S. G. Deeks, T. Wrin, T. Liegler, and et al., *Virologic and immunologic consequences of discontinuing combination antiretroviral-drug therapy in HIV-infected patients with detectable viremia*, N. Engl. J. Med. **344** (2001), no. 7, 472–480.

[29] C. Delaugerre, L. Morand-Joubert, M. L. Chaix, and et al., *Persistence of multidrug-resistant HIV-1 without antiretroviral treatment 2 years after sexual transmission*, Ant. Ther. **9** (2004), no. 3, 415–421.

[30] H. L. Devereux, M. Youle, M. A. Johnson, and C. Loveday, *Rapid decline in detectability of HIV-1 drug resistance mutations after stopping therapy*, AIDS **13** (1999), F123–F127.

[31] J. B. Dinoso, S. Y. Kim, A. M. Wiegand, and et al., *Treatment intensification does not reduce residual HIV-1 viremia in patients on highly active antiretroviral therapy*, Proc. Natl. Acad. Sci. USA **106** (2009), no. 23, 9403–9408.

[32] E. Domingo, L. Menendez-Arias, and J. J. Holland, *RNA virus fitness*, Rev. Med. Virol. **7** (1997), no. 2, 87–96.

[33] M. Eigen, *Self organization of matter and the evolution of biological macromolecules*, Die Naturwissenschaften **58** (1971), no. 10, 465–523.

[34] M. Eigen and P. Schuster, *The hypercycle: A principle of natural self-organization*, Springer-Verlag, Berlin, 1979.

[35] S. H. Eshleman, M. Mracna, A. L. Guay, and et al., *Selection and fading of resistance mutations in women and infants receiving nevirapine to prevent HIV-1 vertical transmission (HIVNET 012)*, AIDS **15** (2001), 1951–1957.

[36] W. E Fiebig, J. D Wright, D. B Rawal, and et al., *Dynamics of HIV viremia and antibody seroconversion in plasma donors: implications for diagnosis and staging of primary HIV infection*, AIDS **17** (2003), 1871–1879.

[37] D. Finzi, J. Blankson, J. D. Siliciano, and et al., *Latent infection of CD4+ T cells provides a mechanism for lifelong persistence of HIV-1, even in patients on effective combination therapy*, Nat. Med. **5** (1999), 512–517.

[38] R. A. Fisher, *The genetical theory of natural selection: A complete variorum edition*, Oxford Press, London, 1930.

[39] S. T. Flys, D. Donnell, A. Mwatha, and et al., *Persistence of K103N containing HIV-1 variants after single dose nevirapine for prevention of HIV-1 mother to child transmission*, J. Infect. Dis. **195** (2007), 711–715.

[40] E. B. Ford, *Ecological genetics*, Chapman and Hall, London, 1964.

[41] I. Frank, *Antivirals against HIV-1*, Clin. Lab. Med. **22** (2002), no. 3, 741–757.

[42] S. D. Frost and A. R. McLean, *Quasispecies dynamics and the emergence of drug resistance during zidovudine therapy of HIV infection*, AIDS **8** (1994), no. 3, 323–332.

[43] R. T. Gandhi, A. Wurcel, E. S. Rosenberg, and et al., *Progressive reversion of human immunodeficiency virus type 1 resistance mutations in-vivo after transmission of a multiply drug-resistant virus*, Clin. Infect. Dis. **37** (2003), no. 12, 1693–1698.

[44] J. G. Garcia-Lerma, R. A. Otten, S. H. Qari, and et al., *Prevention of rectal SHIV transmission in macaques by daily or intermittent prophylaxis with emtricitabine and tenofovir*, PLoS Med. **5** (2008), e28.

[45] D. T. Gillespie, *A general method for numerically simulating the stochastic time evolution of coupled chemical reactions*, J. Comp. Phys. **22** (1976), 403–434.

[46] ———, *Approximate accelerated stochastic simulation of chemically reacting systems*, J. Chem. Phys. **115** (2001), 1716–1733.

[47] N. Goonetilleke, M. K. P. Liu, J. F. Salazar-Gonzalez, and et al., *The first T cell response to transmitted/founder virus contributes to the control of acute viremia in HIV-1 infection*, J. Exp. Med. **206** (2009), no. 6, 1253–1272.

[48] G. S. Gottlieb, D. C. Nickle, M. A. Jensen, and et al., *HIV type 1 superinfection with a dual-tropic virus and rapid progression to AIDS: a case report*, Clin. Infect. Dis. **45** (2007), 501–509.

[49] I. S. Gradshteyn and I. M. Ryzhik, *Routh-Hurwitz Theorem*, In Tables of Integrals, Series, and Products, 6th ed (San Diego), Academic Press, 2000, p. 1076.

[50] R. M. Granich, C. F. Filks, C. Dye, and et al., *Universal voluntary HIV testing with immediate antiretroviral therapy as a stratergy for elimination of HIV transmission: a mathematical model*, Lancet **373** (2009), no. 9657, 48–57.

[51] R. M. Grant, J. R. Lama, P. L. Anderson, and et al., *Preexposure chemoprophylaxis for HIV prevention in men who have sex with men*, N. Engl. J. Med **363** (2010), no. 27, 2587–2599.

[52] G. Gribakin, *Probability and distribution theory*, `http://web.am.qub.ac.uk/users/g.gribakin/Teach_SOR.html`, September 2010, Accessed: 15/09/2010.

[53] J. T. Griffin, T. Garske, and A. C. Ghani, *Joint estimation of the basic reproduction number and generation time parameters for infectious disease outbreaks*, Biostatistics **12** (2011), no. 2, 303–312.

[54] M. Griffith, T. Courtney, A. J. Peccoud, and W. H. Sanders, *Dynamic partitioning for hybrid simulation of the bistable HIV-1 transactivation network*, Bioinformatics **22** (2006), no. 22, 2782–2789.

[55] A. T. Haase, *Population biology of HIV-1 infection: viral and CD4+ T cell demographics and dynamics in lymphatic tissues*, Ann. Rev. Immunol. **17** (1999), no. 1, 625–656.

[56] ———, *Perils at mucosal front lines for HIV and SIV and their hosts*, Nat. Rev. Immunol. **5** (2005), 783–792.

[57] H. Haeno and Y. Iwasa, *Probability of resistance evolution for exponentially growing virus in the host*, J. Theor. Biol. **246** (2007), no. 2, 323–331.

[58] P. Hansasuta and S. L. Rowland-Jones, *HIV-1 transmission and acute HIV-1 infection*, Br. Med. Bull. **58** (2001), 109–127.

[59] T. E. Harris, *The theory of branching processes*, Springer, Berlin, 1963.

[60] E. L. Haseltine and J. B. Rawlings, *Approximate simulation of coupled fast and slow reactions for stochastic chemical kinetics*, J. Chem. Phys. **117** (2002), 6959–6969.

[61] J. M. Heffernan and L. M. Wahl, *Monte Carlo estimates of natural variation in HIV infection*, J. Theor. Biol. **236** (2005), 137–153.

[62] D. D. Ho, A. U. Neumann, A. S. Perelson, W. Chen, J. M. Leonard, and M. Markowitz, *Rapid turnover of plasma virions and CD4 lymphocytes in HIV-1 infection*, Nature **373** (1995), 123–126.

[63] S. D. Holmberg, F. J. Palella, K. A. Lichtenstein, and D. V. Havlir, *The case for earlier treatment of HIV infection*, Clin. Infect. Dis. **39** (2004), 1699–1704.

[64] Y. Iwasa, F. Michor, and M. A. Nowak, *Evolutionary dynamics of escape from biomedical intervention*, Proc. R. Soc. Lond. B **270** (2003), 2573–2578.

[65] ———, *Evolutionary dynamics of invasion and escape*, J. Theor. Biol. **226** (2004), 205–214.

[66] J. Izopet, P. Massip, C. Souyris, and et al., *Shift in HIV resistance genotype after treatment interruption and short-term antiviral effect following a new salvage regimen*, AIDS **14** (2000), 2247–2255.

[67] J. A. Johnson, J-F. Li, X. Wei, and et al., *Minority HIV-1 drug resistance mutations are present in antiretroviral treatment naive populations and associate with reduced treatment efficacy*, PLoS Med. **5** (2008), no. 7, e158.

[68] B. Joos, A. Trkola, M. Fischer, and et al., *Low human immunodeficiency virus envelope diversity correlates with low in vitro replication capacity and predicts spontaneous control of plasma viremia after treatment interruptions*, J. Virol. **79** (2005), no. 14, 9026–9037.

[69] T. H. Jukes and C. R. Cantor, *Evolution of protein molecules*, In Munro HN, editor, Mammalian Protein Metabolism (New York), Academic Press, 1969, pp. 21–132.

[70] Q. Abdool Karim, S. S. Abdool Karim, J. A. Frohlich, and et al., *Effectiveness and safety of Tenofovir Gel, an antiretroviral microbicide, for the prevention of HIV infection in women*, Science **329** (2010), no. 5996, 1168–1174.

[71] B. F. Keele, E. E. Giorgi, J. F. Salazar-Gonzalez, and et al., *Identification and characterization of transmitted and early founder virus envelopes in primary HIV-1 infection*, Proc. Natl. Acad. Sci. USA **105** (2008), 7552–7557.

[72] M. J. Keeling and J. V. Ross, *On methods for studying stochastic disease dynamics*, J. R. Soc. Inter. **5** (2008), 171–181.

[73] T. R. Kiehl, R. M. Mattheyses, and M. K. Simmons, *Hybrid simulation of cellular behavior*, Bioinformatics **20** (2004), 316–322.

[74] H. G. Kijak, M. M. Avila, and H. Salomon, *Mother to child transmission of drug-resistant HIV*, Drug Resistance Updates **4** (2001), 29–37.

[75] M. Kimmel and D. E. Axelrod, *Branching processes in biology*, Springer-Verlag, New York, 2001.

[76] D. M. Knipe and P. M. Howley, *Fields virology, 5th edition, vol 1*, Lippincott Williams & Wilkins, Philadelphia, 2007.

[77] S. Kumar and S. Subramanian, *Mutation rates in mammalian genomes*, Proc. Natl. Acad. Sci. USA **99** (2002), no. 2, 803–808.

[78] V. Lakshmikantham, D. D. Bainov, and P. S. Simeonov, *Theory of impulsive differential equations*, World Scientific, 1989.

[79] H. Y. Lee, E. E. Giorgi, B. F. Keele, and et al., *Modeling sequence evolution in acute HIV-1 infection*, J. Theor. Biol. **261** (2009), 341–360.

[80] H. Y. Lee, A. S. Perelson, S-C. Park, and T. Leitner, *Dynamic correlation between intrahost HIV-1 quasispecies evolution and disease progression*, PLoS Comput. Biol. **4** (2008), no. 12, e1000240.

[81] L. N. Letvin, R. J. Mascola, Y. Sun, and et al., *Preserved CD4+ central memory T cells and survival in vaccinated SIV-challenged monkeys*, Science **312** (2006), 1530–1533.

[82] A. M. L. Lever, *The molecular biology of HIV/AIDS*, John Wiley & Sons, New York, 1996.

[83] H. Lin and J. W. Shuai, *A stochastic spatial model of HIV dynamics with an asymmetric battle between the virus and the immune system*, N. J. Phys. **12** (2010), 043051.

[84] K. J. Liner(2nd), C. D. Hall, and K. R. Robertson, *Impact of human immunodeficiency virus (HIV) subtypes on HIV-associated neurological disease*, J. Neurovirol. **13** (2007), no. 4, 291–304.

[85] S. J. Little, S. D. W. Frost, J. K. Wong, and et al., *Persistence of transmitted drug resistance among subjects with primary human immunodeficiency virus infection*, J. Virol. **82** (2008), no. 11, 5510–5518.

[86] S. J Little, S Holte, and J. P Routy, *Antiretroviral-drug resistance among patients recently infected with HIV*, N. Engl. J. Med. **347** (2002), 385–=–394.

[87] S. J. Little, A. R. McLean, C. A. Spina, D. D. Richman, and D. V. Havlir, *Viral dynamics of acute HIV-1 infection*, J. Exp. Med. **190** (1999), 841–850.

[88] S. Lockman, R. L. Shapiro, L. M. Smeaton, and et al., *Response to antiretroviral therapy after a single, peripartum dose of nevirapine*, N. Engl. J. Med. **356** (2007), no. 2, 135–147.

[89] F. Lori, H. Jessen, J. Lieberman, and et al., *Treatment of human immunodeficiency virus infection with hydroxyurea, didanosine, and a protease inhibitor before seroconversion is associated with normalized immune parameters and limited viral reservoir*, J. Infect. Dis. **180** (1995), no. 6, 1827–1832.

[90] S. Loubser, P. Balfe, G. Sherman, S. Hammer, L. Kuhn, and L. Morris, *Decay of K103N mutants in cellular DNA and plasma RNA after single-dose nevirapine to reduce mother-to-child HIV-1 transmission*, AIDS **20** (2006), 995–1002.

[91] N. Machouf, R. Thomas, V. K. Nguyen, and et al., *Effects of drug resistance on viral load in patients failing antiretroviral therapy*, J. Med. Virol. **78** (2006), no. 5, 608–613.

[92] L. M. Mansky and H. M. Temin, *Lower in-vivo mutation rate of human immunodeficiency virus type 1 than that predicted from the fidelity of purified reverse transcriptase*, J. Virol. **69** (1995), no. 8, 5087–5094.

[93] M. Markowitz, M. Louie, A. Hurley, and et al., *A novel antiviral intervention results in more accurate assessment of human immunodeficiency virus type 1 replication dynamics and T-cell decay in-vivo*, J. Virol. **77** (2003), 5037–5038.

[94] M. Markowitz, H. Mohri, S. Mehandru S, and et al., *Infection with multidrug resistant, dual-tropic HIV-1 and rapid progression to AIDS: a case report*, Lancet **365** (2005), 1031–1038.

[95] R. C. Mata, F. Flor-Parra, P. Viciana, and et al., *Virological and immunological stability in HIV infected patients undergoing partial-treatment interruption*, J. Clin. Virol. **45** (2009), no. 4, 362–366.

[96] J. J. Mattapallil, D. C. Douek, B. Hill, and et al., *Massive infection and loss of memory CD4+ T cells in multiple tissues during acute SIV infection*, Nature **434** (2005), 1093–1097.

[97] J. A. McIntyre, N. Martinson, and G. E. Gray, *Single dose nevirapine combined with a short course of combivir for prevention of mother to child transmission of HIV-1 can significantly decrease the subsequent development of maternal and infant resistant virus*, Ant. Ther. **10** (2005), S4.

[98] A. R. McLean and M. A. Nowak, *Competition between zidovudine-sensitive and zidovudine-resistant strains of HIV*, AIDS **6** (1992), 71–79.

[99] J. A. McMichael, P. Borrow, D. G. Tomaras, N. Goonetilleke, and F. B. Haynes, *The immune response during acute HIV-1 infection: clues for vaccine development*, Nat. Rev. Immunol. **10** (2010), 11–23.

[100] S. Mehandru, M. A. Poles, K. Tenner-Racz, and et al., *Primary HIV-1 infection is associated with preferential depletion of CD4+ T lymphocytes from effector sites in the gastrointestinal tract*, J. Exp. Med. **200** (2004), 761–770.

[101] J. Mellors, S. Palmer, D. Nissley, and et al., *Low frequency non-nucleoside reverse transcriptase inhibitor (NNRTI)-resistant variants contribute to failure of efavirenz-containing regimens in NNRTI-experienced patients with negative standard genotypes for NNRTI mutations*, Antivir. Ther. **8** (2003), S150.

[102] ———, *Low-frequency NNRTI-resistant variants contribute to failure of efavirenz-containing regimens*, Program and abstracts of the 11th Conference on Retroviruses and Opportunistic Infections. Abstract 39 (San Francisco, California), February 8-11 2004.

[103] J. W. Mellors, Jnr Ronaldo C. R, P. Gupta, R. M. White, J. A. Todd, and L. A. Kingsley, *Prognosis in HIV-1 infection predicted by the quantity of virus in plasma*, Science **272** (1996), 1167–1170.

[104] V. Miller, C. Sabin, K. Hertogs, and et al., *Virological and immunological effects of treatment interruptions in HIV-1 infected patients with treatment failure*, AIDS **14** (2000), 2857–2867.

[105] J. E. Mittler, B. Sulzer, A. U. Neumann, and A. S. Perelson, *Influence of delayed viral production on viral dynamics in HIV-1 infected patients*, Math. Biosci. **152** (1998), 143–163.

[106] C. J. Mode and C. K. Sleeman, *An algorithmic synthesis of the deterministic and stochastic paradigms via computer intensive methods*, Math. Biosci. **180** (2002), 115–126.

[107] E. Muro, J. A. Droste, H. T. Hofstede, and et al., *Nevirapine plasma concentrations are still detectable after more than 2 weeks in the majority of women receiving single dose nevirapine, implications for intervention studies*, J. Acquir. Immune Defic. Syndr. **39** (2005), no. 4, 9419–421.

[108] P. W. Nelson, M. A. Gilchrist, D. Coombs, J. M. Hyman, and A. S. Perelson, *An age-structured model of HIV-1 infection that allows for variations in the production rate of viral particles and the death rate of productively infected cells*, Math. Biosci. **1** (2004), no. 2, 267–288.

[109] M. A. Nowak, *HIV mutation rate*, Nature **347** (1990), 522.

[110] ———, *Evolutionary dynamics: Exploring the equations of life*, Harvard University Press, Cambridge, Massachusetts, 2006.

[111] M. A. Nowak, R. M. Anderson, A. R. McLean, T. F. Wolfs, J. Goudsmit, and R. M. May, *Antigenic diversity thresholds and the development of AIDS*, Science **254** (1991), no. 5034, 963–969.

[112] M. A. Nowak, S. Bonhoeffer, G. M. Shaw, and R. M. May, *Anti-viral drug treatment: dynamics of resistance in free virus and infected cell populations*, J. Theor. Biol. **184** (1997), no. 2, 203–217.

[113] ———, *Antiviral drug treatment: dynamics of resistance in free virus and infected cell populations*, J. Theor. Biol. **184** (1997), 203–217.

[114] M. A. Nowak, A. L. Lloyd, G. M. Vasquez, and et al., *Viral dynamics of primary viremia and antiretroviral therapy in simian immunodeficiency virus infection*, J. Virol. **71** (1997), no. 10, 7518–7525.

[115] M. A. Nowak and R. M. May, *Virus dynamics: Mathematical principles of immunology and virology*, Oxford University Press, New York, 2000.

[116] M. A. Nowak, R. M. May, and R. M. Anderson, *The evolutionary dynamics of HIV-1 quasispecies and the development of immunodeficiency disease*, AIDS **4** (1990), 1095–1103.

[117] P. Olofsson and C. A. Shaw, *Exact sampling formulas for multi-type Galton-Watson processes*, Math. Biol. **45** (2002), 279–293.

[118] J. F. Palella, M. K. Delaney, C. A. Moorman, and et al., *Declining morbidity and mortality among patients with advanced human immunodeficiency virus infection*, N. Engl. J. Med. **338** (1998), 853–860.

[119] D. Pao, U. Andrady, J. Clarke, and et al., *Long-term persistence of primary genotypic resistance after HIV-1 seroconversion*, J. Acquir. Immune Defic. Syndr. **37** (2004), no. 5, 1570–1573.

[120] A. S. Perelson, A. U. Neumann, M. Markowitz, J. M. Leonard, and D. D. Ho, *HIV-1 dynamics in-vivo: virion clearance rate, infected cell life-span, and viral generation time*, Science **271** (1996), 1582–1586.

[121] L. Peterson, D. Taylor, R. Roddy, and et al., *Tenofovir disoproxil fumarate for prevention of HIV infection in women: a phase 2, double-blind, randomized, placebo-controlled trial*, PLoS Clin. Tri. **2** (2007), e27.

[122] C. V. Rao and A. P. Arkin, *Stochastic chemical kinetics and the quasi-steady-state assumption: Application to the gillespie algorithm*, J. Chem. Phys. **118** (2003), 4999–5010.

[123] M. Rathinam, L. R. Petzold, Y. Cao, and D. T. Gillespie, *Stiffness in stochastic chemically reaction systems: the implicit tau-leaping method*, J. Chem. Phys. **119** (2003), 12784–12794.

[124] S. Rerks-Ngarm, P. Pitisuttithum, S. Nitayaphan, and et al., *Vaccination with ALVAC and AIDSVAX to prevent HIV-1 infection in Thailand*, N. Engl. J. Med. **361** (2009), no. 23, 2209–2220.

[125] R. M. Ribeiro and S. Bonhoeffer, *A stochastic model for primary hiv-1 infection: optimal timing of therapy*, AIDS **13** (1999), 351–357.

[126] ———, *Production of resistant HIV mutants during antiretroviral therapy*, Proc. Natl. Acad. Sci. **97** (2000), no. 14, 7681–7686.

[127] R. M. Ribeiro, S. Bonhoeffer, and A. M. Nowak, *The frequency of resistant mutant virus before antiviral therapy*, AIDS **12** (1998), 461–465.

[128] R. M. Ribeiro, L. Qin, L. L. Chavez, D. Li, S. G. Self, and A. S. Perelson, *Estimation of the initial viral growth rate and basic reproductive number during acute HIV-1 infection*, J. Virol. **84** (2010), no. 12, 6096–6102.

[129] D. D Richman, *HIV chemotherapy*, Nature **410** (2001), 995–1001.

[130] L. Rong, Z. Feng, and A. S. Perelson, *Emergence of HIV-1 drug resistance during antiretroviral treatment*, Bull. Math. Biol. **69** (2007), no. 6, 2027–2060.

[131] H. J. Ruskin, R. B. Pandey, and Y. Liu, *Viral load and stochastic mutation in a Monte Carlo simulation of HIV*, Physica A **293** (2002), 315–323.

[132] R. Shankarappa, J. B. Margolick, S. J. Gange, and et al., *Consistent viral evolutionary changes associated with the progression of human immunodeficiency virus type 1 infection*, J. Virol. **73** (1999), no. 12, 10489–10502.

[133] H. Shim, C. C. Han, W.S. Ching, S. W. Nam, and J. H. Seo, *Optimal scheduling of drug treatment for HIV-1 infection: continuous dose control and receding horizon control*, Int. J. Contr. Auto. Sys. **1** (2003), 401–407.

[134] R. J. Smith? and L. M. Wahl, *Drug resistance in an immunological model of HIV-1 infection with impulsive drug effects*, Bull. Math. Biol. **67** (2005), no. 4, 783–813.

[135] M. Sourisseau, N. Sol-Foulon, F. Porrot, F. Blanchet, and O O. Schwartz, *Inefficient human immunodeficiency virus replication in mobile lymphocytes*, J. Virol. **81** (2007), no. 2, 1000–1012.

[136] N. I. Stilianikis, C. A. B. Boucher, M. D. De Jong, R. Van Leeuwen, R. Schuurman, and R. De Boer, *Clinical data sets of human immunodeficiency virus type 1 reverse transcriptase-resistant mutants explained by a mathematical model*, J. Virol. **71**, no. 1, 161–168.

[137] M. C. Strain, S. J. Little, E. S. Daar, and et al., *Effect of treatment, during primary infection, on establishment and clearance of cellular reservoirs of HIV-1*, J. Infect. Dis. **191** (2005), no. 9, 1410–1418.

[138] K. Takhasi, K. Kaizu, B. Hu, and M. Tomita, *A multi-algorithm, multi-timescale method for cell simulation*, Bioinformatics **20** (2004), 538–546.

[139] W. Y. Tan and H. Wu, *Stochastic modeling of the dynamics of CD4+ T-cell infection by HIV and some Monte Carlo studies*, Math. Biosci. **147** (1998), 173–205.

[140] D. M. Tebit, I. Nankya, E. J. Arts, and Y. Gao, *HIV diversity, recombination and disease progression: how does fitness fit into the puzzle?*, AIDS Rev. **9** (2007), no. 2, 75–87.

[141] G. D. Tomaras, N. L. Yates, P. Liu, and et al., *Initial B-cell responses to transmitted human immunodeficiency virus type 1: virion-binding immunoglobulin M (IgM) and IgG antibodies followed by plasma anti-gp41 antibodies with ineffective control of initial viremia*, J. Virol. **82** (2008), no. 24, 12449–12463.

[142] H. C. Tuckwell and E. Le Corfec, *A stochastic model for early HIV-1 population dynamics*, J. Theor. Biol. **195** (1998), 451–463.

[143] UNAIDS, *2009 AIDS epidemic update: December 2009*, `http://data.unaids.org/pub/Report/2009/JC1700_Epi_Update_2009_en.pdf`, November 2009, Accessed: 15/11/2010.

[144] L. M. Wahl and M. A. Nowak, *Adherence and drug resistance: predictions for therapy outcome*, Proc. R. Soc. Lond. B **267** (2000), 835–843.

[145] X. Wei, K. S. Ghosh, E. M. Taylor, and et al., *Viral dynamics in human immunodeficiency virus-type 1 infection*, Nature **373** (1995), 117–122.

[146] D. Wick and S. G. Self, *Early HIV infection in-vivo: branching process model for studying timing of immune responses and drug therapy*, Math. Biosci. **165** (2000), no. 2, 115–134.

[147] ———, *On simulating strongly interacting, stochastic population models*, Math. Biosci. **187** (2004), no. 1, 1–20.

[148] ———, *On simulating strongly interacting, stochastic population models. II. Multiple compartments*, Math. Biosci. **190** (2004), 127–143.

[149] W. D. Wick, *Fitting non-linear, stochastic models to data in biology and medicine*, Pre-Print Text Book, SCHARP, Seattle, 2009.

[150] W. D. Wick, O. O. Yang, P. B. Gilbert, F. Li, and S. G. Self, *The ecological genetics of HIV in vivo: How HIV evolves in the host to escape drugs and immune response*, Pre-Print Text Book, SCHARP, Seattle, 2008.

[151] N. A. Wilson, J. Reed, G. S. Napoe, and et al., *Vaccine-induced cellular immune responses reduce plasma viral concentrations after repeated low-dose challenge with pathogenic simian immunodeficiency virus SIVmac239*, J. Virol. **80** (2006), no. 12, 5875–5885.

[152] D. Wodarz and A. L. Lloyd, *Immune responses and the emergence of drug-resistant virus strains in-vivo*, Proc. R. Soc. Lond. B **271** (2004), 1101–1109.

[153] S. B. J. Wong and R. F. Siliciano, *Biology of early infection and impact on vaccine design*, AIDS Vaccine Development: Challenges and Opportunities (United Kingdom), Caister Academic, 2007, pp. 17–22.

[154] N. Wood, T. Bhattacharya, B. F. Keele, and et al., *HIV evolution in early infection: selection sressures, patterns of insertion and deletion, and the impact of APOBEC*, PLoS Path. **5** (2009), no. 5, e1000414.

[155] J. Wu, P. Yan, and C. Archibold, *Modelling the evolution of drug resistance in the presence of antiviral drugs*, BMC Public Health **7** (2007), 300.